waterloopkundig laboratorium
delft hydraulics laboratory

storm surge barrier Oosterschelde

computation of siltation in dredged trenches

mathematical model

R 1267-V/M 1570

September 1980

storm surge barrier Oosterschelde

computation of siltation in dredged trenches

mathematical model

R 1267-V/M 1570

September 1980

CONTENTS

FIGURES

FIGURES (continuation)

PHOTOGRAPHS

1 Instrument for measuring sediment concentration profiles

2 Separation of water and sediment by means of filter material (mesh size = 50 μm)

LIST OF SYMBOLS

A	siltation area	L^2
c	sediment concentration	-
c_a	sediment concentration at the bed (equilibrium profile)	-
$\bar{c}$	depth-averaged concentration	-
D	diameter of sediment particle	L
d	depth of trench	L
E	siltation efficiency	-
g	acceleration of gravity	$L\ T^{-2}$
h	flow depth	L
k	height of bed form	L
k_s	equivalent roughness of Nikuradse	L
L	relaxation length	L
L_A	length of acceleration zone	L
l	length of bed form	L
l_t	top width of trench	L
l_b	bottom width of trench	L
p	porosity of bed material	-
q	discharge per unit width	$L^2\ T$
r	reduction factor	
s_b	bed load transport per unit width	$M\ L^{-1}\ T^{-1}$
s_s	suspended load transport per unit width	$M\ L^{-1}\ T^{-1}$
s_t	total load transport per unit width	$M\ L^{-1}\ T^{-1}$
T	water temperature	^oC
t	time	T
u	longitudinal flow velocity	$L\ T^{-1}$
$\bar{u}$	depth-averaged flow velocity	$L\ T^{-1}$
u_b	maximum flow velocity in outer layer	$L\ T^{-1}$
u_e	maximum flow velocity in layer with reversed flow	$L\ T^{-1}$
u_*	shear velocity	$L\ T^{-1}$
w	vertical flow velocity	$L\ T^{-1}$
w_s	particle fall velocity	$L\ T^{-1}$
x	longitudinal coordinate	L
z	vertical coordinate	L
z_a	boundary level above bed	L

LIST OF SYMBOLS (continuation)

z_b	bed level above a datum	L
z_o	zero-velocity level above bed	L
α_1, α_2, α_3	coefficients in diffusion coefficient distribution	-
β	ratio of diffusion coefficient for sediment and momentum	-
δ_m	thickness of mixing layer	L
ε_m	diffusion coefficient for momentum	L^2 T
$\hat{\varepsilon}_m$	maximum diffusion coefficient for momentum	L^2 T
ε_s	diffusion coefficient for sediment particles	L^2 T
$\hat{\varepsilon}_s$	maximum diffusion coefficient for sediment particles	L^2 T
κ	constant of Von Karman	-
ρ_s	density of sediment	M L^{-3}
ρ_w	density of water	M L^{-3}
σ	standard deviation	-
Θ	numerical implicity factor	-

Indices

b	bed
e	equilibrium
i, j, k	numerical indices
s	sediment
x	longitudinal direction
z	vertical direction
t	time
o	upstream of trench

STORM SURGE BARRIER OOSTERSCHELDE

Mathematical model

1. Introduction and problem statement

The design of the storm surge barrier in the entrance of the Oosterschelde Estuary consists of pre-fabricated (monolith) piers which are founded in a dredged trench. An important objective is the estimation of the siltation of sediment particles in the trench both for the long and short term. Long-term siltation is considered to take place in the period after the dredging of the trench and the maintenance dredging activities just before the arrival of a pier, while short-term siltation is supposed to occur in the period after the last maintenance dredging activities and the arrival and sinking of the pier.

Particularly does the prediction of the short-term siltation require a rather sophisticated prediction method and accurate boundary conditions (input data). The siltation and eriosion processes in a trench can be described as the movement of the suspended sediment particles by diffusion, convection and gravity. The expansion of the flow depth reduces the longitudinal flow velocities, resulting in a reduction of the local transport capacity of the flow. Consequently, the surplus of sediment will settle out by gravity forces, a process intensified by convection due to vertical flow velocities. In the acceleration zone a reversed process occurs, resulting in the erosion of sediment particles from the bed into the flow.

In earlier studies a mathematical model for the prediction of siltation in dredged trenches was developed [4], [6], [11] and [12], based on the diffusion-convection equation for the suspended sediment particles and the continuity equation for the total sediment transport to compute bed level changes. The convection due to vertical flow velocities, however, was neglected. Another drawback was the application of a logarithmic velocity distribution to describe the longitudinal flow velocities, thus restricting the application of the model to gentle-sided trenches only. Furthermore, the siltation due to bed load was not taken into account. This model was actually used to make preliminary computations for a number of representative trench profiles.

To improve the first version of the mathematical model and to extend the prediction method to steep-sided trenches the following subjects were studied:

- the flow field in steep-sided trenches,
- the bed-boundary conditions for the computation of the concentration field, and
- the siltation due to the bed load.

2. Summary, conclusions and suggestions for further research

2.1 Summary

In this report a mathematical model for the prediction of siltation in dredged trenches is described. This (two-dimensional) model simulates the longitudinal and vertical movements of the suspended sediment particles by diffusion, convection and gravity. Bed level changes due to changes in the bed load and suspended load transport are determined on base of the continuity equation, while the flow field is described by a semi-empirical model based on extensive laboratory measurements. Flow separation and reversed flow can also be predicted. Consequently, the model is also suitable for steep-sided trenches. Transport processes due to density differences are not taken into account, while the bed must be moderately or non-graded, and changes in lateral direction must remain relatively small. The method can also be used for tidal conditions by schematizing the tidal period to a number of quasi-steady flow conditions, although in such cases the upstream concentration profiles must be in a quasi-steady state.

Basic equations, simplifications, sediment diffusion coefficient and boundary conditions are described in Chapter 3.
The value of the upstream sediment transport, the form of the upstream concentration profile, and the bed boundary condition are of essential importance. Usually, the upstream concentration profile is supposed to be the equilibrium profile. At the bed, a combined boundary condition (a zero bed-concentration gradient or an equilibrium bed concentration) is applied in case of steep-sided trenches, while for gentle-sided trenches an equilibrium bed concentration determined from the local transport capacity is used.

The numerical solution methods for the diffusion-convection equation and sediment-continuity equation, described in Chapter 4, are given only roughly. To reduce the vertical grid size near the bed (large concentration gradients), the diffusion-convection equation is transformed, using, for the sake of speed and stability of this method a six-point implicit scheme. However, the numerical (pseudo-viscosity) method for the computation of the bed levels may lead to some inaccuracy (smoothing) at sharp transitions in the bed profile, particularly in case of steep-sided trenches.

For the verification of the model both laboratory and field measurements were used. For the laboratory tests, three trenches with different dimensions were utilised (Figure 3), with unchanged flow conditions. The main controlling parameters, like the suspended load rate and the maximum diffusion coefficient at the upstream boundary and the particle fall velocity, were evaluated from measurements. Comparison of measured and computed flow velocities shows reasonable agreement (Figures 6, 7, 8, 11, 12, 15 and 16), and measured and computed concentration profiles show relatively large deviations, particularly near the bed in the deceleration and acceleration zones (Figures 6, 7, 8, 11, 12, 15 and 16). As regards the deceleration zone, the deviations may be caused by the application of a zero-bed concentration gradient and a parabolic-constant vertical distribution for the diffusion coefficient, while for the acceleration zone, the use of the equilibrium bed-concentration method may have led to an underestimation of the bed concentration.
The predicted siltation level after 7.5 and 15.0 hours is quite good (Figures 10, 14 and 18). The predicted erosion level, however, is systematically less than the measured values, resulting from the flow velocities and concentrations near the bed not being represented correctly.
For verification in field conditions, the siltation in a dredged test pit in the entrance of the oosterschelde estuary was used (Figure 29). Flow velocities and sediment concentrations were determined by detailed measurements in the autumn of 1977 and the spring of 1978 (Figures 30 and 31). Representative sediment sizes were determined from samples of the bed and suspended sediment material, while bed roughness was evaluated by means of echo soundings of the bed forms. The main controlling parameters were obtained from measurements. Comparison of measured and computed flow velocities shows good agreement (Figure 34). The predicted siltation level is remarkably good, and no additional calibration was applied (Figure 35).
By means of a sensitivity analysis, the extent to which the siltation in the trench is influenced by the main controlling parameters and boundary conditions was examined. This revealed that the value of the suspended load rate and the maximum diffusion coefficient at the upstream boundary and the particle fall velocity are of essential importance (Figures 20, 22, 24, 37 and 41) and should only be evaluated from detailed measurements. The bed boundary condition also influences the results significantly (Figure 39) less important are the value of the diffusion coefficient in the trench and the flow field (Figures 27 and 36).

2.2 Conclusions

The following conclusions can be drawn from this study:

1 The siltation in a dredged trench can be represented satisfactorily by a mathematical model based on diffusion, convection and gravity processes.

2 The proposed model can be used for tidal conditions if no density currents occur, the bed is moderately or non-graded, and the upstream sediment concentrations are in a quasi-steady state in any phase of the tide.

3 The main controlling parameters, like the value of the suspended load rate and the maximum diffusion coefficient at the suptream boundary and the particle fall velocity, are of essential importance and should only be evaluated from detailed field measurements.

4 The application of a combined bed boundary condition (zero bed-concentration gradient and an equilibrium bed concentration) certainly gives better results than a single bed boundary condition (equilibrium bed concentration), but both methods lead to an underestimation of measured bed concentrations.

5 The value of the diffusion coefficient in the trench does not significantly influence the computed suspended load and siltation level.

6 The flow field does not importantly influence the computed siltation level in the long term, not even for steep-sided trenches, though the concentration profiles and suspended load transport in the initial stage may be influenced considerably.

2.3 Suggestions for further research

The solution method for the diffusion-convection equation is not yet optimal, and possibly a more simple transformation method or another numerical method (finite elements) may be useful. Some attention must also be paid to the solution method of the equation for the bed-level computation, because the applied "pseudo-viscosity" method introduces numerical inaccuracy ("smoothing")

at sharp transitions in the bed profile, particularly in the case of steep-sided trenches. Siltation due to bed load transport must be improved by taking into account the gravity effects on the slopes of the trench.

Further research must especially be focussed on the improvement of the bed boundary condition for the diffusion-convection equation. In the siltation zone, as well as the erosion zone, the bed concentrations computed by means of a zero bed-concentration gradient and/or equilibrium bed concentration are too low compared with measured values. It is believed that the use of an entrainment function which relates the entrainment of the sediment particles (from the bed into the flow) to local flow parameters will produce better results with respect to the prediction of concentration profiles and the sediment erosion in the acceleration zone. Also the computed flow velocities in this zone may be improved. As for the deceleration zone, the predicted concentrations may be improved by applying another boundary condition in combination with a more appropriate distribution for the sediment diffusion coefficient, particularly in case of flow separation. For the latter a "turbulence" model may be considered. However, for the silitation rate in the trench these improvements may be of minor importance, especially as they will be costly.

3. Mathematical model

3.1 Equations and simplifications

Water flow

The water flow in a dredged trench is non-uniform and can be described by solving the equations of continuity and motion [2].
In the case of a trench with relatively gentle slopes such an expensive solution does not seem justified, because the application of logartithmic velocity profiles will not cause much inaccuracy.
In the case of steep-sided trenches, however, the flow velocity and turbulence field is very complex; particularly if flow separation does occur. Therefore an accurate description of the flow field is needed. A method to obtain accurate quantitative information of the flow velocities and turbulence parameters is the use of so-called "turbulence" models. These models are fundamentally related to the "closure" problem; the number of unknown variables exceeds the number of available equations, which can only be solved by assuming additional relations between the unknown variables. These additional functions may be simple algebraic equations relating, for example, the turbulent shear stress to the local flow velocity gradient as well as differential equations. Recently, there has been a tendency for the more complex turbulence models in order to obtain a universal model that can be used for different types of flow. But a major drawback of these models still is the large computer time and hence costs, especially if long-term computations are needed.
Another method to compute the flow velocity field in a trench is the application of a semi-empirical model based on extensive measurements under varying conditions.
In this present research the semi-empirical approach has been followed, which means that the longitudinal flow velocities in each characteristic zone of the trench are described by semi-empirical relations.

In a trench three characteristic zones can be distinguished (see also Figure 1):

- Deceleration zone with or without flow separation. Above the upstream slope of the trench the flow is retarded due to expansion of the flow depth. In the case of a very strong expansion (steep-sided trenches),

the initially equilibrium boundary layer will change into a mixing shear layer with a significant change in the turbulent structure. Even flow separation may occur.

- Relaxation or redistribution zone.
  In the middle zone of the trench the mixing layer will disappear and a new boundary layer flow will develop. The length which is needed to establish an equilibrium flow with unchanged flow characteristics in a longitudinal direction is called the relaxation length, and is about 40-50 times the local flow depth for the outer layer and about 10 times the flow depth for the near-bed layer of the flow.
- Acceleration zone.
  Above the downstream slope of the trench the flow will be accelerated as the result of a (negative) pressure gradient acting in the flow direction. Typical characteristics are a full velocity profile with relatively high velocities near the bed and a considerably upward flow in the near-bed layer.

Detailed information about the semi-empirical model can be found in [3].

In general form (see also Figure a):

$$u_{(z)} = F \text{ (empirical data)} \qquad (3.1)$$

in which:

u = longitudinal flow velocity (m/s)

z = vertical coordinate (m)

The vertical flow velocity is computed from the equation of continuity:

$$\frac{\partial u}{\partial x} + \frac{\partial w}{\partial z} = 0 \qquad (3.2)$$

resulting in:

$$w_{(z)} = w_{(z_b + h)} + \int_{z}^{z_b + h} \frac{\partial u}{\partial x}\, dz \qquad (3.3)$$

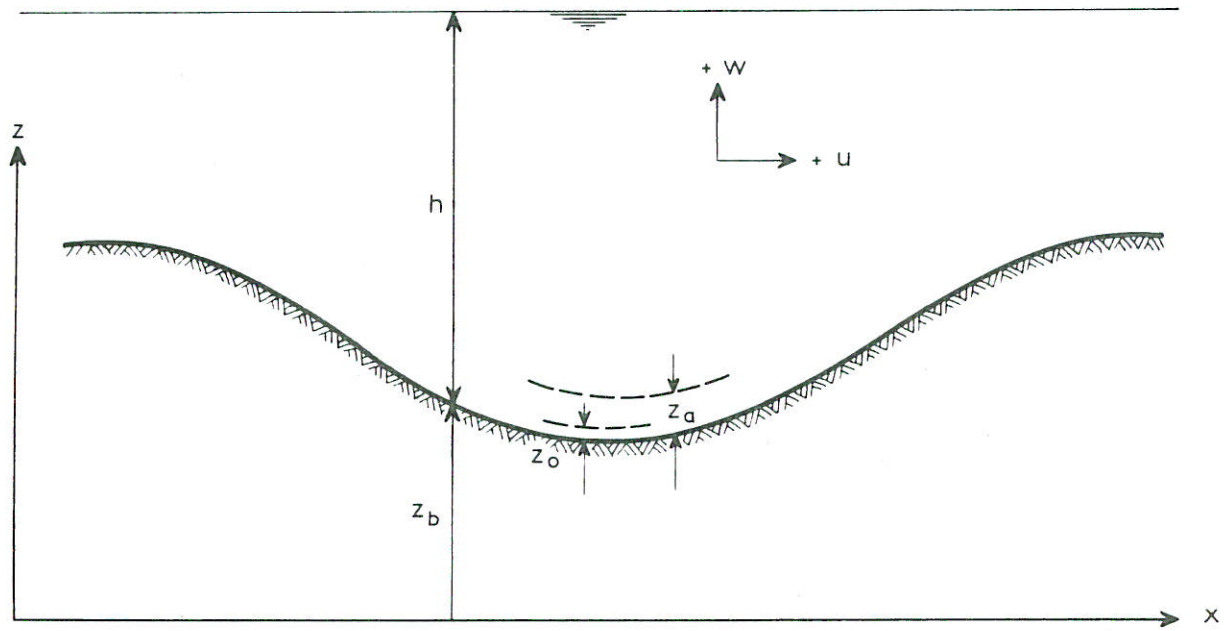

Figure a

Sediment transport

The vertical and longitudinal movements of the suspended sediment particles in a non-permanent and non-uniform flow field can be described by [4]:

$$\frac{\partial c}{\partial t} + u\frac{\partial c}{\partial x} + w\frac{\partial c}{\partial z} - w_s\frac{\partial c}{\partial z} - \frac{\partial}{\partial x}\left(\varepsilon_s\frac{\partial c}{\partial x}\right) - \frac{\partial}{\partial z}\left(\varepsilon_s\frac{\partial c}{\partial z}\right) = 0 \qquad (3.4)$$

convection gravity diffusion

in which:

c	=	local concentration	(kg/m^3)
u	=	longitudinal flow velocity	(m/s)
w	=	vertical flow velocity	(m/s)
w_s	=	particle fall velocity	(m/s)
ε_s	=	turbulent diffusion coefficient	(m^2/s)
x	=	longitudinal coordinate	(m)
z	=	vertical coordinate	(m)
t	=	time	(s)

The turbulent diffusion coefficient is assumed to be a scalar quantity, and the particle fall velocity is assumed to be constant.

By means of scale analysis, it can be shown [11] that in tidal conditions the

time-dependent concentration term can be neglected if the flow depth is not very large (h < 10 m) and the sediment is not very fine (D > 100 μm). Scale analysis also shows that the longitudinal diffusion term is negligibly small with respect to the other terms.

Suspended load

The suspended load transport is computed as:

$$s_s = 0.67\, u_{(z_a)}\, c_{(z_a)}\, (z_a - z_0) + \int_{z_b + z_a}^{z_b + h} u_{(z)}\, c_{(z)}\, dz \qquad (3.5)$$

in which:

$u_{(z_a)}$	=	flow velocity at $z = z_a$	(m/s)
z_a	=	boundary level above bed	(m)
$c_{(z_a)}$	=	concentration at $z = z_a$	(kg/m^3)
z_0	=	zero-velocity level	(m)

The first part of Equation (3.5) represents the suspended load in the layer between the zero-velocity level and the bed-boundary level. The suspended load in this layer is supposed to have a parabolic distribution in a vertical direction. The second part of Equation (3.5) represents the suspended load above the bed boundary level.

Bed load

The bed load, defined as the movement of the sediment particles by rolling and saltating along the bed is represented by a simple empiric formula based on the local (depth-averaged) flow velocity and the sediment properties. Consequently, a change in flow conditions will result in a change of the bed load rate and hence in a bed-level change.
Gravity effects at the side-slopes of the trench, resulting in an increased bed load transport at the upstream slope and a reduced bed load rate at the downstream slope, are not represented in the mathematical model.

Bed level change

Bed level changes can be described by the equation of continuity for the total sediment transport:

$$\frac{\partial z_b}{\partial t} + \frac{1}{(1-p)\ \rho_s} \{\frac{\partial\ (h\bar{c})}{\partial t} + \frac{\partial s_t}{\partial x}\} = 0 \qquad (3.6)$$

in which:

$\bar{c} = \int_{z_b+z_a}^{z_b+h} c_{(z)}\ dz$ = depth-integrated concentration (kg/m^3)

$s_t = s_s + s_b$ = total load transport (kg/sm)

s_s = suspended load transport (kg/sm)

s_b = bed load transport (kg/sm)

z_b = bed level above a datum (m)

z_a = boundary level above bed (m)

h = flow depth (m)

p = porosity (-)

ρ_s = density of sediment (kg/m^3)

By means of scale analysis it can be shown that the storage term $\partial(h\bar{c})/\partial t$ is negligibly small with respect to the other terms.

Summarizing, the following equations are used:

$$u_{(z)} = F \text{ (empirical data)} \qquad (3.7)$$

$$\frac{\partial u}{\partial x} + \frac{\partial w}{\partial z} = 0 \qquad (3.8)$$

$$u\ \frac{\partial c}{\partial x} + w\ \frac{\partial c}{\partial z} - w_s\ \frac{\partial c}{\partial z} - \frac{\partial}{\partial z}\ (\varepsilon_s\ \frac{\partial c}{\partial z}) = 0 \qquad (3.9)$$

$$\frac{\partial z_b}{\partial t} + \frac{1}{(1-p)\ \rho_s}\ \frac{\partial s_t}{\partial x} = 0 \qquad (3.10)$$

3.2 Diffusion coefficient for sediment particles

3.2.1 Uniform flow

Usually, the transport of momentum and mass caused by the turbulent motions is indicated as diffusive transport, the value of which is supposed to be proportional to the local velocity gradient, respectively concentration gradient (Boussinesq hypothesis). From the logarithmic velocity profile of Prandtl, the following expression for the diffusion coefficient of momentum can be derived:

$$\frac{\varepsilon_m}{u_* h} = \kappa \frac{(z - z_b)}{h} \{1 - \frac{(z - z_b)}{h}\} \qquad (3.11)$$

in which:

ε_m	=	diffusion coefficient of mentum	(m^2/s)
u_*	=	shear velocity	(m/s)
h	=	flow depth	(m)
κ	=	constant of Von Karman	(-)
z_b	=	bed level above a datum	(m)
z	=	vertical coordinate	(m)

The maximum value of ε_m is:

$$\frac{\bar{\varepsilon}_m}{u_* h} = 0.1 \text{ , for } \frac{z - z_b}{h} = 0.5 \text{ and } \kappa = 0.4 \qquad (3.12)$$

Usually, the diffusion coefficient for sediment (ε_s) is supposed to be proportional to the diffusion coefficient for momentum (ε_m):

$$\varepsilon_s = \beta \varepsilon_m \qquad (3.13)$$

The proportionality factor β accounts for the centrifugal and inertia forces acting on the sediment particles and for the influence of the sediment particles on the turbulence structure. Research [5] has shown that the β-value may be considerably larger than 1.

On the basis of experiments of Coleman [1], it can be concluded that the diffusion coefficient also depends on the ratio of the particle fall velocity and the shear velocity. The experimental results of Coleman can be represented by [4]:

$$\frac{\varepsilon_s}{u_* h} = 4 \{\alpha_1 + \alpha_2 (\frac{w_s}{u_*})^{\alpha_3}\} \{\frac{(z - z_b)}{h}\} \{1 - \frac{(z - z_b)}{h}\}, \quad \text{for } \frac{z - z_b}{h} < 0.5 \qquad (3.14)$$

$$\frac{\varepsilon_s}{u_* h} = \frac{\hat{\varepsilon}_s}{u_* h} = \alpha_1 + \alpha_2 (\frac{w_s}{u_*})^{\alpha_3} \quad \text{, for } \frac{z - z_b}{h} \geq 0.5 \qquad (3.15)$$

in which:

$\hat{\varepsilon}_s$ = maximum diffusion coefficient for the sediment particles (m^2/s)

α_1 = 0.1 , α_2 = 0.38, α_3 = 4.31 for flumes

α_2 = 0.13, α_2 = 0.20, α_3 = 2.12 for natural channels

If the β-value is defined as the ratio of the maximum diffusion coefficients for sediment and momentum, the following expression can be derived:

$$\beta = \frac{\hat{\varepsilon}_s}{\hat{\varepsilon}_m} = 10 \{\alpha_1 + \alpha_2 (\frac{w_s}{u_*})^{\alpha_3}\} \qquad (3.16)$$

in which:

$\hat{\varepsilon}_s$ = maximum vertical diffusion coefficient of sediment (m^2/s)

$\hat{\varepsilon}_m$ = maximum vertical diffusion coefficient of momentum (m^2/s)

Equation (3.16) is represented graphically in Figure 2, showing a β-value which is always larger than 1.

In the case of uniform flow the diffusion-convection Equation (3.9) can be simplified to:

$$w_s c + \varepsilon_s \frac{dc}{dz} = 0 \qquad (3.17)$$

Substitution of (3.14) and (3.15) into (3.17) and integration over the flow depth yields:

$$\frac{c_{(z)}}{c_a} = \left[\left(\frac{z_a}{h - z_a}\right)^{\frac{h\, w_s}{4\, \hat{\varepsilon}_s}}\right]\left[e^{-\frac{w_s\,(z - z_b - 0.5\, h)}{\hat{\varepsilon}_s}}\right], \quad \text{for} \quad \frac{z - z_b}{h} \geq 0.5 \qquad (3.18)$$

$$\frac{c_{(z)}}{c_a} = \left[\left\{\frac{h - (z - z_b)}{z - z_b}\right\}\left\{\frac{z_a}{h - z_a}\right\}\right]^{\frac{h\, w_s}{4\, \hat{\varepsilon}_s}}, \quad \text{for} \quad \frac{z - z_b}{h} < 0.5 \qquad (3.19)$$

in which:

c_a = bed concentration at the bed boundary level (kg/m^3)

In uniform condition Equation (3.18) and (3.19) are used to describe the vertical concentration distribution.

3.2.2 Non-uniform flow

In non-uniform flow additional memory effects, namely, the reaction of the turbulence to a change in flow conditions (mean velocity field), will occur. These additional effects should not be confused with memory effects inherent to the turbulence itself, which are also present in stationary and homogeneous flow. Experiments on boundary layer flow with a sudden change in the imposed pressure gradient or a sudden flow expansion have revealed that the inner region (near the wall) will reach an equilibrium state sooner than the outer region. Consequently, the response of turbulence to a disturbance seems to depend on the size of the turbulent eddies. A small eddy in the inner region, with a small time-scale, will show a smaller additional memory effect than a larger eddy in the outer region, with a larger time-scale. Therefore, in principle the transport by diffusion in a non-uniform flow cannot be described by a simple gradient-type transport model. For reasons of simplicity, however, this approach is still applied.

Flow separation

In case of flow separation, the maximum value of the diffusion coefficient is supposed to be proportional to the thickness of the mixing layer and the velocity difference across this layer [3].
Considering the form of Equations (3.14) and (3.15), the diffusion coefficient is supposed to be constant in the upper half of the flow depth and parabolic in the lower half. But it must be stressed that this approach will give rise to deviations because the maximum ε_s-value will undoubtedly occur in the mixing layer, which also exists in the lower half of the flow depth. The derivations of constants and empirical functions are given in [3].

Deceleration zone

$$\hat{\varepsilon}_s = \beta \chi \delta_m (u_e - u_b) \qquad (3.20)$$

in which:

β	=	ratio of diffusion coefficient for sediment and momentum	(-)
χ	=	constant = 0.0085	(-)
δ_m	=	thickness of the mixing layer	(m)
u_e	=	maximum flow velocity in the outer layer	(m/s)
u_b	=	maximum flow velocity in the layer with reversed flow	(m/s)

Relaxation zone

The relaxation of the $\hat{\varepsilon}_s$-value at the end of the deceleration zone ($\hat{\varepsilon}_{s,R}$) to an equilibrium value ($\hat{\varepsilon}_{s,L}$) is described by:

$$\frac{\hat{\varepsilon}_{s,x} - \hat{\varepsilon}_{s,L}}{\hat{\varepsilon}_{s,R} - \hat{\varepsilon}_{s,L}} = 1 - \tanh \{7.2 \left(\frac{x - x_R}{L}\right)\}, \qquad (3.21)$$

in which:

$\hat{\varepsilon}_{s,L}$	=	equilibrium value of $\hat{\varepsilon}_s$ according to Equation (3.15)	(m^2/s)
$\hat{\varepsilon}_{s,R}$	=	value of $\hat{\varepsilon}_s$ at the end of the deceleration zone according to Equation (3.20)	(m^2/s)
L	=	relaxation length = 40 h_R	(m)
h_R	=	flow depth at the end of the deceleration zone	(m)
x_R	=	longitudinal coordinate of the end of the deceleration zone	(m)

Acceleration zone

$$\frac{\hat{\varepsilon}_{s,x} - \hat{\varepsilon}_{s,A}}{\hat{\varepsilon}_{s,B} - \hat{\varepsilon}_{s,A}} = \left(\frac{x - x_A}{L_A}\right)^2 \qquad (3.22)$$

in which:

$\hat{\varepsilon}_{s,A}$ = value of $\hat{\varepsilon}_s$ at the end of the relaxation zone according to Equation (3.21) (m^2/s)

$\hat{\varepsilon}_{s,B}$ = value of $\hat{\varepsilon}_s$ at the end of the acceleration zone according to Equation (3.15) (m^2/s)

L_A = length of the acceleration zone (m)

x_A = longitudinal coordinate of the end of the relation zone (m)

No flow separation

As no information about the diffusion coefficient in these conditions is available, the diffusion coefficient is described by the relations for uniform flow (Equations (3.14) and (3.15)).

3.3 Boundary conditions

Bed profile

The initial (t = 0) bed profile $z_{b(x,0)}$ must be given.

At the upstream boundary the bed level $z_{b(0,t)}$ must be given as a function of time.

Water flow

Upstream boundary

Discharge $q_{(0,t)}$ and flow depth $h_{(0,t)}$ must be given as a function of time.

Surface boundary

The water surface is supposed to be horizontal, resulting in:

$w = 0$ at $z = z_b + h$

(By means of Equation (3.3) and assuming $u = 0$ at $z = z_b + z_0$, it can be shown that $w = 0$ at $z = z_b + z_0$.)

Sediment transport

Upstream boundary

The concentration profile $c_{(0,z)}$, must be given as a function of time. Usually, this will be the equilibrium profile.

Surface boundary

The vertical sediment transport is supposed to be zero, resulting in:

$$w_s \, c_{(z_b + h)} + \varepsilon_{s,(z_b + h)} \frac{\delta c_{(z_b + h)}}{\delta z} = 0 \qquad (3.23)$$

Bed boundary

At the bed boundary the concentration gradient $\partial c_{(x,z_b + z_a)}/\partial z$ or the bed concentration $c_{(x,z_b + z_a)}$ must be specified.

In the model both conditions are applied:

Steep-sided trenches

$$\frac{\partial c_b}{\partial z} = 0 \ , \quad \text{in the zone where} \quad \frac{\partial s}{\partial x} < 0 \qquad (3.24)$$

$$c_b = c_{b,e} \ , \text{ in the zone where} \quad \frac{\partial s}{\partial x} \geq 0 \qquad (3.25)$$

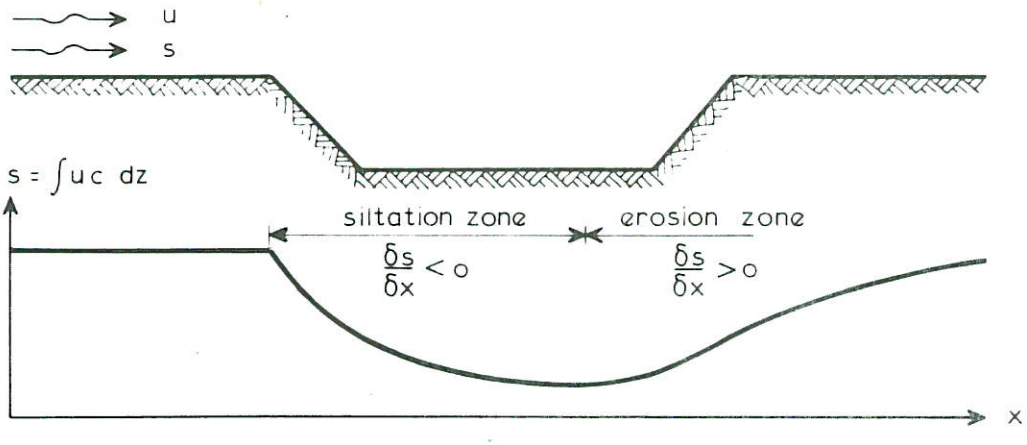

Figure b

The zone in which the siltation process dominates is characterised by a decreasing sediment transport (Figure b). In this zone a zero bed-concentration gradient is applied. This bed boundary condition implies no re-entrainment of sediment from the bed into the flow, which may be a rather (too) crude assumption.
In case of flow separation and the establishment of a layer with reversed flow, the zero bed-concentration gradient is applied at the dividing stream line, defined as the line above which the discharge remains constant. The use of a new bed boundary is necessary because the diffusion-convection Equation (3.9) cannot be solved for negative longitudinal flow velocities. The recirculation zone is treated as a "black box" in which the sediment concentrations in a vertical direction are supposed to be equal to the concentration at the new "bed" boundary (= dividing stream line).

The equilibrium bed concentration ($c_{b,e}$) applied in the erosion zone is determined from the local transport capacity of the suspended load, which can be estimated by an adequate transport formula for equilibrium conditions. The transport capacity can also be computed by:

$$s_{s,e} = \int_{z_b + z_a}^{z_b + h} u_{(z)}\, c_{e,(z)}\, dz \qquad (3.26)$$

in which the equilibrium concentration profile $c_{e,(z)}$ follows from Equations (3.18) and (3.19). Using the transport capacity according to Equation (3.26) and the applied transport formula the equilibrium bed concentration ($c_{b,e}$) can be determined.

Gentle-sided trenches

In the case of gentle slopes (maximum slope 1:20) allowing the application of logarithmic velocity profiles, an equilibrium bed concentration is applied at the bed boundary:

$$c_b = c_{b,e} \qquad (3.27)$$

3.4 Armoured bed layer

The top layer of the bed of a channel can become armoured by natural segregation processes or by an artificial construction. Generally the siltation process will not be influenced by an armoured layer, but the erosion process, however, will be completely hindered, if no bed material is available on top of the armoured layer.
In the mathematical model the bed can be eroded until:

$$s_{s,i} + s_{b,i} = s_{s,i-1} + s_{b,i-1} + \Delta s \qquad (3.28)$$

in which:

$\Delta s = \frac{\Delta d\ \Delta x\ (1-p)\ \rho_s}{\Delta t}$ = sediment transport due to the entrainment of sediment particles present on top of the armoured layer (kg/sm)

Δd = sediment layer on top of the armoured bed (m)

Δt = time step (s)

p = porosity (-)

ρ_s = density of sediment (kg/m^3)

$s_{s,i}$; $s_{s,i-1}$ = suspended load transport without an armoured bed (kg/sm)

$s_{b,i}$; $s_{b,i-1}$ = bed load transport without an armoured bed (kg/sm)

If $s_{t,i} - s_{t,i-1} > \Delta s$, then the computed sediment concentrations, and hence the sediment transport, is reduced by:

$$r = \frac{s_{t,i-1} + \Delta s}{s_{t,i}} \qquad (3.29)$$

For $\Delta s = 0$, the sediment transport remains constant.

4. Numerical aspects

4.1 Solution method for diffusion-convection equation

Transformations

Due to the large vertical concentration gradients close to the bed, it is desirable to reduce the vertical grid size near the bed. This is done by means of a transformation (Figure c):

$$x' = x \tag{4.1}$$

$$z' = \int_{z = z_b + z_a}^{z} f_{(x,z)}\, dz \tag{4.2}$$

bed boundary $(z = z_b + z_a)$: $z' = 0$

surface boundary $(z = z_b + h)$: $z' = \int_{z_b + z_a}^{z_b + h} f_{(x,z)}\, dz = z'_{max}$

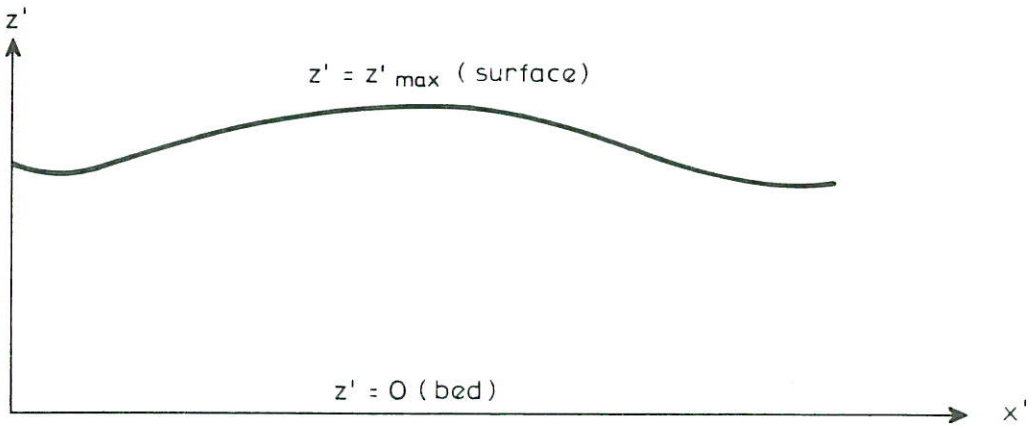

Figure c

The differentiation operators are:

$$\frac{\partial}{\partial x} = \frac{\partial}{\partial x'} + \frac{\partial z'}{\partial x}\frac{\partial}{\partial z'} \quad \text{and} \quad \frac{\partial}{\partial z} = \frac{\partial z'}{\partial z}\frac{\partial}{\partial z'}$$

in which:

$$\frac{\partial z'}{\partial x} = \int_{z_b+z_a}^{z} \frac{\partial f_{(x,z)}}{\partial x}\, dz - f_{(x,z_b+z_a)} \frac{d(z_b+z_a)}{dx} \tag{4.3}$$

$$\frac{\partial z'}{\partial z} = f_{(x,z)} \tag{4.4}$$

The transformed diffusion-convection equation reads:

$$(w-w_s)\, f_{(x,z)} \frac{\partial c}{\partial z'} + u \left(\frac{\partial c}{\partial x'} + \frac{\partial z'}{\partial x} \frac{\partial c}{\partial z'}\right) - f_{(x,z)} \frac{\partial c}{\partial z'} \left(\varepsilon_s\, f_{(x,z)} \frac{\partial c}{\partial z'}\right) = 0 \tag{4.5}$$

To obtain a rectangular grid pattern for each bottom configuration, a second transformation is applied (Figure d):

$$x'' = x' \tag{4.6}$$

$$x'' = \frac{z'}{z'_{max}} \tag{4.7}$$

bed boundary ($z' = 0$): $z'' = 0$

surface boundary ($z' = z'_{max}$): $z'' = 1$

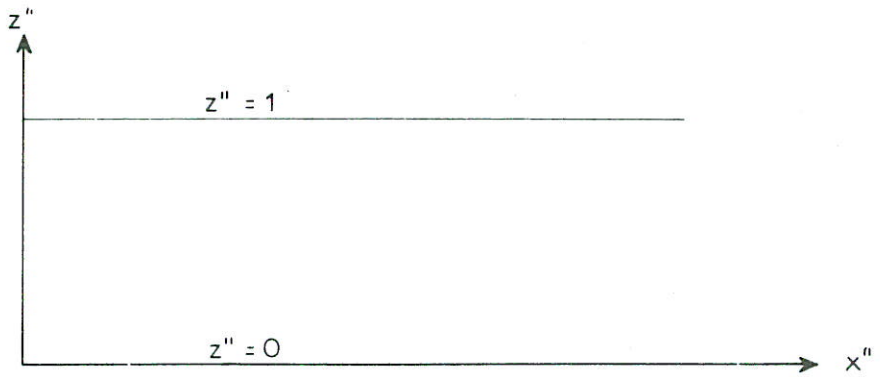

Figure d

The differentiation operators are:

$$\frac{\partial}{\partial x'} = \frac{\partial}{\partial x''} + \frac{\partial z''}{\partial x'} \frac{\partial}{\partial z''} \qquad \text{and} \qquad \frac{\partial}{\partial z'} = \frac{\partial z''}{\partial z'} \frac{\partial}{\partial z''}$$

in which:

$$\frac{\partial z''}{\partial x'} = - \frac{z'}{(z'_{max})^2} \frac{dz'_{max}}{dx'} \tag{4.8}$$

$$\frac{\partial z''}{\partial z'} = \frac{1}{z'_{max}} \tag{4.9}$$

The diffusion-convection equation finally reads:

$$\lambda \frac{\partial c}{\partial z''} - \frac{\partial c}{\partial x''} + \mu \frac{\partial}{\partial z''} (\varepsilon_s f_{(x,z)} \frac{\partial c}{\partial z''}) = 0 \tag{4.10}$$

in which:

$$\lambda = - \left[\{ (\frac{w-w_s}{u}) f_{(x,z)} + \frac{\partial z'}{\partial x} \} \frac{1}{z'_{max}} + \frac{\partial z''}{\partial x'} \right] \tag{4.11}$$

$$\mu = \frac{f_{(x,z)}}{u} \frac{1}{(z'_{max})^2} \tag{4.12}$$

The function $f_{(x,z)}$ used in the mathematical model is defined as:

$$f_{(x,z)} = \frac{w_s}{\varepsilon_s} \tag{4.13}$$

in which:

w_s = fall velocity (m/s)

ε_s = vertical diffusion coefficient for the sediment particles (after equations (3.14) and (3.15)) (m^2/s)

Numerical scheme

Application of a six-point implicit scheme yields the following set of equations (see Figure e):

$$\alpha^j_{i+1}\, c_{i+1,j-1} + \beta^j_{i+1}\, c_{i+1,j} + \gamma^j_{i+1}\, c_{i+1,j+1} = \alpha^j_i\, c_{i,j-1} + \beta^j_i\, c_{i,j} + \gamma^j_i\, c_{i,j+1} \tag{4.14}$$

in which:

$$\alpha^j_{i+1} = \frac{\Theta}{2\Delta z''} \{- \lambda_{i+1,j} + \frac{\mu_{i+1,j}}{\Delta z''} (\varepsilon_{s,i+1,j}\, f_{i+1,j} + \varepsilon_{s,i+1,j-1}\, f_{i+1,j-1})\} \tag{4.15}$$

$$\beta^j_{i+1} = - \{\frac{1}{\Delta x''} + \frac{\Theta\, \mu_{i+1,j}}{2(\Delta z'')^2} (\varepsilon_{s,i+1,j+1}\, f_{i+1,j+1} + 2\, \varepsilon_{s,i+1,j}\, f_{i+1,j} + \varepsilon_{s,i+1,j-1}\, f_{i+1,j-1})\} \tag{4.16}$$

$$\gamma^j_{i+1} = \frac{\Theta}{2\Delta z''} \{\lambda_{i+1,j} + \frac{\mu_{i+1,j}}{\Delta z''} (\varepsilon_{s,i+1,j+1}\, f_{i+1,j+1} + \varepsilon_{s,i+1,j}\, f_{i+1,j})\} \tag{4.17}$$

$$\alpha^j_i = \frac{1-\Theta}{2\Delta z''} \{\lambda_{i,j} - \frac{\mu_{i,j}}{\Delta z''} (\varepsilon_{s,i,j}\, f_{i,j} + \varepsilon_{s,i,j-1}\, f_{i,j-1})\} \tag{4.18}$$

$$\beta^j_i = \{- \frac{1}{\Delta x''} + (1-\Theta) \frac{\mu_{i,j}}{2(\Delta z'')^2} (\varepsilon_{s,i,j+1}\, f_{i,j+1} + 2\, \varepsilon_{s,i,j}\, f_{i,j} + \varepsilon_{s,i,j-1}\, f_{i,j-1})\} \tag{4.19}$$

$$\gamma^j_i = - \frac{(1-\Theta)}{2\Delta z''} \{\lambda_{i,j} + \frac{\mu_{i,j}}{\Delta z''} (\varepsilon_{s,i,j+1}\, f_{i,j+1} + \varepsilon_{s,i,j}\, f_{i,j})\} \tag{4.20}$$

Θ = implicity factor

$i = 0,1,2,....$

$j = 1,2,3,....,k-1$

Together with the boundary conditions, this set of equations can be solved yielding the concentration field.

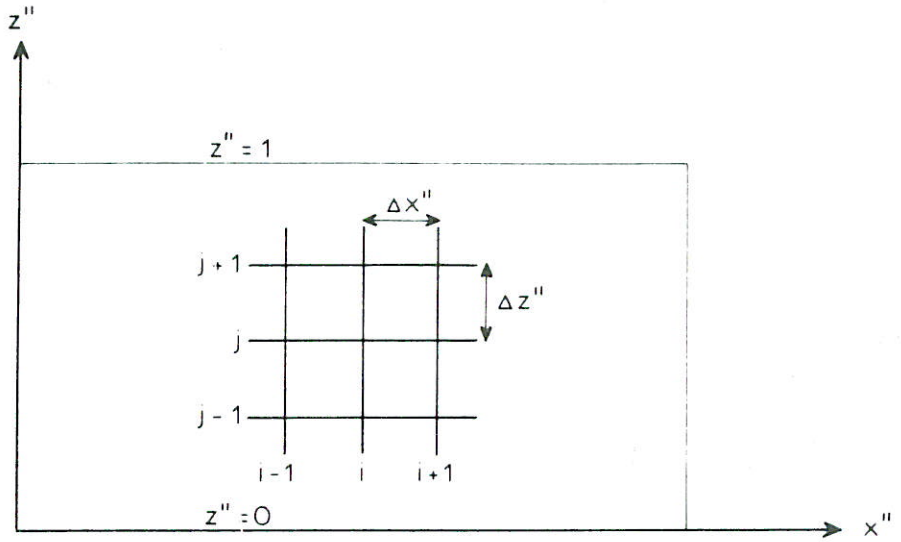

Figure e

Finally, some remarks must be made about the numerical modelling of the term $\partial z'/\partial x$ in Equation (4.11). Test computations have shown that a forward, central or backward discretisation of this term does influence the vertical distribution of the concentrations at sharp transitions in the bed.
At this stage the most stable solution is obtained for a numerical scheme with forward differences. To improve the solution method, further reasearch is needed. Possibly a more simple transformation method or another numerical method (finite elements) may be useful.

4.2 Solution method for sediment-continuity equation

Bed level changes are described by the continuity equation for the total sediment transport:

$$\frac{\partial z_b}{\partial t} + \frac{1}{(1-p)\ \rho_s}\ \frac{\partial s}{\partial x} = 0 \qquad (4.21)$$

For the computation of the new bed level at time $t+\Delta t$ from the known bed level at time t, the following numerical scheme is used:

$$z_{b,i}^{t+\Delta t} = z_{b,i}^{t} - \frac{\Delta t}{2\ (1-p)\ \rho_s\ \Delta x}\ (s_{i+1}^{t} - s_{i-1}^{t}) + \tfrac{1}{2}\ \alpha\ (z_{b,i+1}^{t} - 2\ z_{b,i}^{t} + z_{b,i-1}^{t}) \qquad (4.22)$$

in which:

z_b	=	bed level	(m)
Δt	=	time step	(s)
Δx	=	longitudinal space step	(m)
p	=	porosity of the bed material	(-)
s	=	total load transport	(kg/sm)
ρ_s	=	density of sediment	(kg/m^3)

The α-factor in Equation (4.22) determines to what extent the bed level of the surrounding points of $z_{b,i}$ are taken into account for the computation of the new bed level $z_{b,i}$ at time $t+\Delta t$.
This method causes numerical smoothing at sharp transitions in the bed level profile (steep-sided trenches), but numerical inaccuracies can be minimized by selecting the proper longitudinal space step (Δx), time step (Δt) and migration velocity of a small disturbance at the bed. A detailed analysis of this so-called "pseudo viscosity" method can be found in [6], [14].

The entire computational procedure can be described thus:

1 Compute the longitudinal and vertical flow velocities for a given bed level;
2 compute the sediment concentrations;
3 compute the suspended load and the bed load transport for each vertical; and
4 compute the new bed level.

5 Verification for flume tests

5.1 General outline

To verify the mathematical model computational results were compared with laboratory measurements concerning the siltation in a trench, using three tests with different trench dimensions.
The trench dimensions and flow conditions for each test are given in Figure 3. The only variable was the geometry of the trench; the hydraulic conditions upstream of the trench were not changed. Consequently, also the siltation efficiency of a trench in relation to its geometry can be evaluated.
The tests were done in a laboratory flume with a "flow-through" system. The flume has a width of 0.5 m, a depth of 0.7 m and a length of about 30 m. In the flume a sediment bed with a thickness of 0.2 m was installed. To ensure equilibrium conditions, sand was supplied at a constant rate at the upstream side of the flume, and the discharge was regulated by means of a circular weir.
Each test consisted of:

- The determination of the equilibrium sediment transport and bed level at the governing flow conditions;
- the measurement of the flow parameters in equilibrium conditions;
- the measurement of flow velocities and sediment concentrations in the trench at the initial stage; and
- the determination of the bed level in the trench as a function of time.

To apply the mathematical model a number of controlling parameters must be determined. Parameters which can be determined from measurements are the upstream flow velocity ($\bar{u}_0$) and depth (h_0), the suspended load transport ($s_{s,0}$), and the particle fall velocity (w_s). The maximum value of the diffusion coefficient was evaluated on basis of curve fitting of measured and computed sediment concentrations in equilibrium conditions (upstream of the trench).

Computed flow velocity profiles, sediment concentration profiles and bed level profiles are compared with measured profiles, while a detailed sensitivity analysis with respect to the influence of the controlling parameters and boundary conditions is also given. Finally, the influence of the trench geometry in relation to the siltation efficiency is considered.

5.2 Hydraulic conditions

Flow data

Flow velocities were measured with an Ott-current meter, and average flow velocity was about 0.5 m/s. The flow depth, defined as the distance between the average bed level and the water surface was about 0.40 m. The bed level was recorded continuously in longitudinal direction by means of an automatic sounding system.

Sediment data

Bed sediment

The initial sediment bed consisted of fine sand with diameters: D_{10} = 115 µm, D_{50} = 160 µm and D_{90} = 195 µm, but due to segregation, the composition of the bed material became somewhat coarser during the tests. The longitudinal distribution of the bed material size is shown in Figure 4.

Total load

To ensure equilibrium conditions (no scour or siltation) upstream of the trench, sand was supplied at a constant rate of 0.040 kg/sm. This sediment had the same composition as the initial bed sediment.

Suspended load

The suspended load transport was determined from concentration and flow velocity measurements and the sand concentrations by taking water-sediment samples in the centre line of the flume with a siphon sampler, which consisted of a hose run connected to an intake nozzle (Photograph 1). In a vertical direction, 10 measurements were made simultaneously. The intake velocity was about 0.8 m/s, which was just sufficient to transport the sediment particles through the hose without settlement (visual observation). The separation of water and sediment was done by means of filtration with nylon filter material (50 µm). The sand concentrations were determined as the ratio of the dry weight of the sediment particles and the volume (= 10 liters) of the water sample.
From the measured sand concentrations and flow velocities in the centre line, the suspended load transport was estimated to be in the range of 0.030 $\pm$ 0.006 kg/sm, and the total load transport was 0.040 kg/sm (sand feed). Consequently, the contribution of the suspended load transport to the total load transport was in the range of 0.6 - 0.9.

The relation between the suspended load transport and the average flow velocity necessary to compute the equilibrium concentrations at the bed boundary level is represented by a simple exponential function:

$$s_{s,e} = a\,\bar{u}^{b} \qquad (5.1)$$

in which:

$s_{s,e}$ = suspended load transport (in equilibrium conditions) (kg/sm)
$\bar{u}$ = depth-averaged flow velocity (m/s)

Earlier measurements [6] indicated an exponent of 5.5. The a-coefficient was determined from the condition:

$s_{s,e} = 0.030$ kg/sm, for $\bar{u} = 0.5$ m/s.

Bed load

As the suspended load transport was about 0.030 kg/sm, the bed load transport must have been about 0.010 kg/sm. To compute bed-level changes due to changes in the bed load transport, the bed load transport was related to the average flow velocity. The exponent was supposed to have a value of 3, which is a generally accepted value for bed load formulas. The a-coefficient was determined from the condition:

$s_{b,e} = 0.010$ kg/sm, for $\bar{u} = 0.5$ m/s.

Particle fall velocity

Based on sieve analysis of suspended sediment samples, the size (D_{50}) of the suspended sediment particles was found to vary from 120 μm (near the water surface) to 150 μm (near the bed). The vertical distribution is shown in Figure 4. For a water temperature of about 15°C, the representative particle fall velocity will be in the range of 0.011 - 0.015 m/s.

Bed forms and roughness

During the test with equilibrium flow, small-scale ripples were formed on the bed, the ripple length varying from 0.10 - 0.25 m, and the height from 0.015 - 0.035 m.

The equivalent sand roughness of Nikuradse was computed from the water surface slope, the average flow velocity and the depth resulting in a value of 0.025 m.

Side-wall effects were taken into account according to the Vanoni-Brooks method [13].

5.3 Estimation of maximum diffusion coefficient

An accurate prediction of the siltation level in the trench can only be made if the value and distribution of the sediment concentrations at the upstream boundary are represented correctly.
Assuming equilibrium conditions at the upstream boundary, the vertical concentration distribution is determined by Equations (3.18) and (3.19) in which the particle fall velocity and the maximum diffusion coefficient are of essential importance.
Assuming a known particle fall velocity, a good estimate of the maximum diffusion coefficient for the sediment particles can be obtained by the combining of measured and computed concentrations.

According to Equation (3.12) and assuming $h_0 = 0.4$, $u_* = 0.033 - 0.049$ m/s, the maximum diffusion coefficient $\hat{\varepsilon}_{m,0}$ is in the range of 0.0013 - 0.0020 m^2/s. According to Equation (3.15), which is based on the experiments of Coleman, the maximum diffusion coefficient $\hat{\varepsilon}_{s,0}$ is in the range of 0.0014 - 0.0021 m^2/s. On the basis of these results, the maximum diffusion coefficient is supposed to be in the range of 0.0013 - 0.0021 m^2/s
For a particle fall velocity of 0.013 m/s, the best fit was obtained for $\hat{\varepsilon}_{s,0}$ = 0.00165 m^2/s (Figure 5); this is the value used in the mathematical model.

5.4 Input data

The computations of the sediment concentrations, longitudinal sediment transport and bed levels for trenches T1, T2 and T3 were made with the following data:

		T1	T2	T3
suspended load	($s_{s,0}$)	0.030	0.030	0.030
total load	($s_{t,0}$)	0.040	0.040	0.040
flow velocity	($\bar{u}_0$)	0.50	0.51	0.51
flow depth	(h_0)	0.40	0.39	0.39
maximum diffusion coefficient	($\hat{\varepsilon}_{s,0}$)	0.00165	0.00165	0.00165
particle fall velocity	(w_s)	0.013	0.013	0.013
equivalent sand roughness	(k_s)	0.025	0.025	0.025
porosity of bed sediment	(p)	0.4	0.4	0.4
density of sediment	(ρ_s)	2650	2650	2650
density of water	(ρ_w)	1000	1000	1000
water temperature	(T)	15	18	15
boundary level above bed	(z_a)	0.0125	0.0125	0.0125
longitudinal space step	(Δx)	0.25	0.25	0.25
vertical space step	(Δz)	variable (10 grid points	variable (10 grid points)	variable (10 grid points
time step	(Δt)	900	900	900

5.5 Measured and computed flow velocities, sediment concentrations, sediment transport and bed levels

T1

Flow velocities

The trench in Test T1 had steep side-slopes (1:3). At the initial state flow separation did occur. Measured and computed flow velocities are given in Figures 6, 7 and 8. The flow velocities in the recirculation zone and the vertical flow velocities were too low to be measured. It should be noted that the computed vertical flow velocities are represented on a ten times larger scale. As regards profiles 1...5 (deceleration zone), the agreement is reasonable. In the relaxation and acceleration zones (Profiles 6...8) relatively large deviations occur, and particularly near the bed are the computed velocities too low.

Finally, it must be stressed that all measurements were made in the centre line of the flume, while the computations are based on an average discharge per unit width. As a result the measured values will generally be somewhat higher (see Profile 1). If the measured flow velocity profile at the upstream boundary had been taken as a boundary condition in the computations, the overall agreement would have been better [3].

Sediment concentrations and transport

Computed and measured concentrations are shown in Figures 6, 7 and 8, and the longitudinal distribution of the maximum diffusion coefficient used to compute the concentration field is given in Figure 9. In a vertical direction a parabolic-constant distribution was used. Comparison of measured and computed concentration profiles in the deceleration zone (Profiles 2...5) show large deviations in the lower part of the profiles, with the measured values being much higher than the computed values. The form of the concentration profiles is represented satisfactorily. The high concentrations near the bed may be generated by a relatively intensive diffusion mechanism which cannot be represented by the parabolic-constant distribution used in the model. Also, the assumption of a zero bed-concentration gradient at the dividing streamline expressing no re-entrainment of sediment may be too crude.

In the middle part of the trench the agreement between measured and computed concentrations is considerably better (Profile 6), although close to the bed large deviations still exist.

In the acceleration zone the computed near-bed concentrations are somewhat too low. This is probably due to the fact that the relatively high shear stresses and flow velocities generated at the steep slope are not fully represented by the model (Profile 7).

Downstream of the trench the flow velocities and concentrations are computed assuming equilibrium conditions. Measured values in Profile 8 (Figure 8) indicate that this assumption is not correct. Both the measured velocities and concentrations near the bed are much higher than the computed values. Very close to the bed sediment concentrations of about 3000 ppm were measured.

The longitudinal distribution of the sediment transport is shown in Figure 9. Undulations in this distribution at the (sharp) transition from the upstream section to the trench section due to a non-optimal numerical solution method have been smoothed.

In the deceleration zone a rapid decrease in the total load transport can be observed which is mainly caused by changes in the bed load transport. The measured suspended load transport in this zone is somewhat higher than the computed values, but in the middle part of the trench the agreement between measured and computed values is quite good.

In the acceleration zone a remarkable phenomenon is the rapid increase of the suspended load transport, probably because the relatively high longitudinal and vertical flow velocities close to the bed result in a relatively high entrainment rate. At the downstream end of the trench the transport capacity of the flow is even exceeded. This trend is also represented by the model, though absolute values deviate considerably.
The largest reduction of the total load transport (= siltation efficiency) at the initial stage is about 60%.

Bed levels

Figure 10 represents measured and computed bed levels at 7.5 and 15.0 hours. Except in the acceleration zone the agreement between measured and computed values is remarkably good. The large erosion in the acceleration zone is not represented by the model, firstly because the high flow velocities near the bed are not represented and secondly because the applied bed boundary condition ($c_b = c_{b,e}$) leads to an underestimation of the bed concentration in this part of the trench (Figure 8). This last deficiency may be eliminated by applying an entrainment function based on local flow parameters. Much theoretical and experimental research will undoubtedly be needed to improve the bed boundary condition.
Finally, some remarks must be made about numerical inaccuracies in the bed level computation. Particularly on the side slopes the inaccuracy may be relatively high because the longitudinal space step (0.25 m) is relatively large in comparison with the length of the side slope (0.50 m). However, a smaller space step is not always an appropriate solution, because mostly also a smaller time step is needed resulting in more computational steps to cover the same time period. As more computations lead to more inaccuracy, the overall inaccuracy may be in the same order compared with a computation on base of a larger space step, while the computer costs will definitely be higher.

T2

Flow velocities

Measured and computed flow velocities are given in Figures 11 and 12.
Except in Profile 3, the longitudinal flow velocities are represented satisfactorily. Flow separation was not observed.

Sediment concentrations and transport

The maximum diffusion coefficient used to compute the concentrations is described by Equations (3.14) and (3.15), resulting in an approximately constant value in a longitudinal direction ($\hat{\varepsilon}_{s,x} \approx \hat{\varepsilon}_{s,0}$).
Measured and computed concentration profiles are shown in Figures 11 and 12. The agreement between measured and computed values is remarkably good except for Profile 3, where considerably large deviations can be observed.
The longitudinal distribution of the computed sediment transport is given in Figure 13, showing good agreement with measured values.

Bed levels

Measured and computed bed level profiles after 7.5 and 15.0 hours are shown in Figure 14. Particularly after 15.0 hours the computed siltation level shows good agreement with the measurements. As in Test T1, the computed erosion level is systematically less than the measured values.

T3

Flow velocities

Flow velocities are shown in Figures 15 and 16. The largest deviations between measured and computed values occur in the near-bed region; see, for example, Profiles 3 and 5.
As already stated, the measurements were made in the centre line of the flume, while the computed velocities are based on an average discharge per unit width.

Sediment concentration and transport

Measured and computed concentrations are represented in Figures 15 and 16. In the near-bed region of the deceleration zone the measured profiles show high concentrations and relatively large gradients, expressing that a zero concentration gradient as bed boundary condition is not correct in the case of a trench with relatively gentle slopes. In the acceleration zone, where an equilibrium bed concentration is used, the agreement between measured and computed concentration profiles is much better. Downstream of the trench very high concentrations were measured in the near-bed region.
Measured and computed sediment transport are shown in Figure 17. In all zones of the trench the measured suspended load is larger than the computed values, while downstream of the trench the suspended load even exceeds the transport capacity of the flow.

Bed levels

Measured and computed bed level profiles after 7.5 and 15.0 hours are represented in Figure 18. The measurements show a relatively flat upstream sideslope, which is not fully represented by the model. The predicted siltation level in the middle part of the trench shows good agreement with the measured level, particularly after 15.0 hours.
As in Tests T1 and T2, the computed erosion level is less than the measured level.

Summarizing, it can be concluded that, apart from the acceleration zone, the flow velocity profiles are predicted satisfactorily. In the acceleration zone the predicted flow velocities near the bed are somewhat too low.
The prediction of the concentration field is less satisfactory. Particularly, does the application of a zero bed-concentration gradient in the deceleration zone seem to be too crude. Improvement of the bed boundary condition may be obtained by applying an entrainment function which relates the entrainment (pick-up) of sediment from the bed to local flow parameters. However, much research will be needed to develop such a function.
The prediction of the overall siltation rate in the trench is quite good and is not very much influenced by inaccurate predictions of local concentrations in some parts of the trench.
The predicted erosion levels are systematically too low, which is caused by an underestimation of the longitudinal flow velocities and the sediment concentrations in the near-bed region of the acceleration zone.
Finally, it must be stressed that the results have been obtained on base of measured input data without using additional calibration procedures.

5.6 Sensitivity analysis

Longitudinal distribution of the maximum diffusion coefficient

In the case of non-uniform flow conditions the vertical and longitudinal distribution of the diffusion coefficient is not known. To estimate the influence of the maximum diffusion coefficient ($\hat{\varepsilon}_{s,x}$), the concentration profiles and suspended load transport were also computed for increased $\hat{\varepsilon}_{s,x}$ values, with the upstream value ($\hat{\varepsilon}_{s,0}$) remaining constant. The trench of Test T1 was used for this analysis because the diffusion coefficient, expressing the turbulent mixing process, is supposed to be largest in a steep-sided trench due to flow separation and large vertical velocity gradients. The "normal" longitudinal distribution of the maximum diffusion coefficient for trench T1 is given in Figure 9. The maximum value of the relative diffusion coefficient is approximately 1.4. For a value of 2.8 there was no significant influence on the computed concentration profiles and suspended load (not shown).

In a vertical direction the distribution of the diffusion coefficient remained parabolic-constant. Nor were the results changed by using a vertically constant distribution in the deceleration zone only.

From this analysis it can be concluded that the upward sediment transport by diffusion in the deceleration zone of the trench is of minor importance. Apparently the siltation process is dominated by the particle fall velocity and the downward orientated vertical flow velocities.

Suspended load

The influence of the contribution of the suspended load to the total load ($s_{s,0}/s_{t,0}$) on the longitudinal distribution of the computed total load for Test T2 is given in Figure 19. The main influence can be observed in the deceleration zone of the trench, which can be explained by considering that in the case of a relatively small transport ratio ($s_{s,0}/s_{t,0} = 0.6$) a relatively large amount of sediment is transported as bed load which is supposed to react directly to changed flow conditions.

As regards the siltation in the trench, the steepness and the migration velocity of the upstream side slope will be relatively high for a small transport ratio (Figure 20). On the other hand, the siltation level in the middle part of the trench will be less for a small transport ratio because of the relatively large contribution of the bed load. This process can be understood more easily

by considering the siltation due to bed load only. In that case the trench will migrate in a downstream direction only with minor changes in geometry.

Particle fall velocity

The representative particle fall velocity was found to be in the range of 0.011 - 0.015 m/s. The influence of the particle fall velocity on the computed suspended load and bed level in trench T2 is shown in Figures 21 and 22. The main influence can be observed on the upstream side slope of the trench. To understand this effect, it must be realized that a change in particle fall velocity modifies the form of the initial concentration profile (boundary condition). For example, a larger particle fall velocity results in a steeper concentration profile with higher concentrations near the bed and lower concentrations near the water surface. Consequently, the "average" settling length will decrease, which explains the large siltation and migration velocity at the upstream side slope.

Maximum diffusion coefficient at the upstream boundary

At the upstream side of the trench, the maximum diffusion coefficient ($\hat{\varepsilon}_{s,0}$) is estimated to be in the range of 0.0012 - 0.0021 m^2/s.
Figures 23 and 24 show the influence of the $\hat{\varepsilon}_{s,0}$ value on the computed suspended load transport and the bed level for Test T2. In a longitudinal direction the $\hat{\varepsilon}_s$ value remained approximately constant. In a vertical direction a parabolic-constant distribution was used. As can be observed, the influence of the $\hat{\varepsilon}_{s,0}$ value is largest on the upstream slope of the trench. Like the particle fall velocity, the maximum diffusion coefficient modifies the initial concentration profile (Figure 5). For example, a small $\hat{\varepsilon}_{s,0}$ value causes a relatively large sediment transport just above the bed. Consequently, the "average" settling length will be relatively small, which explains the increased siltation on the upstream side slope for a small $\hat{\varepsilon}_{s,0}$ value.
The best agreement between measured and computed bed levels after 15.0 hours is observed for $\hat{\varepsilon}_{s,0} = \hat{\varepsilon}_{m,0} = 0.00165$ m^2/s.

Bed boundary condition

In the case of a steep-sided trench the diffusion-convection equayion is solved for a combined bed boundary condition: a zero bed-concentration gradient in the sedimentation zone and an equilibrium bed concentration in the erosion zone. To

estimate the influence of the bed boundary condition, the bed concentration and suspended load were also computed for an equilibrium bed concentration only. The results for Test T2 are given in Figure 25.
Although it is remarkable that both methods only cause minor differences, this result has no general significance because the bed concentration computed on base of the equilibrium bed concentration method is greatly dependent on the character of the formula used for the transport capacity As the applied relation between the transport capacity and the average flow velocity is a fifth power function, the reduced flow velocity in the trench results in a relatively low transport capacity. Consequently, the bed concentration computed from this transport capacity will also be relatively low.
Measured (bed) concentrations at 0.01 m above the bed indicate that the computed bed concentrations are somewhat too low.

Flow velocity field

To analyse the influence of the flow field, the suspended load transport for Test T1 (steep-sided trench) was also computed using logarithmic velocity profiles. As bed boundary condition the equilibrium bed concentration method was used.
It must be remarked that in the case of logarithmic velocity profiles the bed boundary condition is applied at a level close to the bed, while for velocity profiles with reversed flow (semi-empiric model) the bed boundary condition is applied at the dividing stream line. The latter method results in concentration profiles with higher concentrations in the deceleration zone because the effective flow depth is reduced by the presence of a zone with reversed flow, resulting in a reduced siltation efficiency. Consequently, the suspended load transport is considerably higher than the corresponding values computed for logarithmic velocity profiles (Figure 26).
The best agreement with the measured suspended load is obtained for the flow velocity field according to the semi-empiric model, although the large values in the erosion zone are not predicted. As already stated, the use of an entrainment function in the erosion zone may be advantageous.
Although in the initial stage the deviations may be large, the consequences for the long-term predictions remain relatively small. For example after 7.5 hours the differences in the suspended load for both flow velocity fields are already negligibly small. The bed levels after 7.5 and 15.0 hours also show minor deviations (Figure 27).

5.7 Siltation efficiency

In the laboratory experiments the only variable was the geometry of the trench; the hydraulic conditions upstream of the trench were not changed. Consequently, the measurements can be used to relate the siltation efficiency to the trench geometry.

The siltation efficiency (E) is defined as the ratio of the reduction (Δs_t) in the total sediment transport caused by the trench and the initial value ($s_{t,0}$) of the total sediment transport (Figure f).

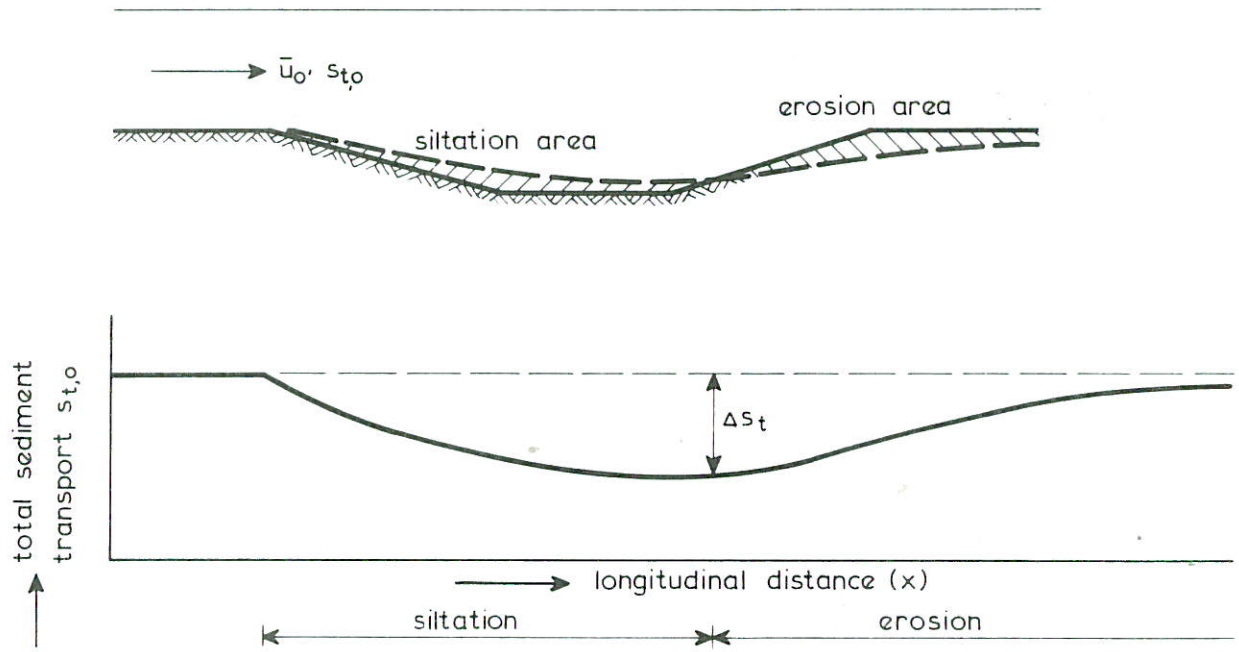

Figure f

$$E = \frac{\Delta s_t}{s_{t,0}} \qquad (5.2)$$

in which:

Δs_t = reduction in the total sediment transport (kg/sm)

$s_{t,0}$ = initial total sediment transport (kg/sm)

In the mathematical model the reduction in the total sediment transport is obtained as a computational result. For laboratory or field data, however, this value cannot be determined easily, so in that case the reduction in sediment transport can be determined indirectly by:

$$\Delta s_t = \frac{(1 - p)\ \rho_s\ A}{\Delta t} \qquad (5.3)$$

in which:

p	= porosity of the bed	(-)
ρ_s	= density of sediment	(kg/m^3)
A	= siltation area for a small time interval Δt	(m^3)
Δt	= time interval	(s)

Computed values of the siltation efficiency, for both the mathematical model and the laboratory experiments, are presented as a function of relative depth in Figure 28. Although the differences are relatively small, the mathematical model results indicate that the largest amount of sediment will be trapped by trench T1 with the largest bottom width and the smallest top width, while the smallest amount of sediment will be caught by trench T2 with the smallest bottom and top width. Due to the scatter in the values for the experiments, the small relative differences in the siltation efficiency computed by the mathematical model for trenches T1, T2 and T3 cannot be confirmed clearly.

6 Verification for a testpit in the Oosterschelde estuary

6.1 General outline

In the entrance of the Oosterschelde Estuary a large storm surge barrier will be built, with large openings which will be closed by iron lift gates in case of a major storm. The piers on both sides of the openings will be founded in a dredged trench (perpendicular to the flow direction). To estimate the siltation in the trench, a test pit was dredged in the autumn of 1977 in the Schaar van Roggeplaat, one of the three main channels in the entrance to the estuary (Figure 29).

The depth of the test pit was about 4.5 m (Figure 35), while the local flow depth outside the trench was about 21.5 m with respect to the mean sea level. The test pit had a bottom width (in the flow direction) of about 80 m and a top width of about 200 m. The slopes of the trench varied from 1:6 to 1:8. Outside the trench the bed of the channel was protected with a sand-tight mattress supplemented by concrete blocks. The total length of the mattress was about 400 m. (on both sides), and soundings have indicated that the mattress and the blocks have been covered by a layer of sediment.
After the dredging works the test pit was sounded regularly, while upstream of the pit flow velocity and concentration measurements were carried out several times and bed samples were also taken.

6.2 Tidal conditions

For the sake of simplicity, the neap-spring tidal cycle is represented by an average tide, although the average tide is not representative for the average sediment transport during the neap-spring cycle because the sediment transport is not linearly dependent on the flow velocity.
To account for the relative higher contribution of the flow velocities during spring tide to the total amount of sediment transport in a neap-spring tidal cycle and for unfavourable meteorological influences the flow velocities must be increased.
The value of this increase can be related to the ratio (α) of the maximum flow velocities during spring tide and the average tide, the standard deviation (σ) of the maximum flow velocity of the average tide due to meteorological influen-

ces only, and the power (b) of the relation between the sediment transport and the flow velocity [7].
For $\alpha = 1.15$, $\sigma = 0.15$ and $b = 4$, the flow velocities of the average tide must be increased by about 4%, resulting in the (so called) design tide for the sediment transport. This tide, shown in Figure 30, is schematized in 4 quasi-stationary flow periods of 2 hours each, and the flow velocities of these periods are computed in such a way that the amount of sediment transported in the full ebb and flood periods of the design tide equals the amount of sediment transported in the 8-hour period of the schematized tide.
The tidal range of the average tide is shown in Figure 31.

6.3 Sediment Transport

Suspended load

Detailed knowledge of the relation between suspended load transport and flow velocity was obtained by means of flow velocity and concentration measurements upstream of the testpit [8].
On base of these measurements the relation between the suspended load transport and the average flow velocity was found to depend on the state of the tide. Detailed information is given in [8].
For accelerating flow:

$$s_s = 0.11\ \bar{u}^{5.5} \qquad \text{(kg/sm)} \qquad (6.1)$$

For decelerating flow:

$$s_s = 0.19\ \bar{u}^{2.9} \qquad \text{(kg/sm)} \qquad (6.2)$$

These formulas were used to determine the (equilibrium) concentration profiles of the upstream boundary and that at the bed boundary. At the upstream boundary the concentration profile was assumed (based on measurements) to be the equilibrium profile in any state of the tide.

Bed load

The bed load transport was evaluated from regular echo-soundings of the bed forms. For this purpose a special anchored vessel was used on which a movable echo-sounding system was installed. Most of the measurements were made in the Room-

pot, the largest channel in the entrance to the estuary, in the period 5-26 February, 1976. During tidal periods of 13 hours the bed configuration was sounded over a length of about 30 m, while simultaneously the flow velocity at 0.2, 0.7 and 1.0 m above the bed was measured.
From these measurements the following bed load formula was derived [9]:

$$s_b = 0.06\ \bar{u}^3 \qquad \text{(kg/sm)} \qquad (6.3)$$

Because the flow depth was relatively large in comparison with the height of the bed forms, Equation (6.3) is not supposed to be very accurate. Another drawback is formed by the fact that no measurements were made in the direct surroundings of the test pit. Furthermore, the local bed load may be influenced by the presence of the sand-tight mattress.
For a flow velocity of about 1.0 m/s, the bed load transport is approximately 25-30% of the total load transport which seems to be reasonable value for medium-fine sediment.

Bed sediment

Just after the dredging of the test pit, a number of bed samples in and outside the test pit were taken by means of a scrab, and the size composition was determined by means of sieve analysis.
Outside the test pit the D_{10} varied from 210-240 μm, the D_{50} from 295-325 μm, and the D_{90} from 400-450 μm, while in the test pit these values were 170-250 μm, 250-235 μm and 330-430 μm respectively. On the average, the bed sediment in the test pit was slightly finer at the initial state [8].
After a siltation period of two months another set of bed samples were taken by means of a free-fall instrument which penetrated into the bed, and again size analysis was done by means of sieving. The size composition of the samples taken in the test pit was about the same as that of the samples outside the test pit, indicating that the siltation had been caused mainly by sediment particles transported close to the bed.

Particle fall velocity

Suspended sediment samples were used to determine the size of the particles by means of sieving and settling experiments. Based on these tests, the D_{50} of the suspended sediment particles was estimated to vary from 150-200 μm. Taking into account an average water temperature of 5°C (winter period), the representative particle fall velocity was supposed to be in the range of 0.012 - 0.0185 m/s.

Detailed information about the size of the sediment in suspension is given in [8].

Bed forms and roughness

The bed forms outside the test pit were determined by means of echo soundings. The average height was about 0.35 m, and the average length was approximately 10 m. The hydraulic roughness of the bed can be related to the dimensions of the bed forms by means of a simple function [10]:

$$\frac{k_s}{k} = 1.75 + 0.75 \log \left(\frac{k}{l}\right) \qquad (6.4)$$

in which:

k_s = equivalent roughness of Nikuradse (m)

k = average height of the bed forms (m)

l = average length of the bed forms (m)

Using the above-mentioned dimensions of the bed forms, an equivalent roughness of 0.25 m is obtained, a value which is also supposed to be valid for the bed in the test pit. The bed boundary condition is applied at a distance above the bed equal to half the equivalent roughness of Nikuradse (= 0.25 m).

6.4 Estimation of the maximum diffusion coefficient

An accurate prediction of the siltation level in the trench can only be obtained if the vertical distribution of the sand concentrations at the upstream boundary are represented correctly. From Equations (3.18) and (3.19) it can be concluded that the particle fall velocity and the maximum diffusion coefficient are of essential importance.
A good estimate of the maximum diffusion coefficient can be obtained by the curve fitting of measured and computed sand concentrations for equilibrium conditions, provided the representative particle fall velocity is known.

According to Equation (3.12), and assuming a flow velocity of about 1.10 m/s, a flow depth of 22.0 m and an equivalent roughness of 0.25 m, the maximum diffusion coefficient for momentum is about 0.14 m^2/s. According to Equation (3.15) based on the experiments of Coleman, the maximum diffusion coefficient for the sediment particles is about 0.20 m^2/s. On base of these results, the maximum

diffusion coefficient is supposed to be in the range of 0.14 - 0.20 m^2/s.

Assuming a particle fall velocity of 0.015 m/s (measurements), the best agreement between measured and computed concentrations can be observed for a maximum diffusion coefficient of 0.14 m^2/s according to Equation (3.12), (Figures 32 and 33). Based on this, Equation (3.12) is used to describe the upstream maximum diffusion coefficient. The measured concentrations in Figures 32 and 33 represent the average value of the period with maximum flow, while also the smallest and largest values are indicated.

6.5 Input data

The computations of the concentration profiles, longitudinal sediment transport and bed level profiles for the test pit in the Oosterschelde Estuary were done with the following data:

Ebb :	flow velocity	$(\bar{u}_0)$	= 1.15, 1,05	(m/s)
	flow depth	(h_0)	= 22.0 , 20.7	(m)
	maximum diffusion coefficient	$(\hat{\varepsilon}_{s,0})$	= 0.14, 0.13	(m^2/s)
Flood:	flow velocity	$(\bar{u}_0)$	= 0.70, 1.10	(m/s)
	flow depth	(h_0)	= 20.85, 22,05	(m)
	maximum diffusion coefficient	$(\hat{\varepsilon}_{s,0})$	= 0.10, 0.14	(m^2/s)
	particle fall velocity	(w_s)	= 0.015	(m/s)
	density of sediment	(ρ_s)	= 2650	(kg/m^3)
	equivalent roughness	(k_s)	= 0.25	(m)
	porosity of the bed	(p)	= 0.4	(-)
	water temperature	(T)	= 5	(^oC)
	bed-boundary level	(z_a)	= 0.125	(m)
	vertical space step	(Δz)	= variable (10 grid points)	
	time step	(Δt)	= 7200	(s)

transport capacity: $s_s = 0.11\ \bar{u}^{5.5}$ kg/sm (accelerating flow)

$s_s = 0.19\ \bar{u}^{2.9}$ kg/sm (decelerating flow)

$s_b = 0.06\ \bar{u}^{3}$ kg/sm

6.6 Measured and computed flow velocities, sediment concentrations and bed levels

The longitudinal and vertical flow velocities (ebb), predicted by the semi-empiric model, are shown in Figure 34, although in this the vertical flow velocities are indicated on a 10 times larger scale.
The agreement between computed and measured values is satisfactory. For comparison the longitudinal flow velocities in the trench were also computed from the logarithmic distribution, but this resulted in less good agreement with measured values.
Figure 34 also presents computed concentration profiles. The longitudinal distribution of the maximum diffusion coefficient (Equations (3.20), (3.21) and (3.22)) used to compute the concentration field at the initial stage is given as curve A in Figure 36.
Computed and measured bed level profiles are shown in Figure 35. Due to the asymmetrical form of the tide, the siltation level at the eastern slope is relatively large. The agreement between measured and computed bed levels after 180 days is remarkably good, especially when is considered that the results are obtained without using additional calibration.

6.7 Sensitivity analysis

Longitudinal distribution of the maximum diffusion coefficient

To analyse the influence of variations in the longitudinal value of the maximum diffusion coefficient, the longitudinal suspended load transport was also computed for higher (curve B in Figure 36) and lower (curve C) values of the diffusion coefficient. The value of the maximum diffusion coefficient at the upstream boundary was kept constant.
As can be observed in Figure 36, the influence is relatively small in the siltation zone and relatively large in the erosion zone. An explanation may be the minor role of the diffusion process in the siltation zone because the upward transport by diffusion is relatively low due to small concentration gradients caused by the zero bed-concentration gradient condition.
In the erosion zone, where an equilibrium bed concentration is applied, the concentration gradients are considerably larger. Consequently, an increase in the diffusion coefficient will lead to an increase of the concentrations and hence to an increase of the suspended load transport. Downstream of the trench, the

suspended load transport has a (different) constant value for each curve because no erosion is supposed to take place (sand-tight mattress). In the case of (normal) erosion downstream of the trench, the suspended load transport had become equal to the downstream transport capacity for all three curves. The influence of variations in the longitudinal values of the maximum diffusion coefficient on the computed bed level after 180 days was relatively small and is, therefore, not shown.

Maximum diffusion coefficient at the upstream boundary

The maximum diffusion coefficient in uniform conditions based on the experiments of Coleman (Equation (3.15)) is about 40% higher than the diffusion coefficient for momentum (Equation (3.12)). Both values were used to predict the siltation level in the trench so that the influence of a change in the $\hat{\varepsilon}_{s,0}$-value can be considered.

The results are given in Figure 37, showing a significant lower siltation level for an increased $\hat{\varepsilon}_{s,0}$ value. This behaviour can be explained by considering the influence of the $\hat{\varepsilon}_{s,0}$ value on the form of the concentration profile. As an increased $\hat{\varepsilon}_{s,0}$ value modifies the concentration profile into a more uniform profile, the "average" settling length will be increased, resulting in less siltation in the trench.

Particle fall velocity

Figure 37 also shows the influence of an increased particle fall velocity. For a value of 0.0185 m/s a relatively large increase in the siltation level can be observed.

Bed boundary condition

Normally, in a longitudinal direction a combined bed boundary condition is used ($\partial c_b/\partial z = 0$ and $c_b = c_{b,e}$). The influence of the bed boundary condition was analysed by applying a single bed boundary condition ($c_b = c_{b,e}$) also. Computed bed concentrations and suspended load transport for both methods are given in Figure 38. For both the ebb and flood periods the single bed boundary condition produces the highest bed concentrations and suspended load transport which can be explained by considering the local transport capacities. The relatively small depth of the test pit only causes a small reduction of the average flow velocity. Consequently, the local transport capacities from which the bed concentrations are determined in case of a single boundary condition remain relatively large. Therefore, the bed concentrations and the suspended load transport are also rela-

tively large.
The difference in the reduction of the bed concentration for decelerating (flood) and accelerating (ebb) flow is due to the character of the transport formula used. For decelerating flow a 2.9 power function was used, while for accelerating flow a 5.5 power function was applied (Equations (6.1) and (6.2)), resulting in a smaller reduction of the transport capacity for decelerating flow.
The influence of the bed boundary condition on the computed bed level of the test pit is shown in Figure 39, which shows that the application of a combined bed boundary condition produces a significantly larger siltation level. Furthermore, the computed bed level after 180 days shows much better agreement with the measured values.

Flow velocity field

The longitudinal flow velocities, described by the semi-empiric model, correspond reasonably well with measured values. To estimate the influence of the applied flow velocity field, the suspended load transport and siltation level were also computed for a simple logarithmic velocity distribution. Although the use of such a distribution produces less good velocity profiles (Figure 34), the overall effect on the longitudinal suspended load transport and siltation level is negligibly small (not shown). On base of these results, it seems justified to use a simple logarithmic velocity distribution in case of gentle-sided trenches (no flow separation).

Bed load

The relation between the bed load transport and the average flow velocity was evaluated from echo soundings of the bed forms. This method is not very accurate because of the small heights of the bed forms with respect to the flow depth. Furthermore, as the measurements were not made at the location of the test pit, the accuracy of the applied bed load formula (Equation 6.3) is supposed to be relatively poor.
To estimate the influence of the bed load transport on the siltation level, this value was also computed for double the original bed load transport and without bed load transport. The results are presented in Figure 40.
However, some considerations about the siltation due to bed load must be made. Assuming equal flow velocity on both sides of the trench and neglecting gravity effects on the side slopes of the trench, the amount of siltation due to bed load will

always be equal to the amount of erosion. As a result, there will be no net amount of siltation in case of a symmetrical tidal curve. At the location of the test pit, however, the ebb flow dominates, which results in a relatively high siltation level at the eastern side slope of the trench (Figure 40). For double the original bed load transport, this effect will be even more clear. Consequently, the effective width of the trench is reduced, which means a lower siltation efficiency for the suspended load. Therefore, the siltation level in the middle part of the trench shows a reduction for double the original bed load transport. The bed level profiles computed without bed load show the largest siltation level in the middle part of the trench, while at the eastern slope a reduced siltation level can be observed.

Suspended load

Due to seasonal, temporal and spatial variations, the formulas (Equations (6.1) and (6.2)) used to describe the relation between the transport capacity for the suspended load and the average flow velocity are not very accurate. For example, only 50-60% of the measured values are within the range of half and double the average suspended load transport, as predicted by Equations (6.1) and (6.2). Considering the importance of the transport capacity (sediment input), the siltation level in the test pit was also computed for half and double the original suspended load transport. The results are shown in Figure 41, which shows that the siltation level is almost linearly dependent on the value of the suspended load at the upstream boundary.

From the results concerning the upstream sediment transport the following conclusions can be made:

Firstly, a minor misjudgement in the representative flow velocity and thus in the sediment transport results in a significantly different prediction of the siltation.

Secondly, a realistic prediction can only be made if detailed and accurate prototype measurements over a long period are available, and even then it will be difficult to estimate the controlling parameters with sufficient accuracy.

Thirdly, the mathematical model can be calibrated easily if siltation levels (test pit) are known.

LITERATURE

1 COLEMAN, N.L.,
Flume Studies of the Sediment Transfer Coefficient,
Water Resources Research, Vol. 6, No. 3, June 1970

2 DELFT HYDRAULICS LABORATORY,
Computational Methods for the Vertical Distribution of Flow in Shallow Water,
Report on Literature Study, Report W 152, August 1973

3 DELFT HYDRAULICS LABORATORY,
Semi-empirical Model for the Flow in Dredged Trenches,
Report R 1267-III/M 1536, 1980

4 DELFT HYDRAULICS LABORATORY,
Morphological Computations for Suspended Sediment Transport,
Research Report S 78-VI, March 1978

5 DELFT HYDRAULICS LABORATORY,
Sand Transport in Suspension, Study Diffusion Theory,
Report R 783-I, December 1973 (in Dutch)

6 DELFT HYDRAULICS LABORATORY,
Siltation in Trenches, Numerical Model for Non-steady Suspended Load Transport,
Report R 975-II, August 1977 (in Dutch)

7 DELFT HYDRAULICS LABORATORY,
Sediment Transport in Estuaries,
Note R 1267-1, October 1977 (in Dutch)

8 DELFT HYDRAULICS LABORATORY,
Sediment Transport in the Entrance of the Oosterschelde Estuary,
Report R 1267-IV/M 1572, 1980 (in Dutch)

9 DELFT HYDRAULICS LABORATORY,
Determination of Bed Load Transport by Migration of Bed Forms,
Interim Report R 1267-4, 1980 (in Dutch)

LITERATURE (continued)

10 DELFT HYDRAULICS LABORATORY,
Flow Resistance in Open Channels with an Alluvial Bed,
Interim Report R 1267-3, 1980 (in Dutch)

11 KERSSENS, P.M.J., PRINS, A. and RIJN, L.C. van,
Model for Suspended Sediment Transport,
Journal of the Hydraulics Division, ASCE, May 1979

12 KERSSENS, P.M.J., RIJN, L.C. van and WIJNGAARDEN, N.J. van,
Model for Non-steady Suspended Sediment Transport,
Paper A15, 17th Congress IAHR, Baden-Baden, Germany, August 1977

13 VANONI, V.A. and BROOKS, N.H.,
Laboratory Study of the Roughness and Suspended Load of Alluvial Streams,
Sedimentation Laboratory No. E-68, California Institute of Technology,
Pasadena, California, December 1957

14 VRIES, M. de,
Solving River Problems by Hydraulic and Mathematical Models,
Publication No. 76 II, Delft Hydraulics Laboratory, September 1971

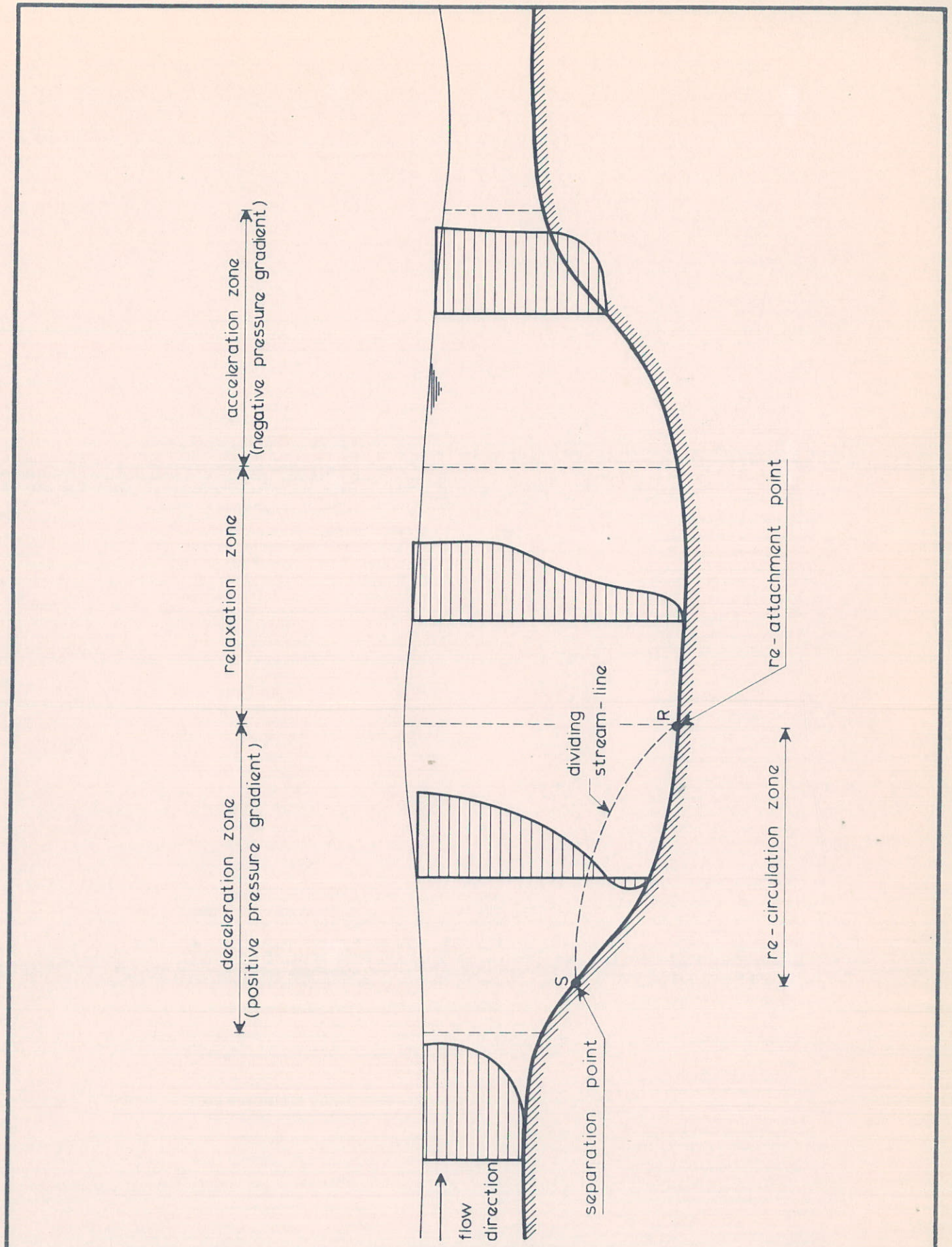

SKETCH OF FLOW VELOCITY PROFILES
IN A DREDGED TRENCH

DELFT HYDRAULICS LABORATORY

R1267-V/M1570

FIG. 1

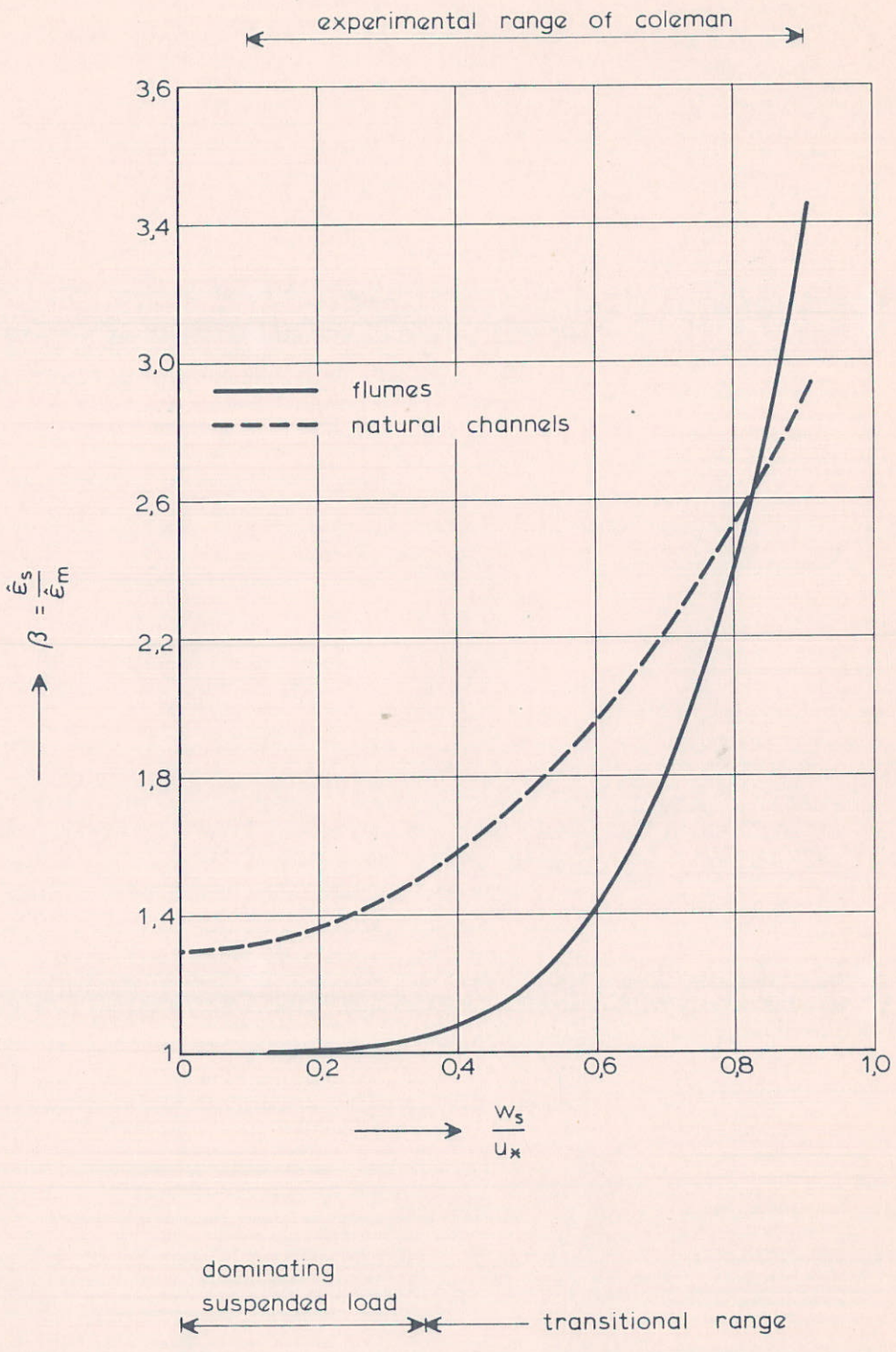

RATIO OF DIFFUSION COEFFICIENT FOR SEDIMENT AND MOMENTUM AS A FUNCTION OF PARTICLE FALL VELOCITY AND SHEAR VELOCITY

DELFT HYDRAULICS LABORATORY | R1267-V/M1570 | FIG. 2

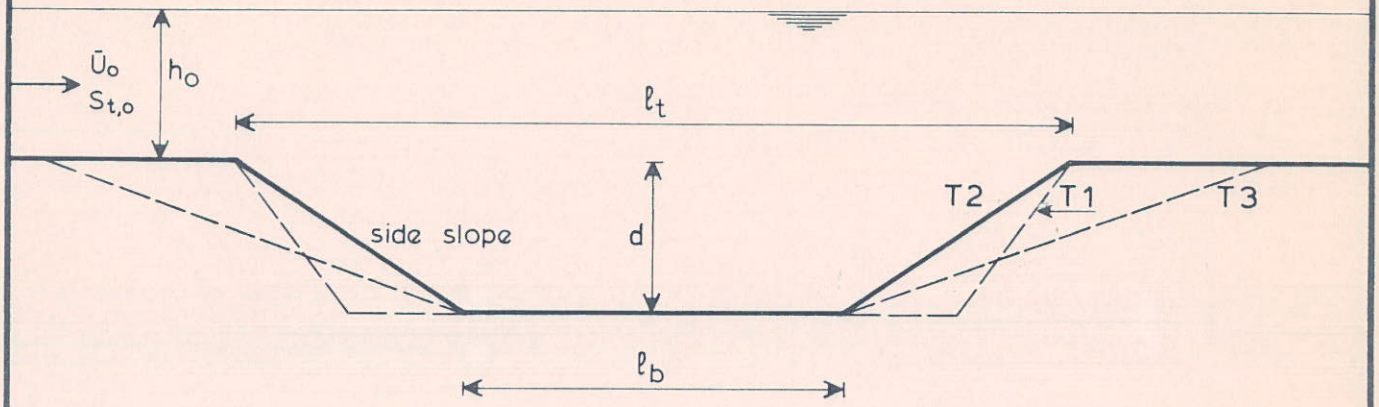

		T0	T1	T2	T3	
top width	(ℓ_t)	-	5.0	5.0	6.0	(m)
bottom width	(ℓ_b)	-	4.0	2.5	3.0	(m)
trench depth	(d)	-	0.178	0.17	0.15	(m)
side slope		-	1:3	1:7	1:10	
upstream flow depth	(h_o)	0.40	0.40	0.39	0.39	(m)
upstream flow velocity	($\bar{U}_o$)	0.50	0.50	0.51	0.51	(m/s)
upstream sediment transport	($S_{t,o}$)	0.04	0.04	0.04	0.04	(kg/sm)
particle fall velocity	(W_s)	0.013	0.013	0.013	0.013	(m/s)
equivalent roughness of Nikuradse	(k_s)	0.025	0.025	0.025	0.025	(m)
water temperature	(T)	15	15	18	15	(°C)

GENERAL DATA FOR FLUME TESTS

DELFT HYDRAULICS LABORATORY | R1267-V/M1570 | FIG. 3

vertical distribution of suspended sediment size

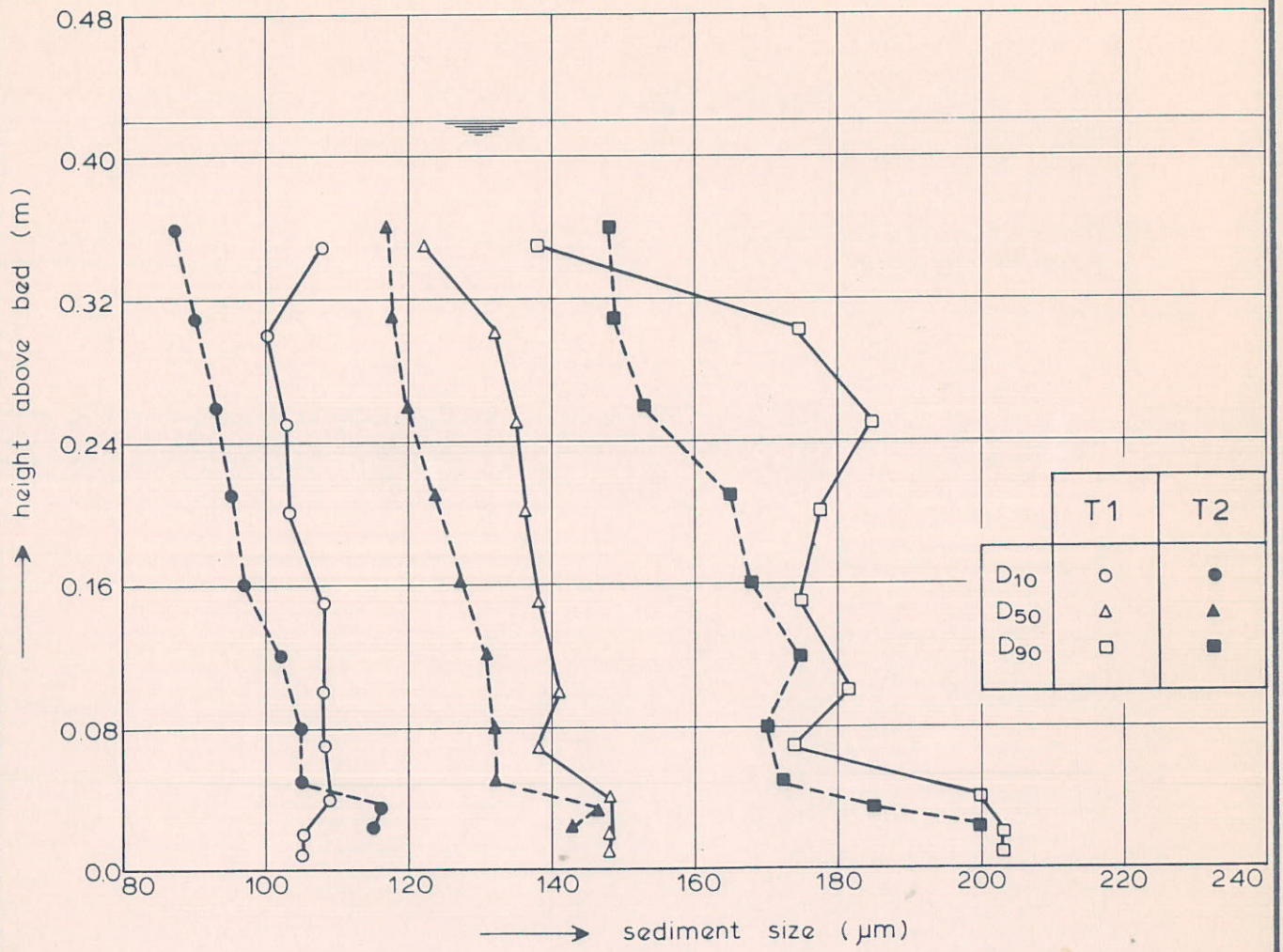

longitudinal distribution of bed material size (T_0)

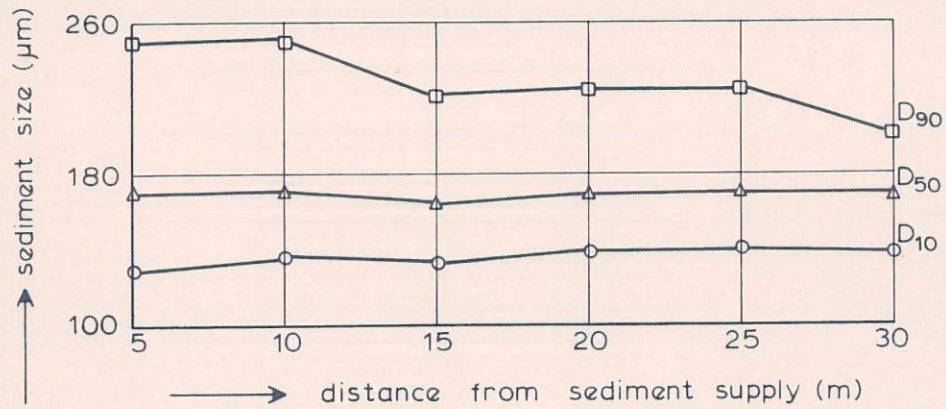

SEDIMENT FEED
D_{10} = 115 μm D_{50} = 160 μm D_{90} = 195 μm

SEDIMENT SIZE DISTRIBUTIONS (FLUME TESTS)

DELFT HYDRAULICS LABORATORY | R 1267-V/M1570 | FIG. 4

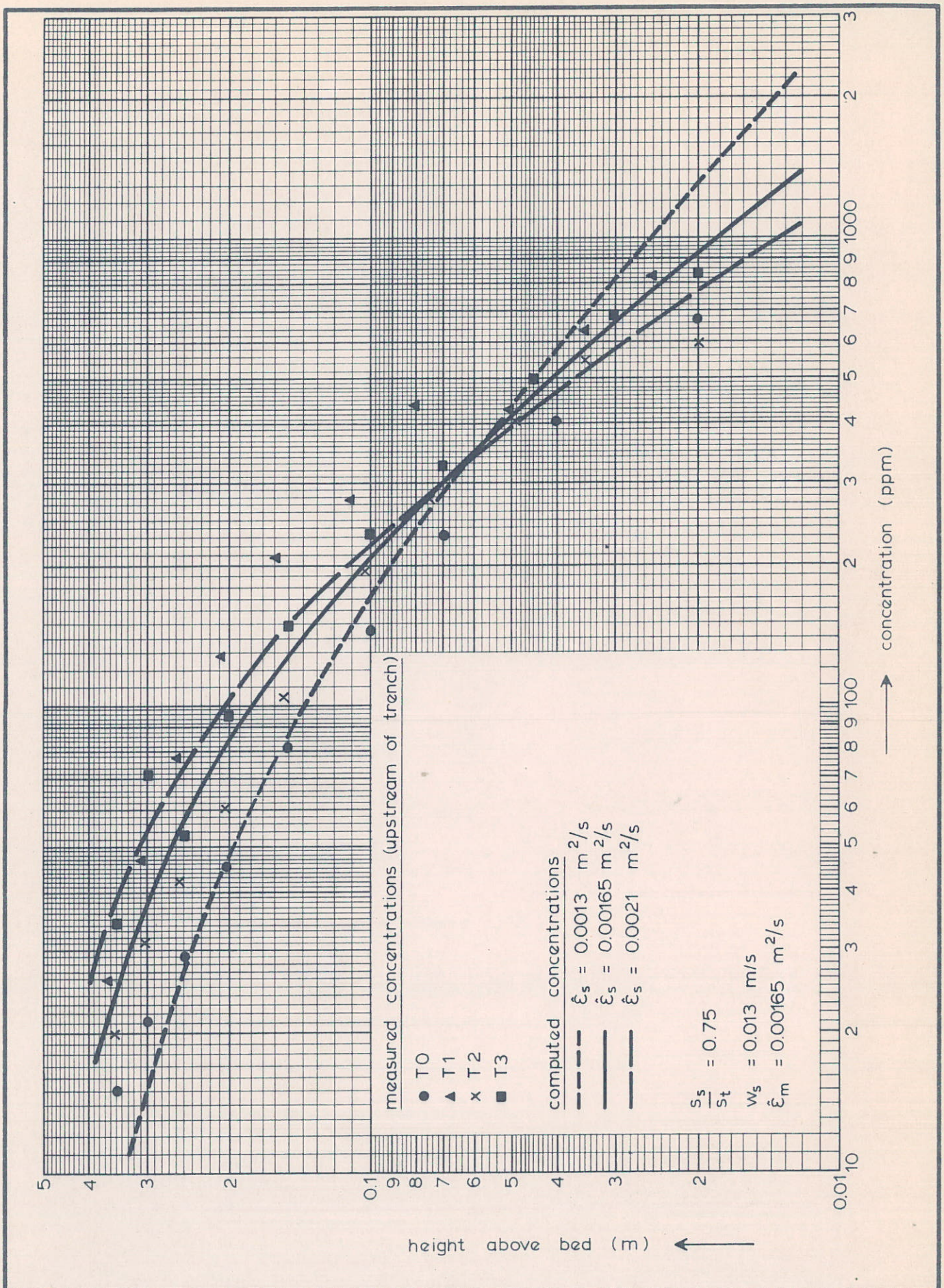

INFLUENCE OF DIFFUSION COEFFICIENT ON EQUILIBRIUM CONCENTRATION PROFILE (FLUME TESTS)

DELFT HYDRAULICS LABORATORY

R1267-V/M1570

FIG. 5

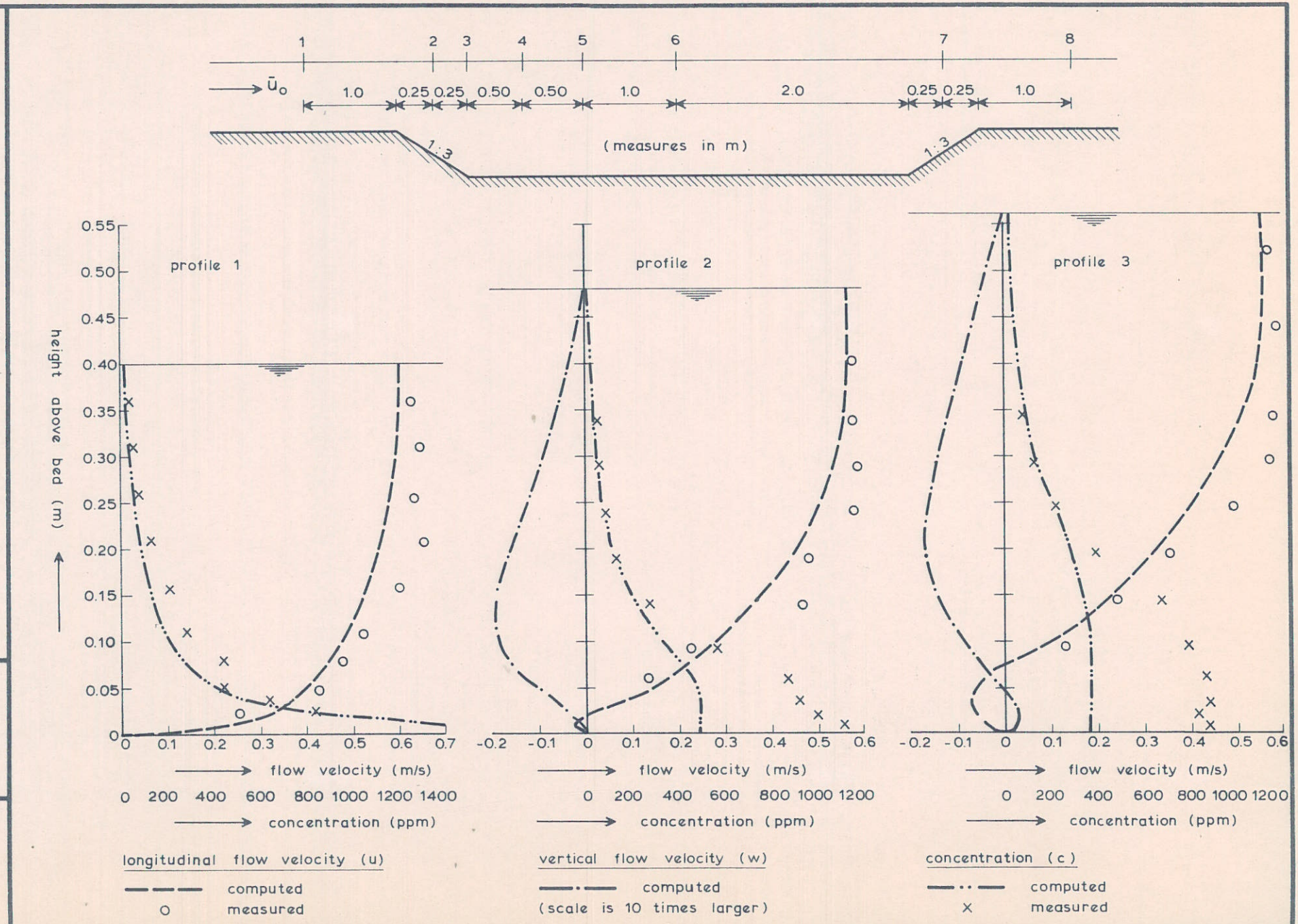

FLOW VELOCITY AND SEDIMENT CONCENTRATION PROFILES (1, 2, 3)

DELFT HYDRAULICS LABORATORY

T 2

R1267-V/M1570

FIG. 6

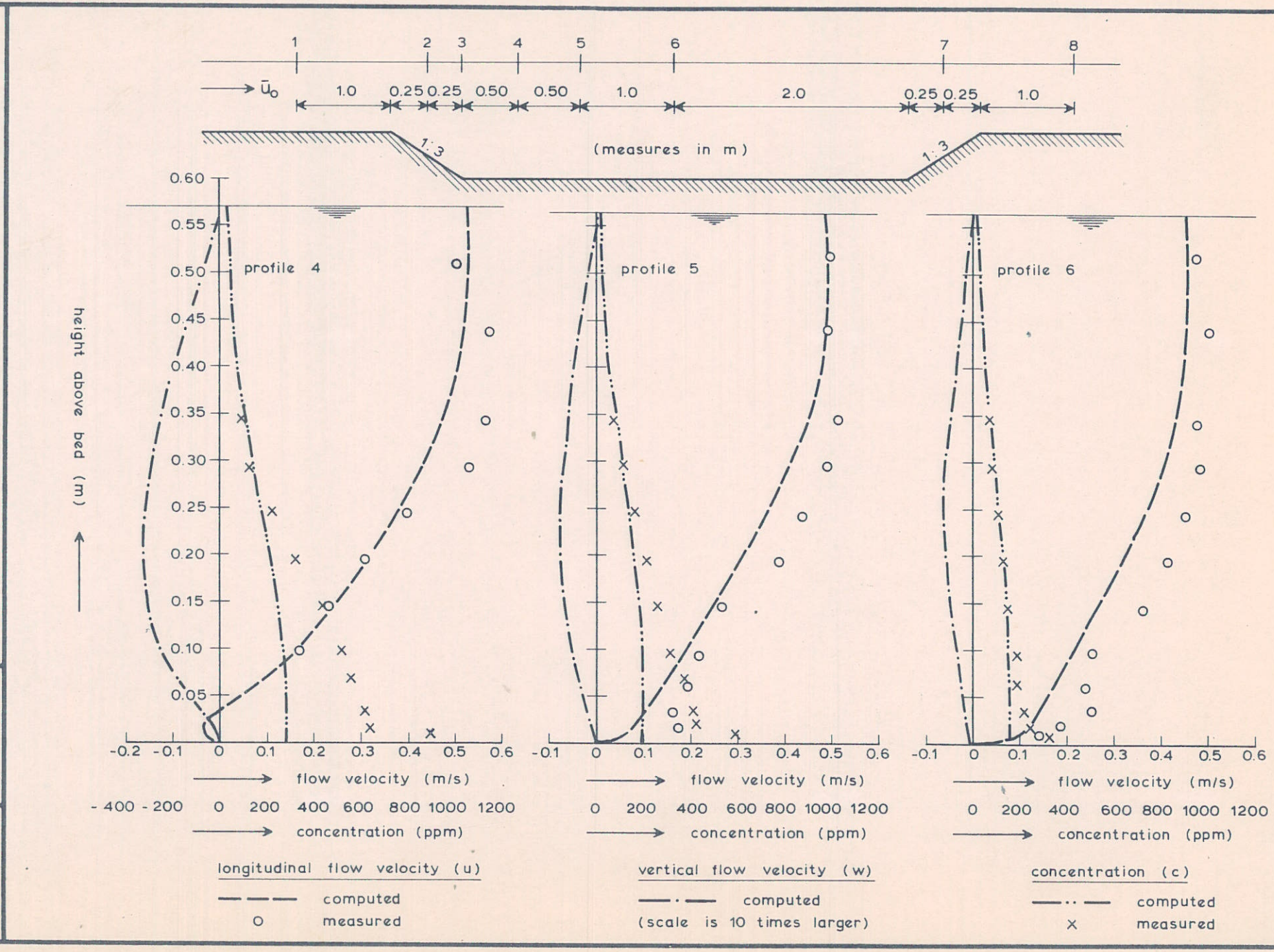

FLOW VELOCITY AND SEDIMENT CONCENTRATION PROFILES (4,5,6)

DELFT HYDRAULICS LABORATORY

T 2

R1267-XI/M1570

FIG. 7

DELFT HYDRAULICS LABORATORY

FLOW VELOCITY AND SEDIMENT CONCENTRATION PROFILES (7,8)

T 2

R1267-V/M1570

FIG. 8

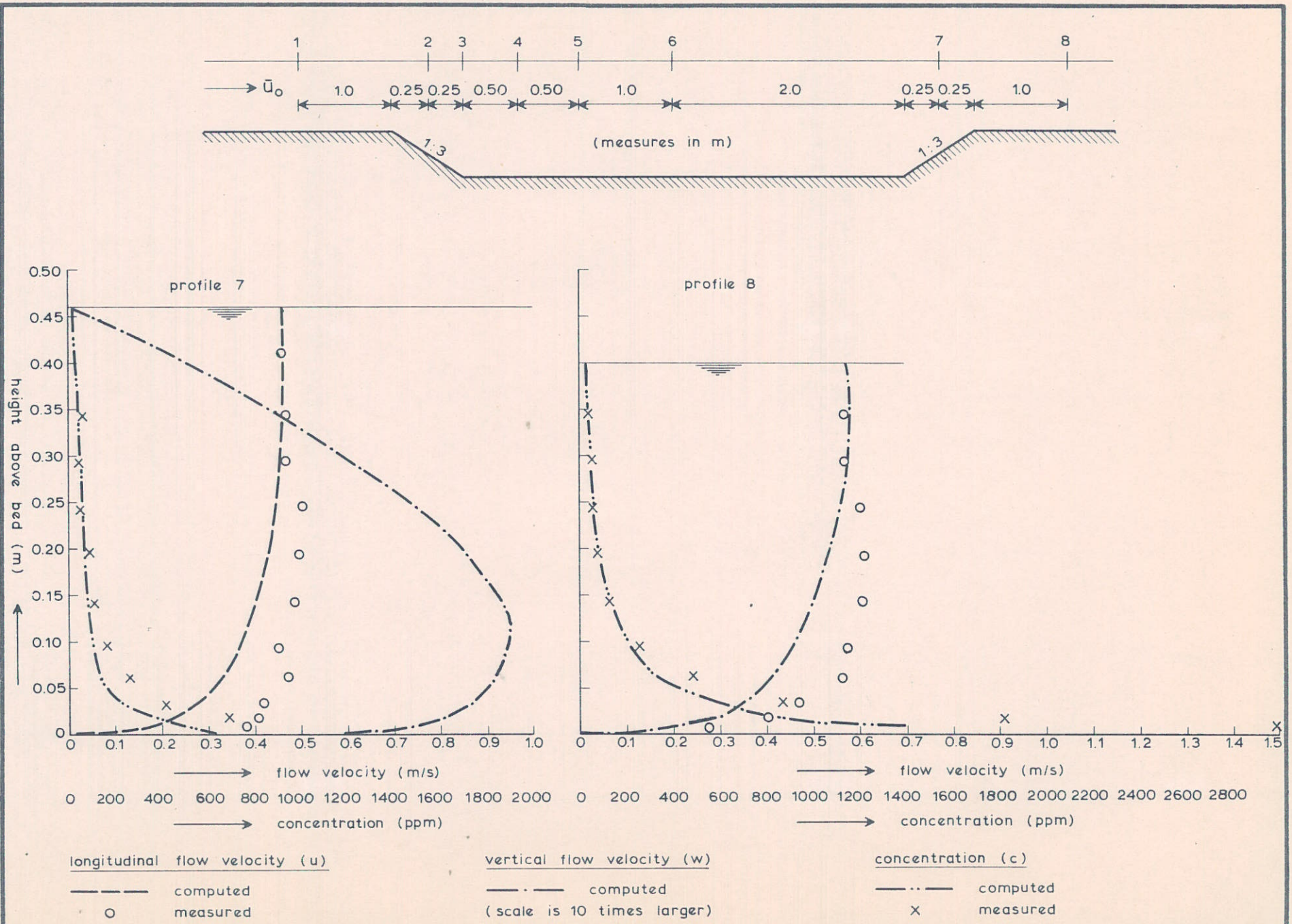

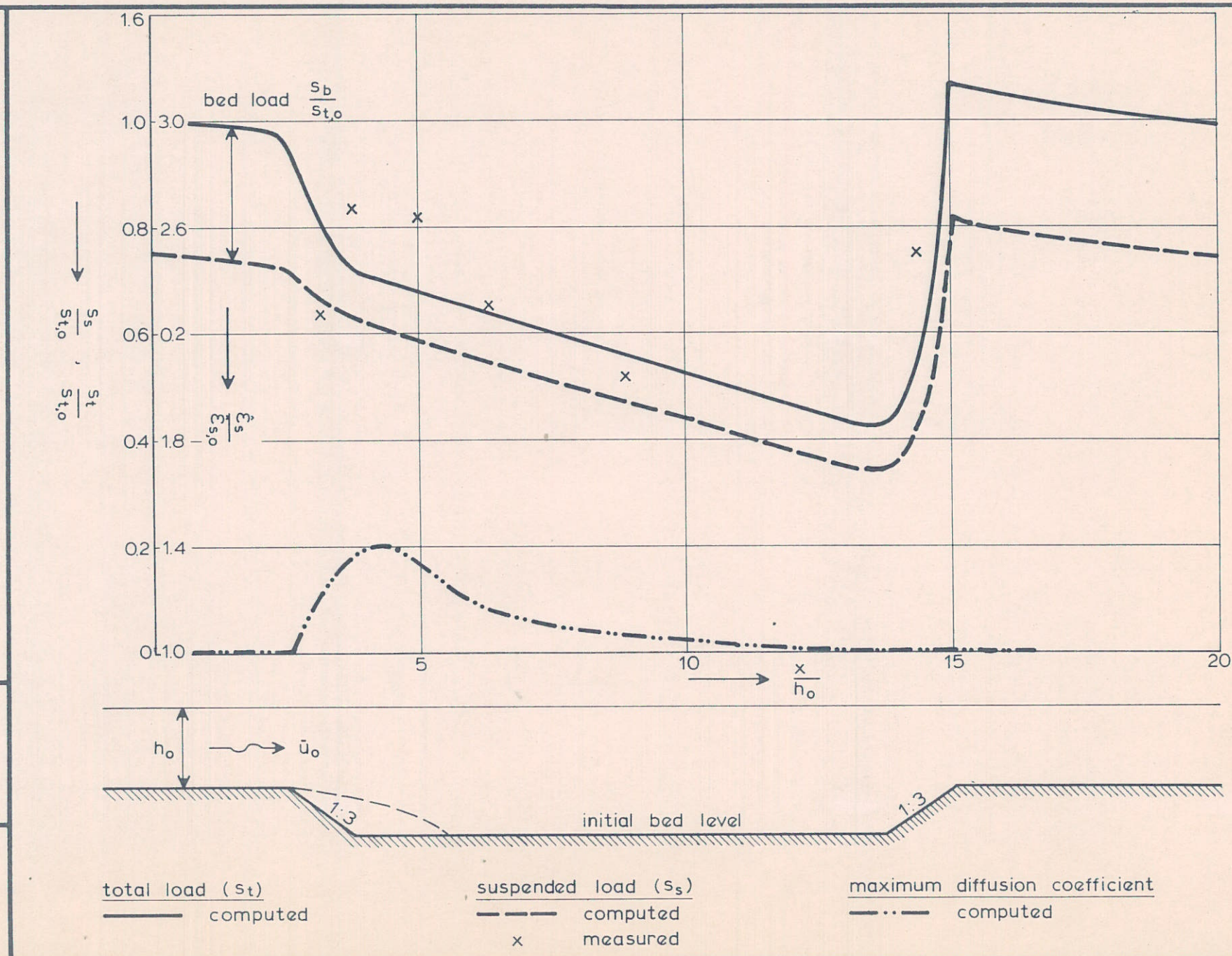

LONGITUDINAL SEDIMENT TRANSPORT AND DIFFUSION COEFFICIENT

T 1

DELFT HYDRAULICS LABORATORY

R1267-I/M1570

FIG. 9

DELFT HYDRAULICS LABORATORY

BED LEVELS

T 1

R1267-IV/M1570 FIG. 10

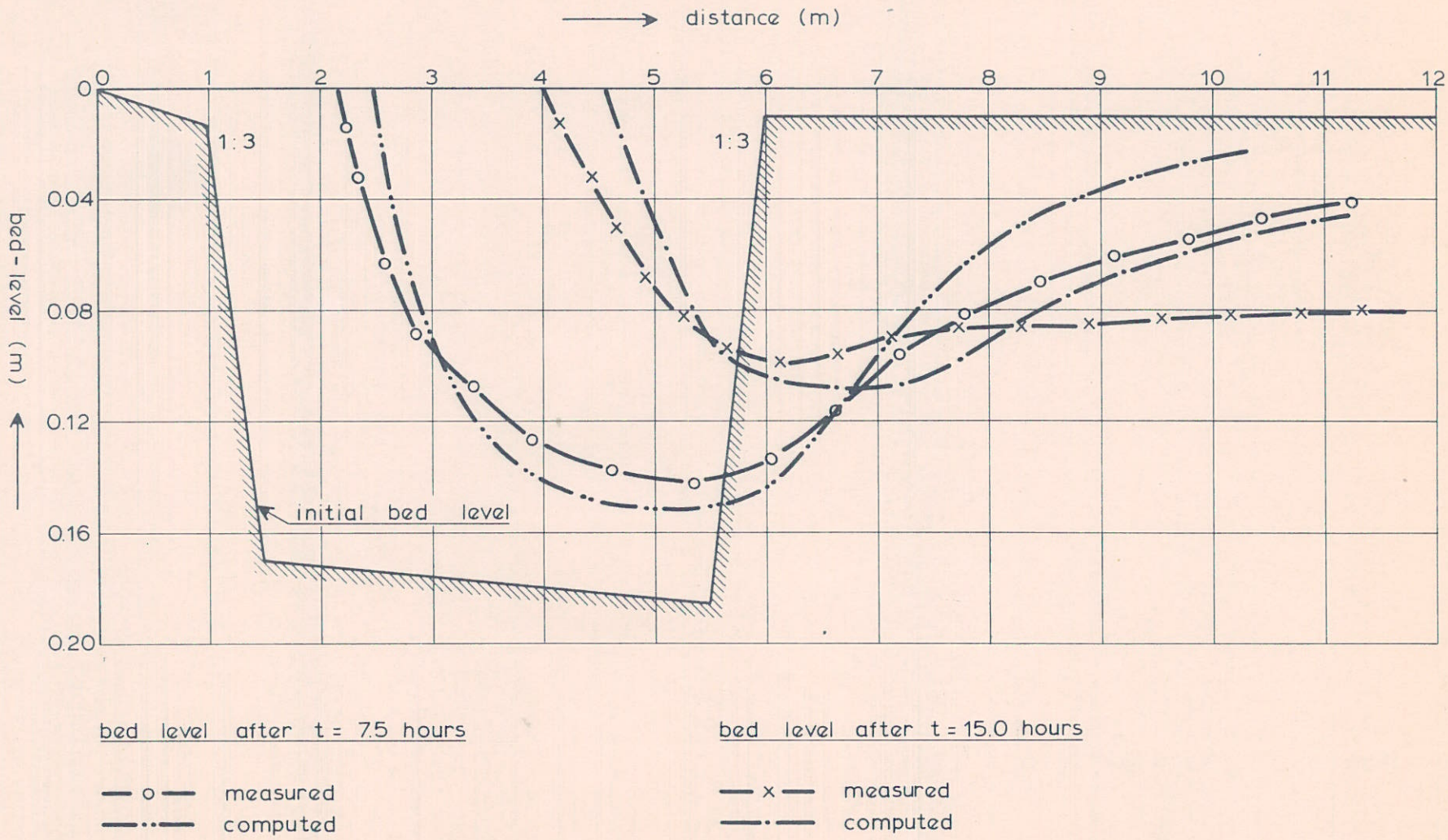

DELFT HYDRAULICS LABORATORY

FLOW VELOCITY AND SEDIMENT CONCENTRATION PROFILES (1,2,3)

T2

R1267-IV/M1570

FIG. 11

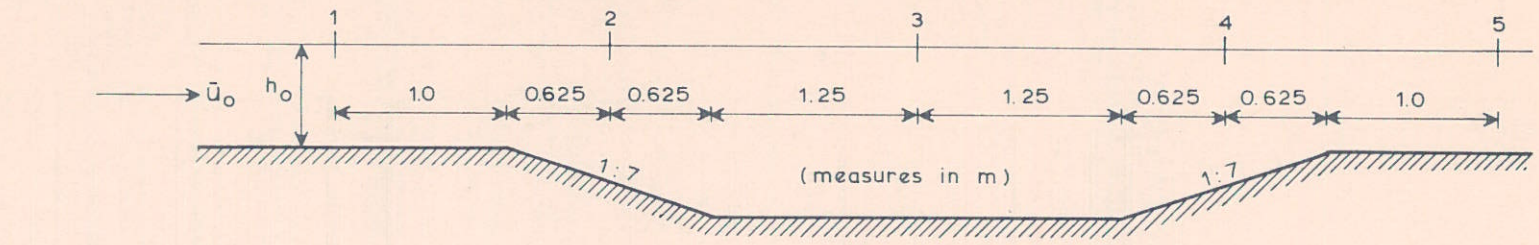

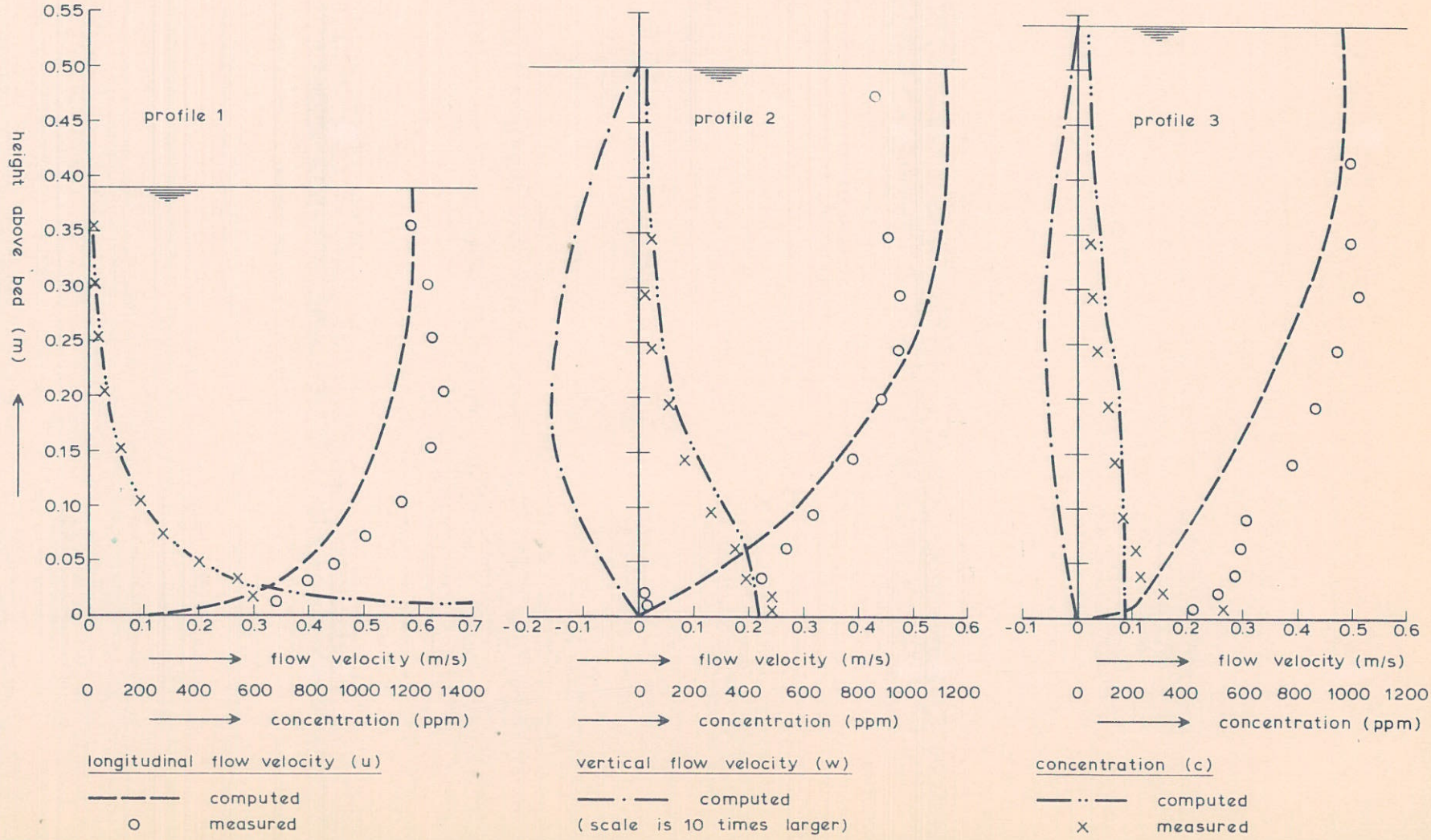

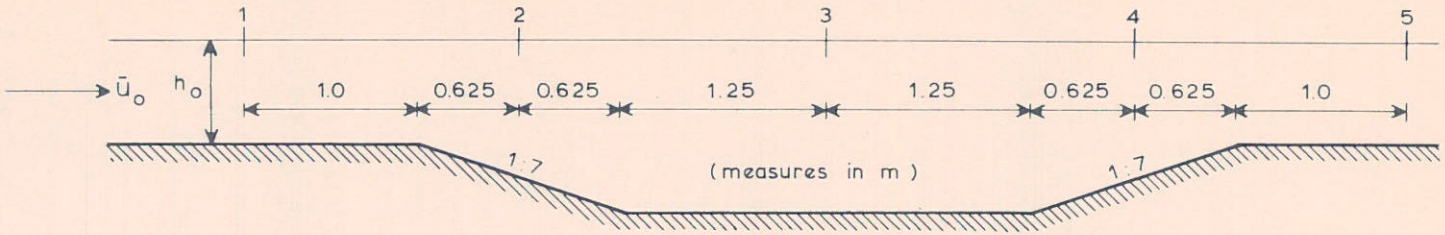

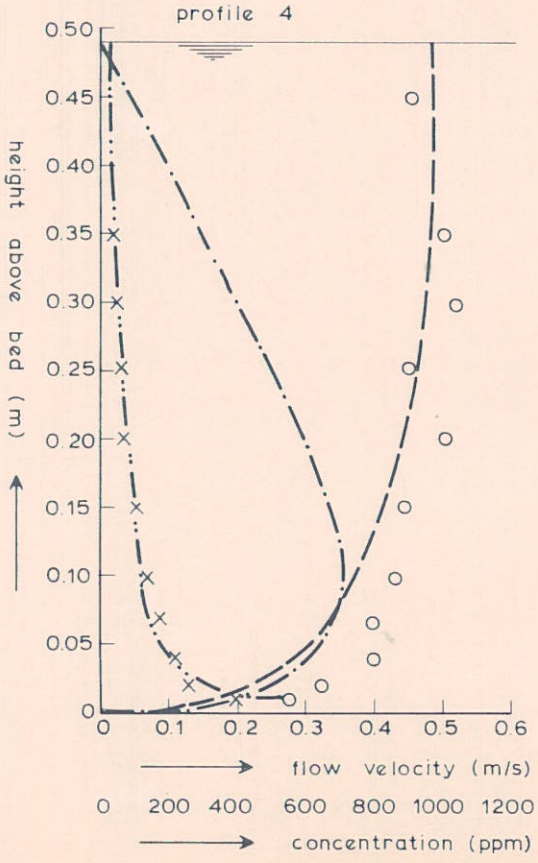

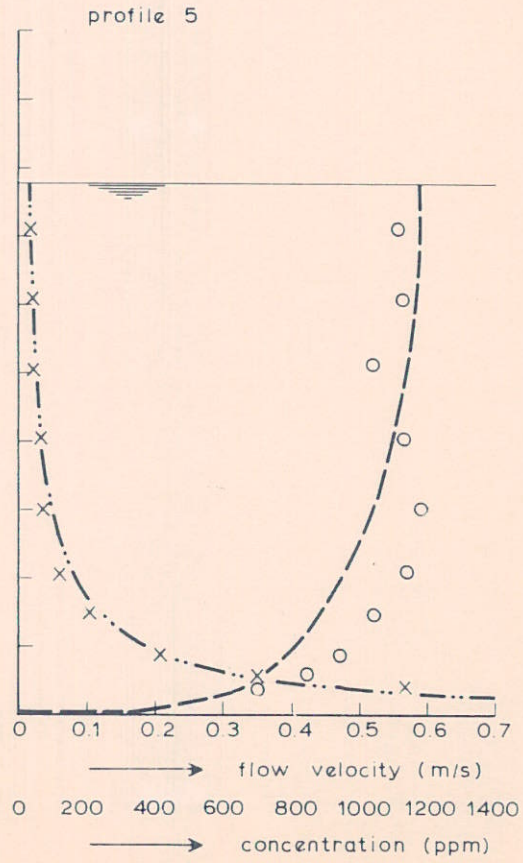

longitudinal flow velocity (u)
——— computed
o measured

vertical flow velocity (w)
—·— computed
(scale is 10 times larger)

concentration (c)
—··— computed
x measured

FLOW VELOCITY AND SEDIMENT CONCENTRATION PROFILES (4,5)

T 2

R1267-IV/M1570

FIG. 12

DELFT HYDRAULICS LABORATORY

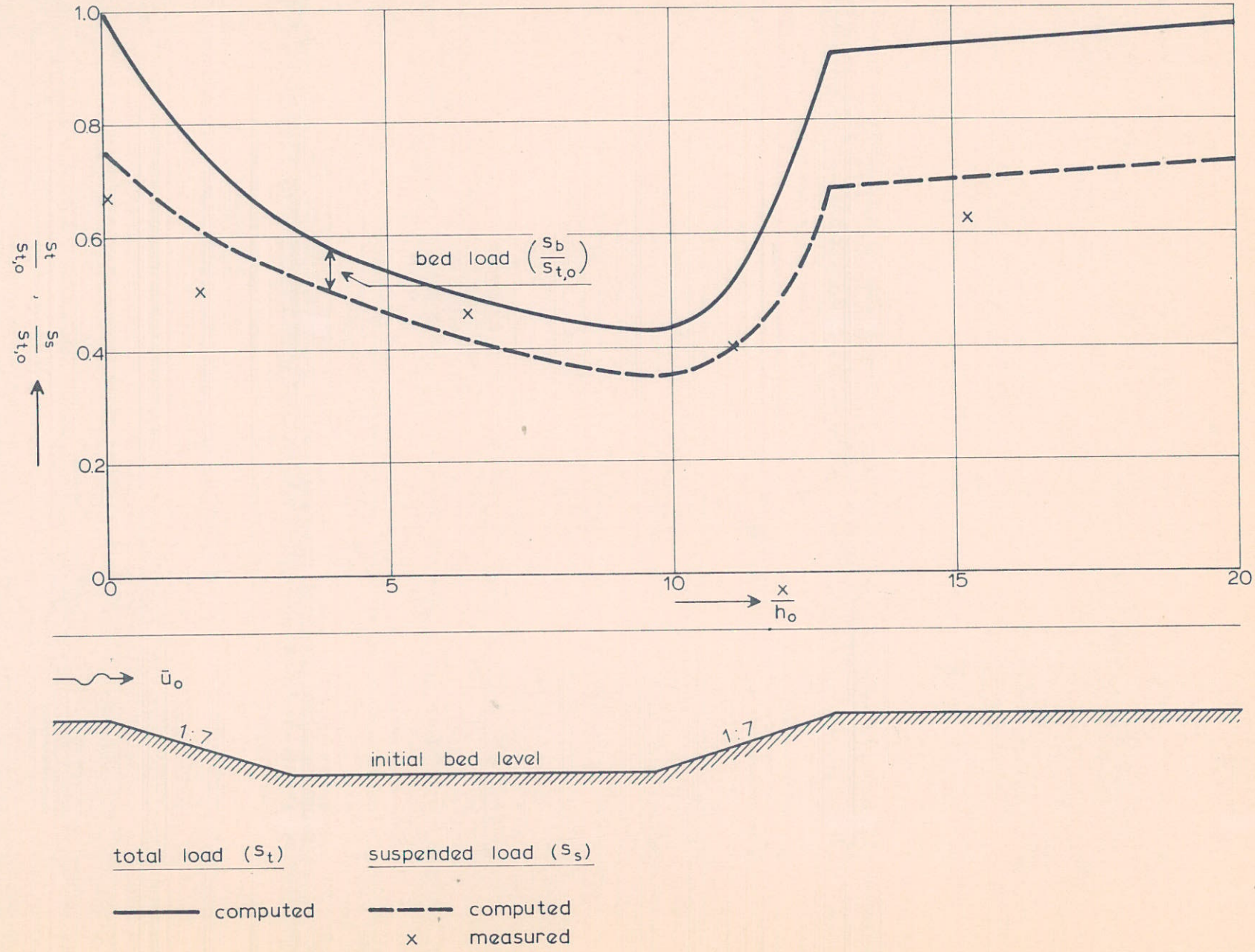

LONGITUDINAL SEDIMENT TRANSPORT

DELFT HYDRAULICS LABORATORY

R1267-IV/M1570

T 2

FIG. 13

DELFT HYDRAULICS LABORATORY

BED LEVELS

T 2

R267-II/M1570

FIG. 14

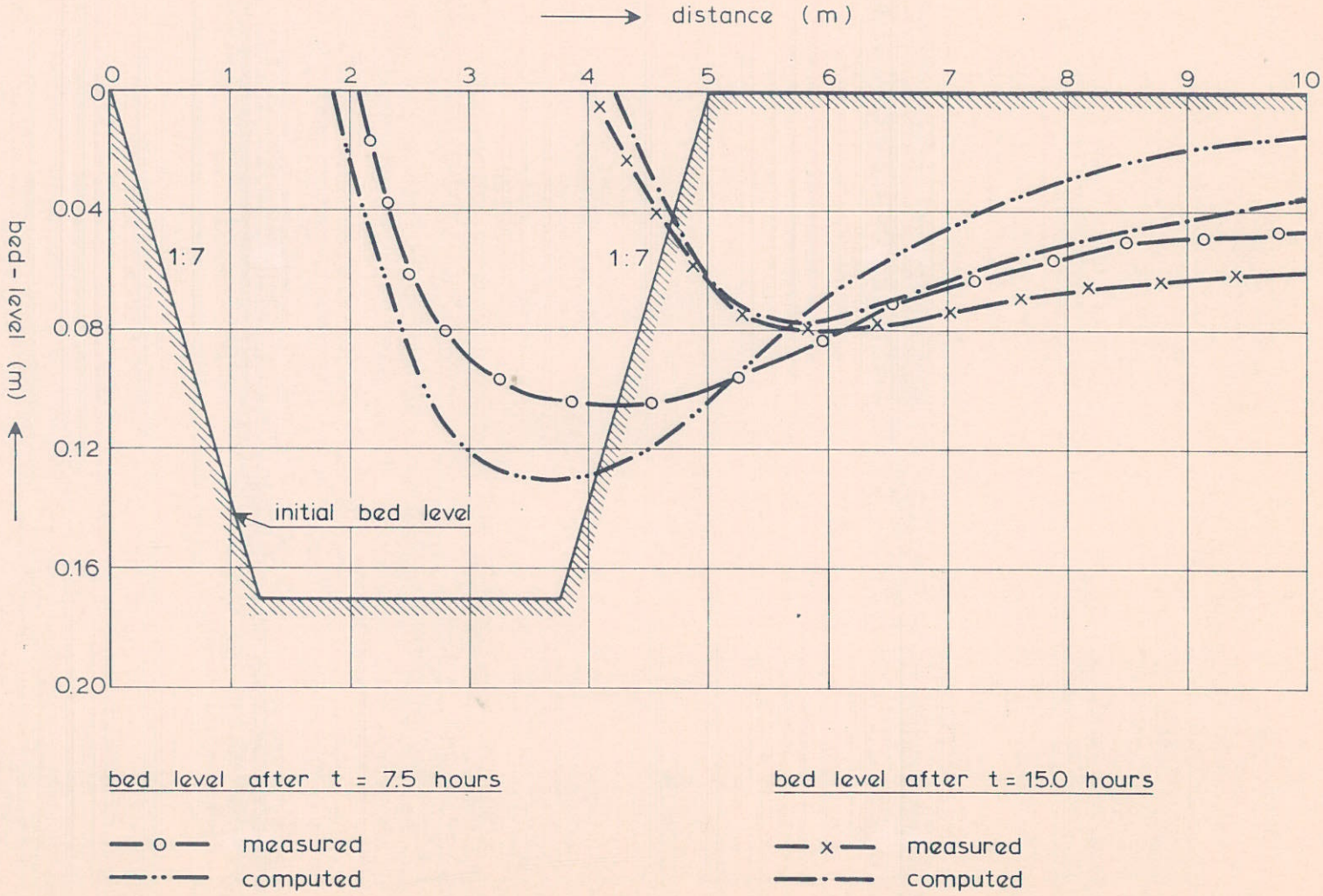

DELFT HYDRAULICS LABORATORY

FLOW VELOCITY AND SEDIMENT CONCENTRATION PROFILES (1, 2, 3)

T 3

R1267-IV/M1570

FIG. 15

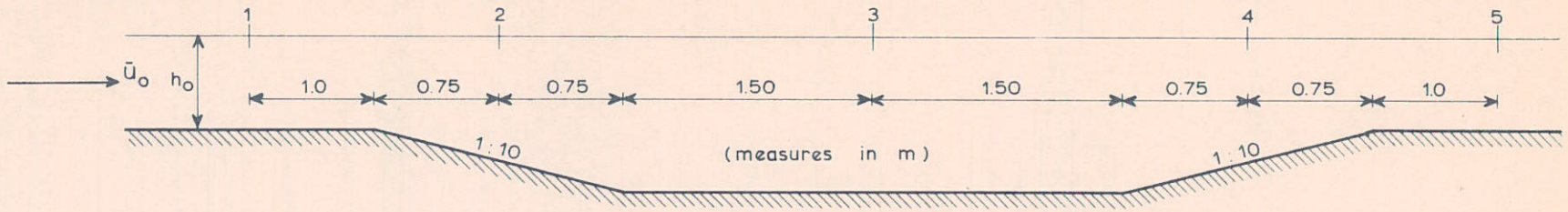

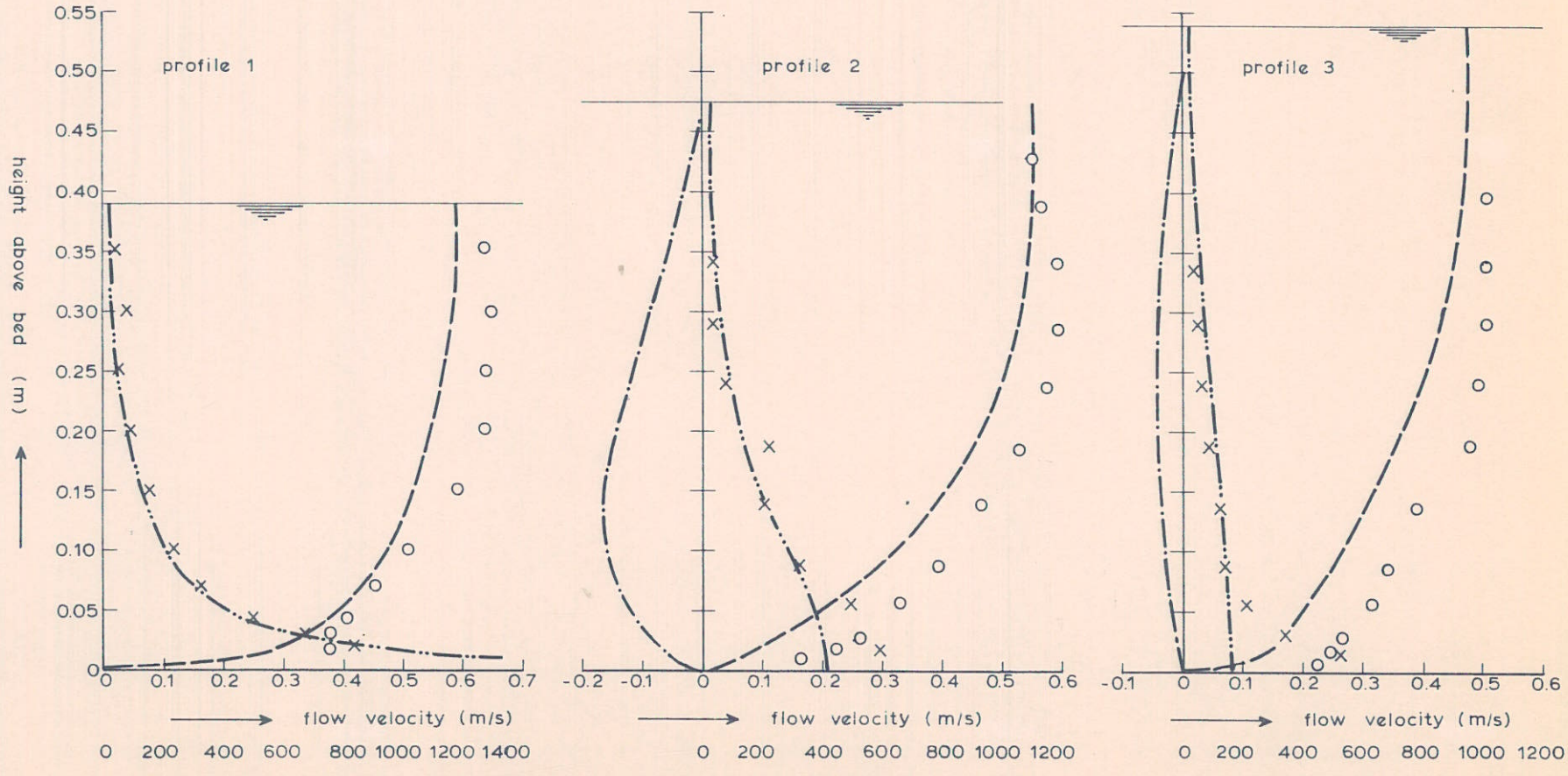

longitudinal flow velocity (u)

— — — computed

o measured

vertical flow velocity (w)

—·— computed

(scale is 10 times larger)

concentration (c)

—··— computed

× measured

DELFT HYDRAULICS LABORATORY

FLOW VELOCITY AND SEDIMENT CONCENTRATION PROFILES (4,5)

T 3

R1267-IV/M1570

FIG. 16

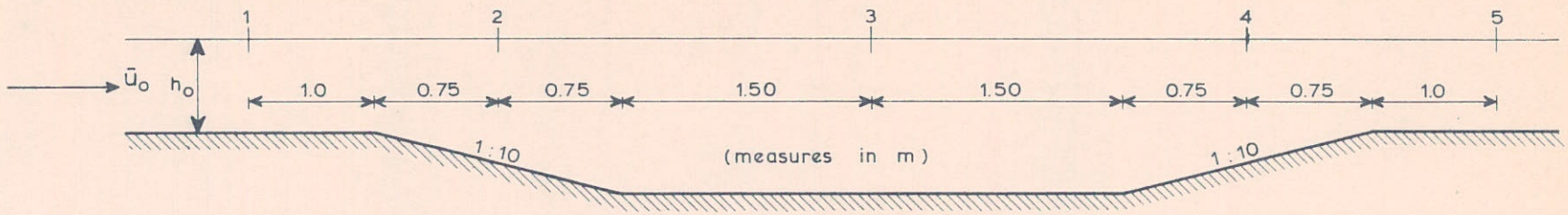

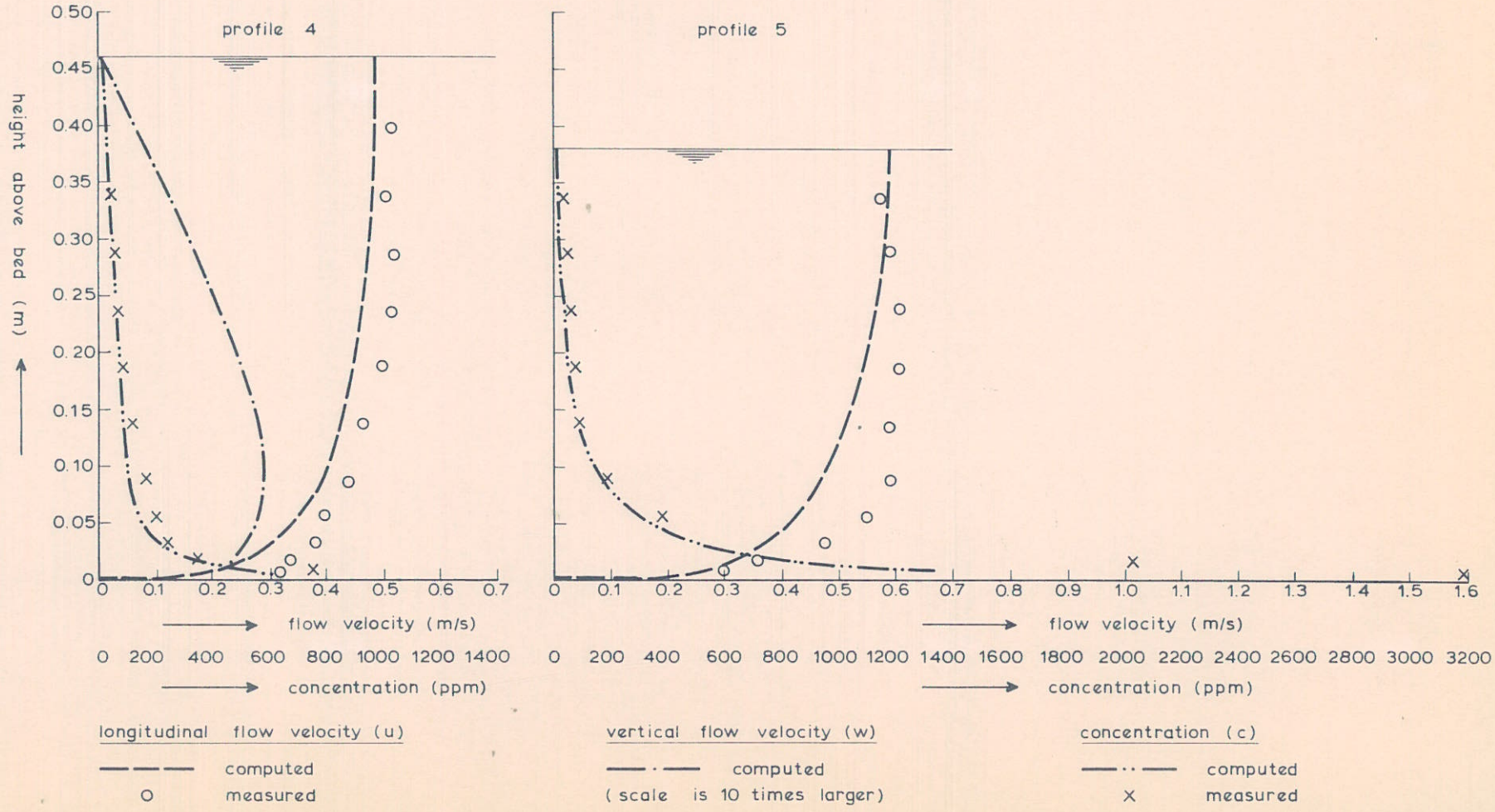

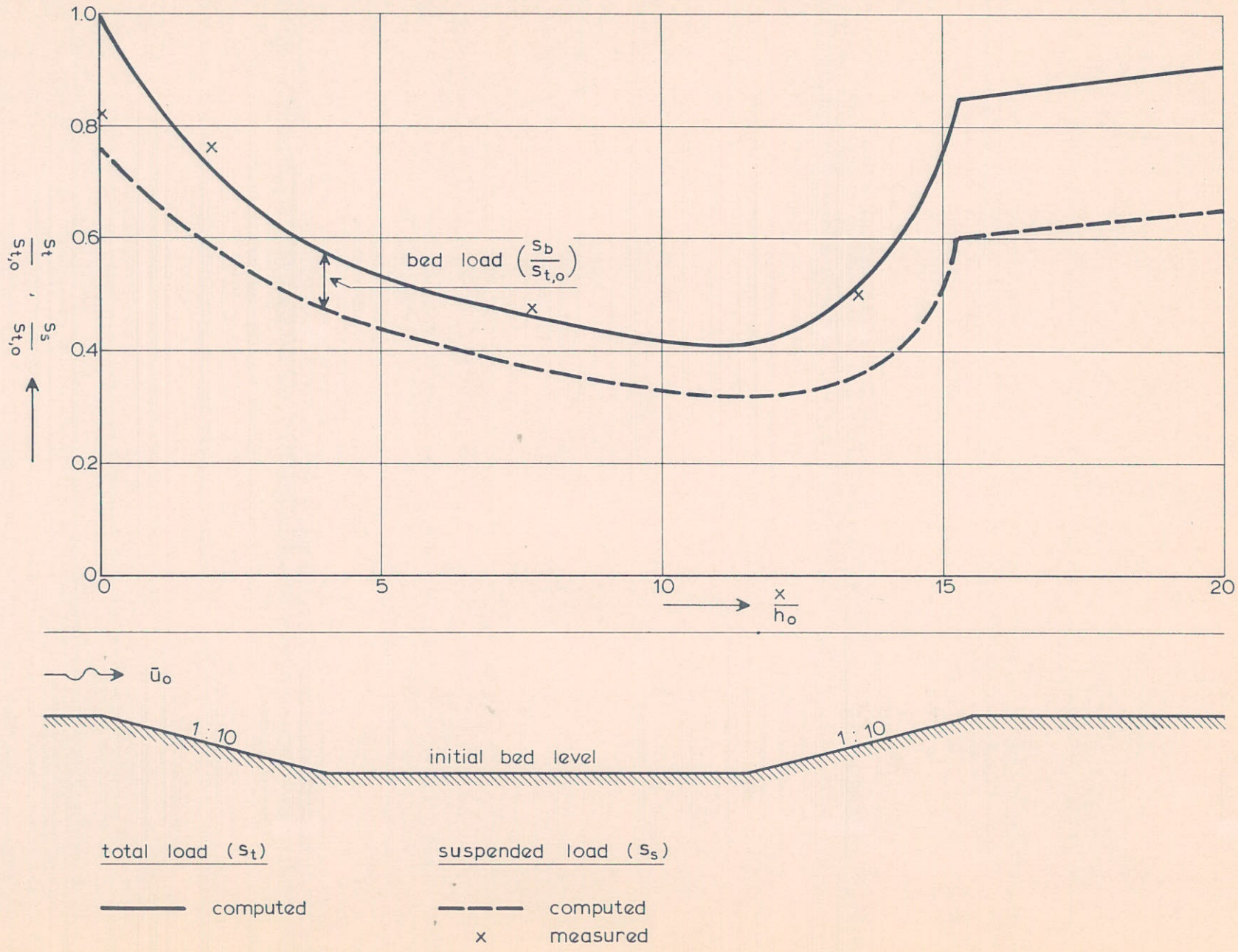

DELFT HYDRAULICS LABORATORY

LONGITUDINAL SEDIMENT TRANSPORT

T 3

R1267-II/M1570

FIG. 17

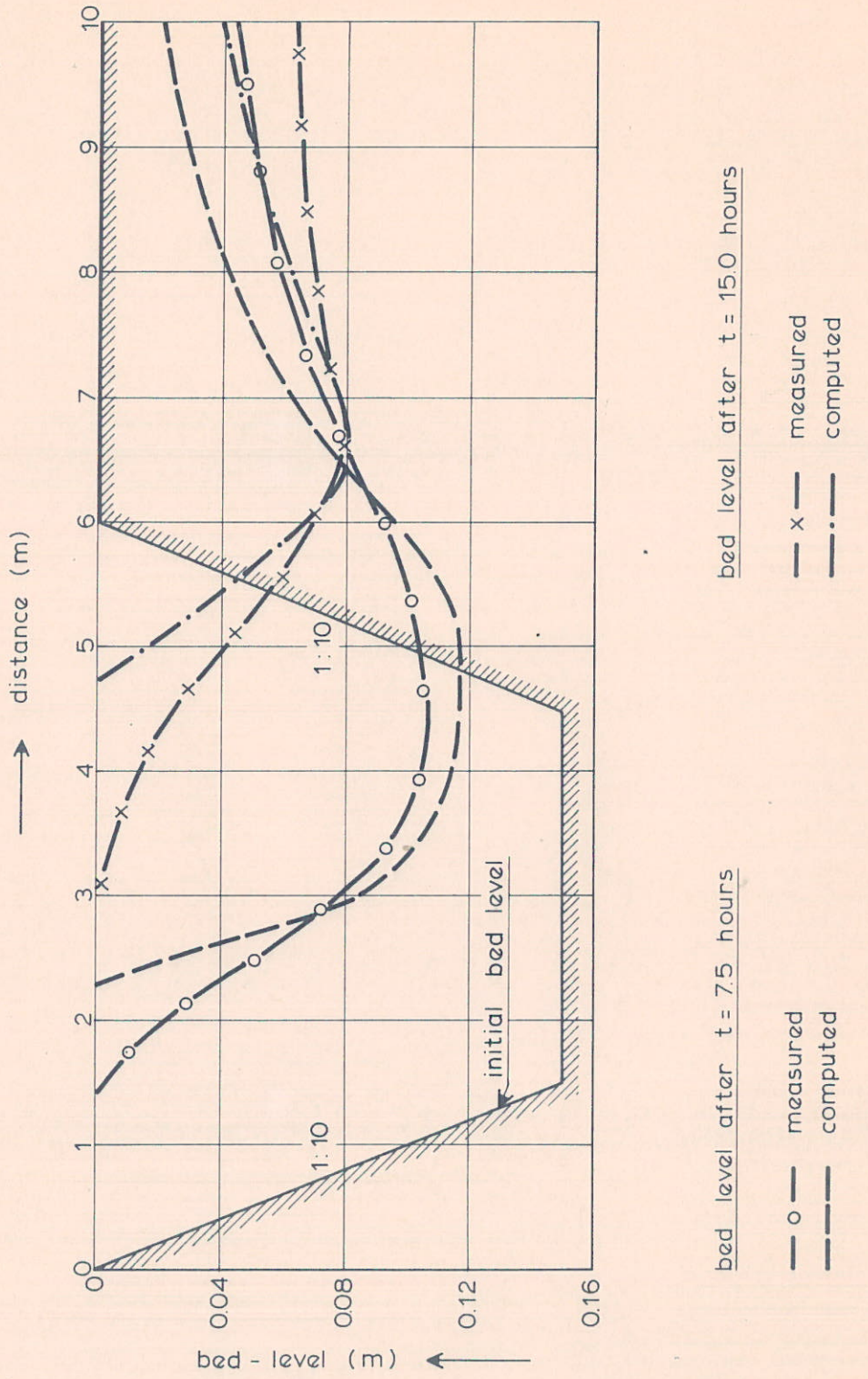

BED LEVELS

T 3

DELFT HYDRAULICS LABORATORY

R1267-V/M1570

FIG. 18

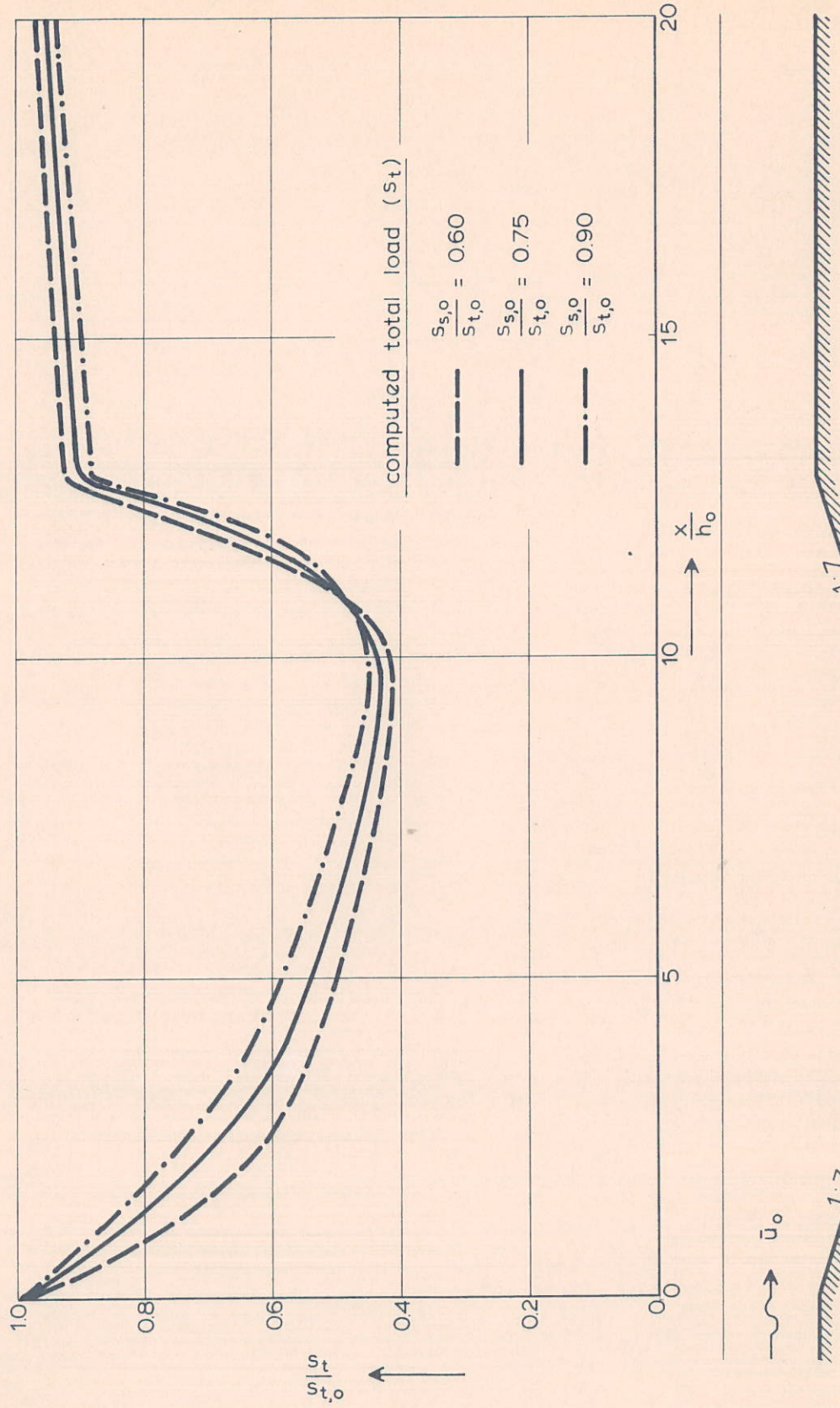

INFLUENCE OF UPSTREAM SUSPENDED LOAD ON LONGITUDINAL TOTAL LOAD	T 2	
DELFT HYDRAULICS LABORATORY	R1267-V/M1570	FIG. 19

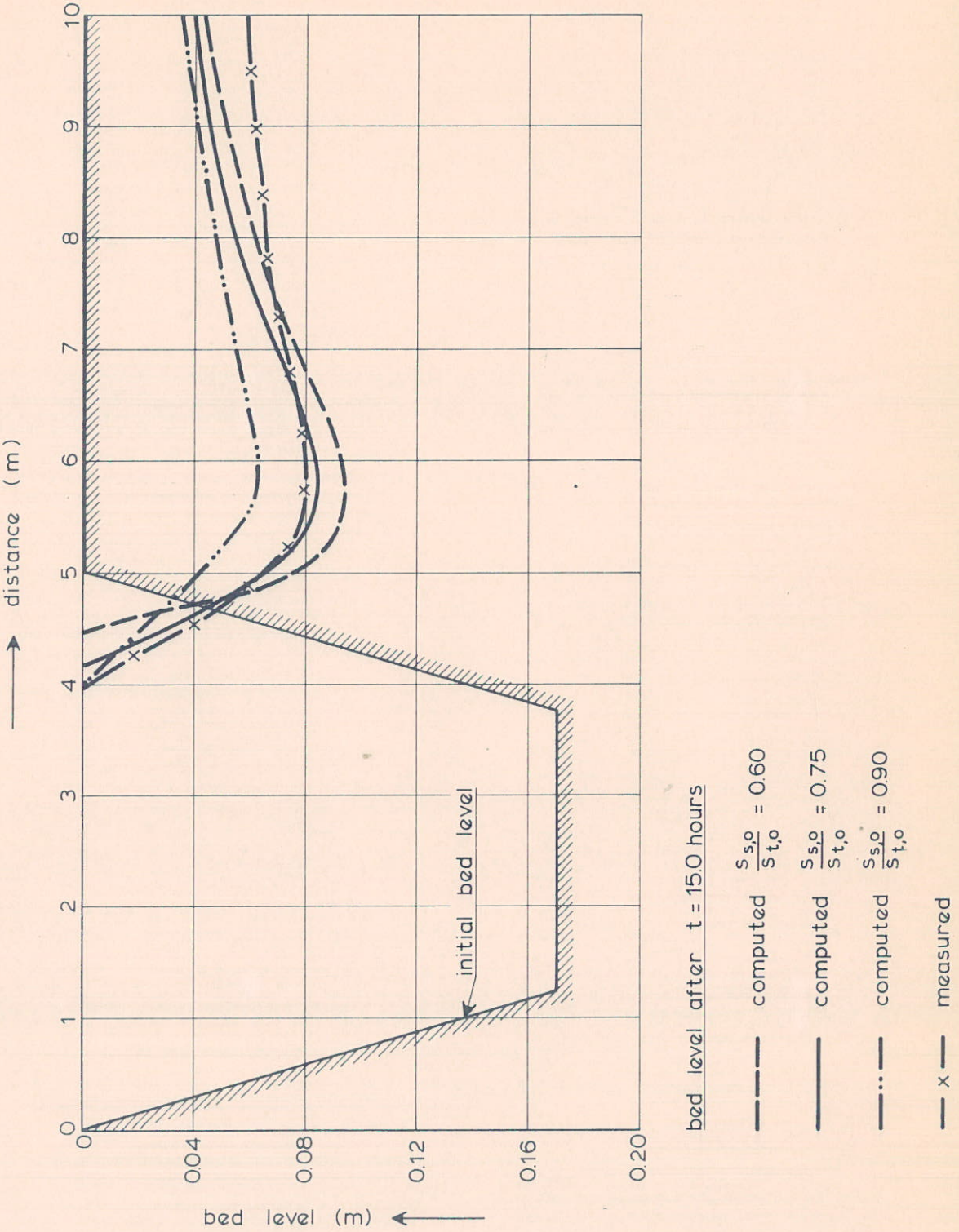

INFLUENCE OF UPSTREAM SUSPENDED LOAD ON BED LEVEL	T 2	
DELFT HYDRAULICS LABORATORY	R1267-V/M1570	FIG. 20

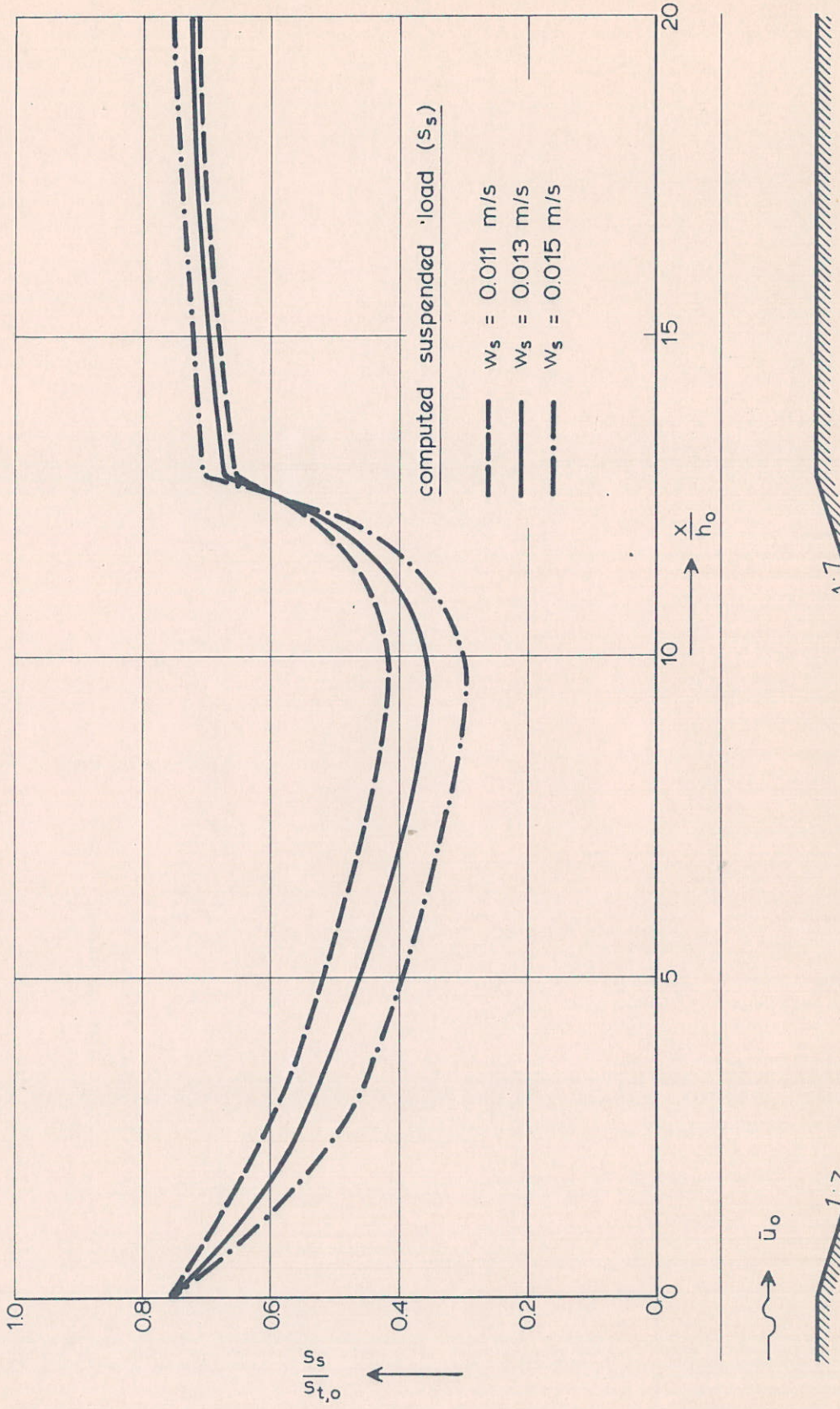

INFLUENCE OF PARTICLE FALL VELOCITY ON LONGITUDINAL SUSPENDED LOAD

T 2

DELFT HYDRAULICS LABORATORY

R1267-V/M1570

FIG. 21

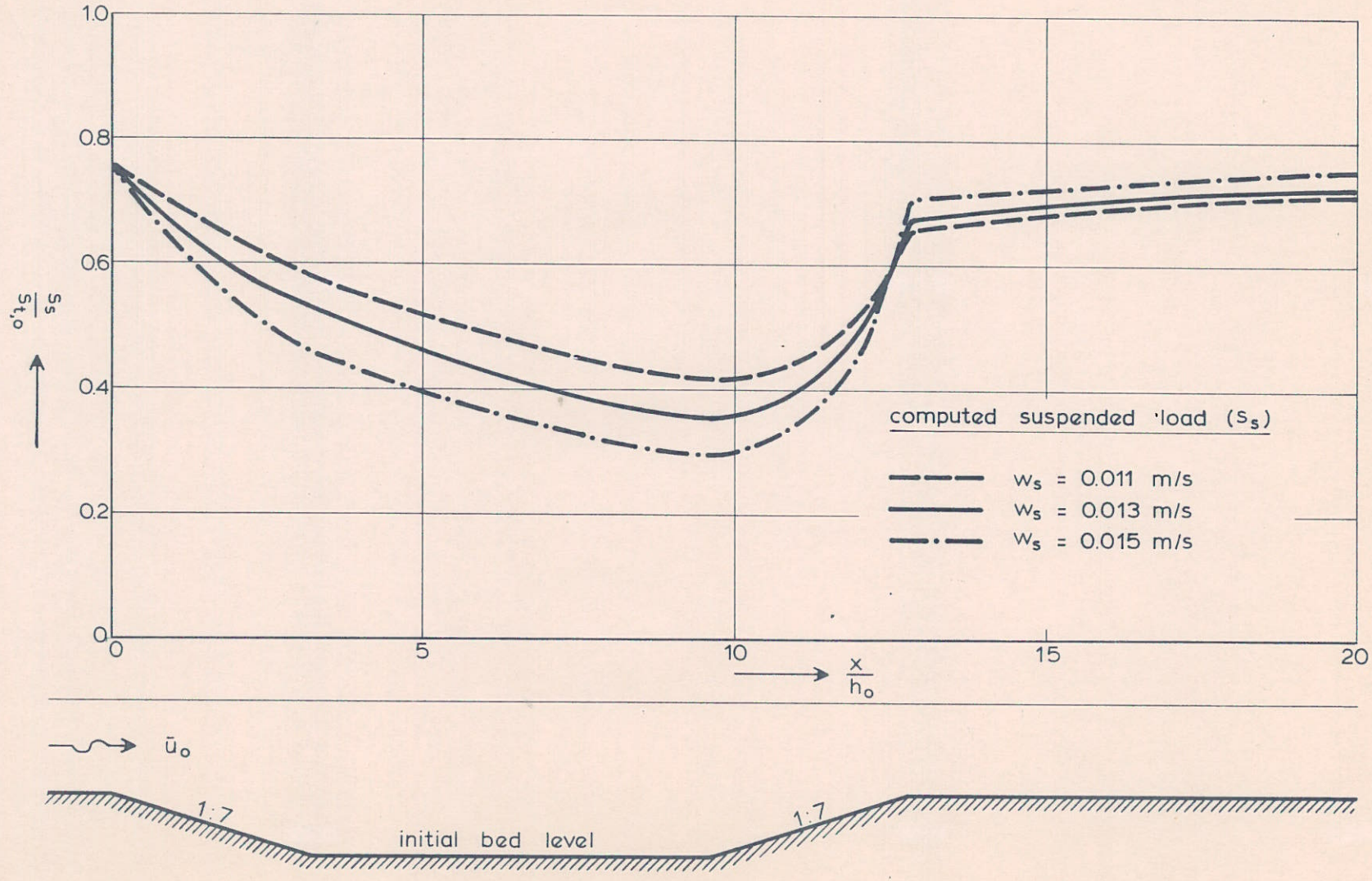

INFLUENCE OF PARTICLE FALL VELOCITY ON LONGITUDINAL SUSPENDED LOAD

DELFT HYDRAULICS LABORATORY

R1267-V/M1570

T 2

FIG. 21

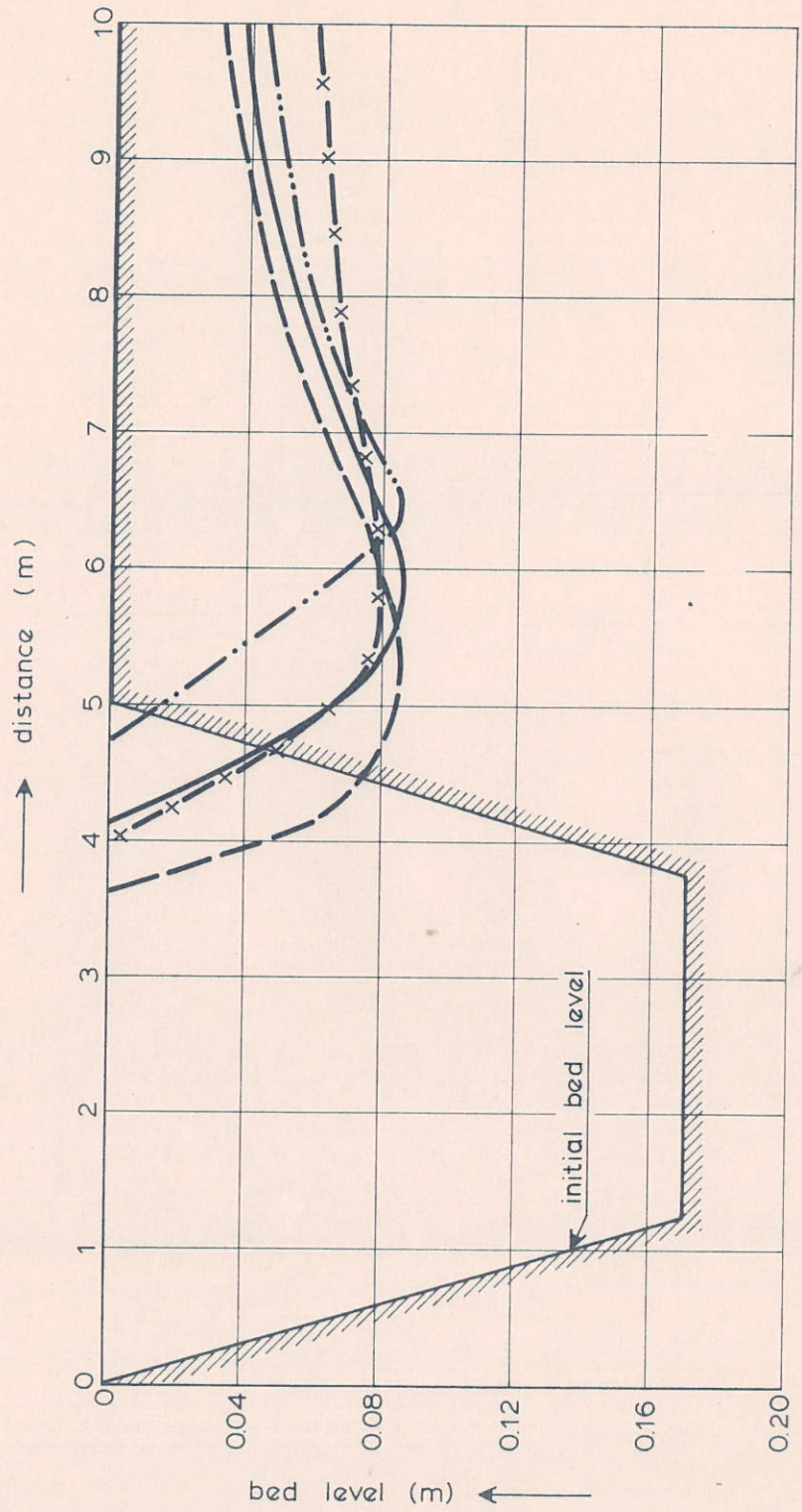

INFLUENCE OF PARTICLE FALL VELOCITY ON BED LEVEL	T 2	
DELFT HYDRAULICS LABORATORY	R1267-V/M1570	FIG. 22

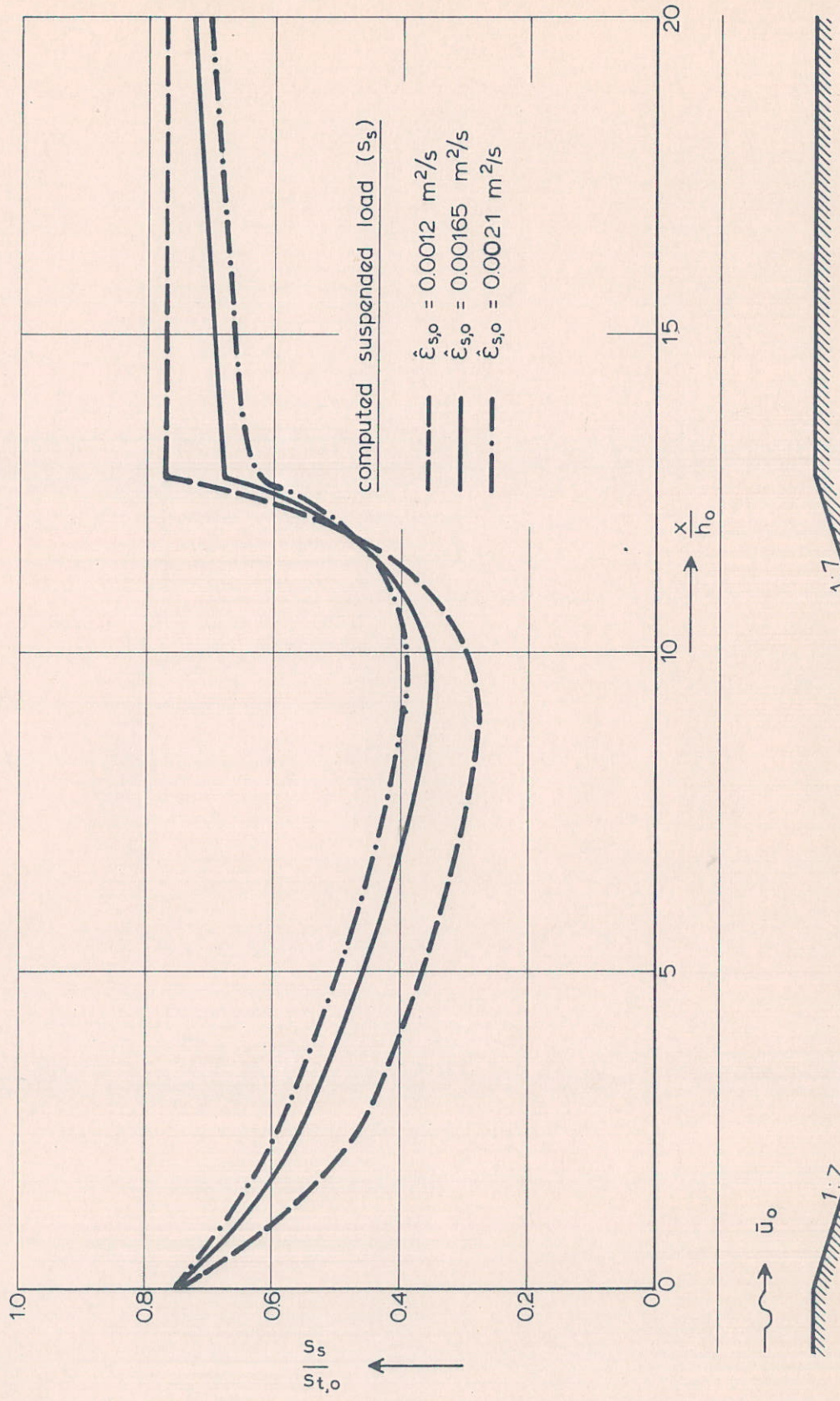

INFLUENCE OF UPSTREAM DIFFUSION COEFFICIENT ON LONGITUDINAL SUSPENDED LOAD

T2

DELFT HYDRAULICS LABORATORY

R1267-V/M1570

FIG. 23

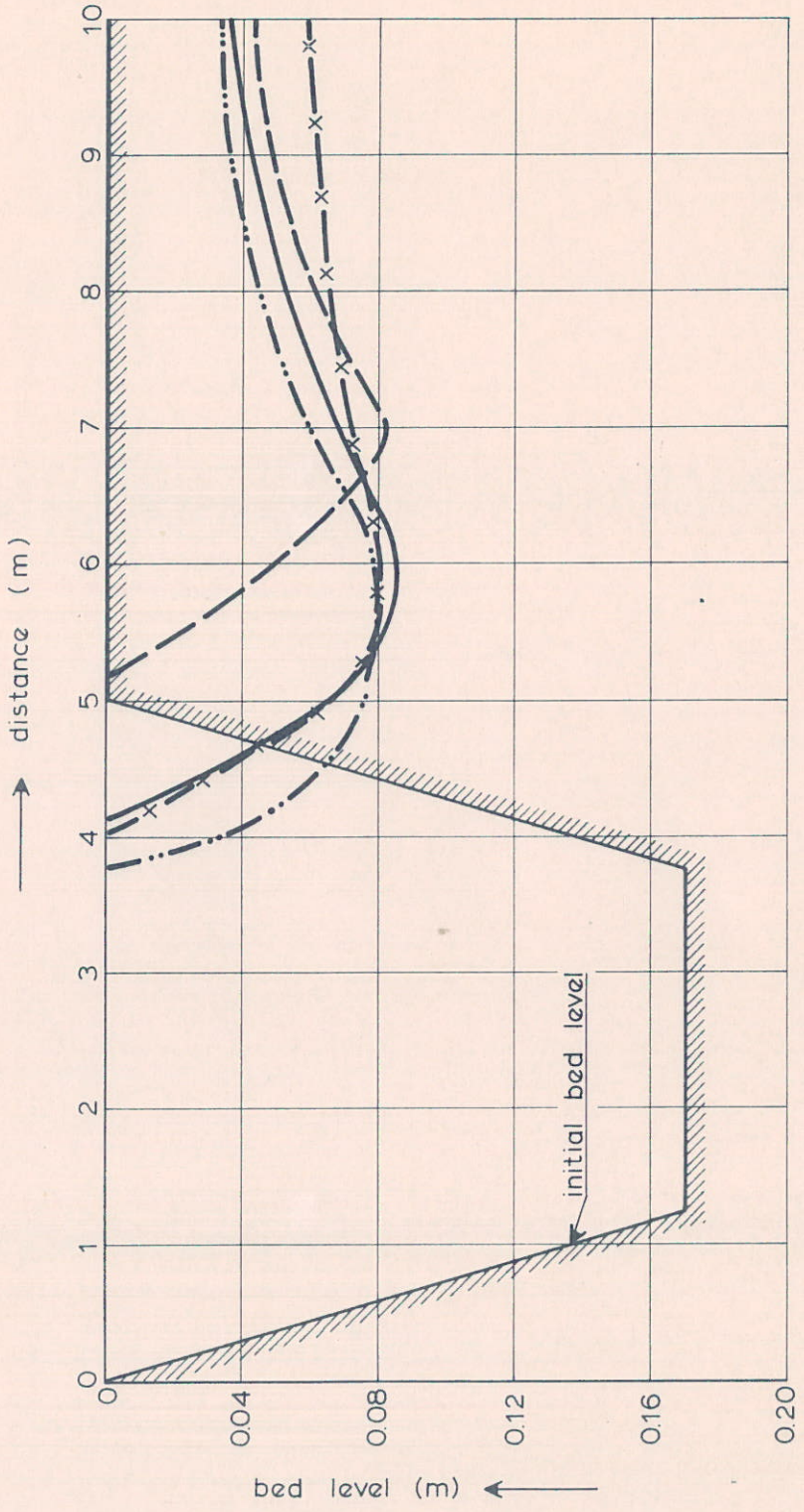

INFLUENCE OF UPSTREAM DIFFUSION COEFFICIENT ON BED LEVEL

T 2

DELFT HYDRAULICS LABORATORY

R1267-V/M1570

FIG. 24

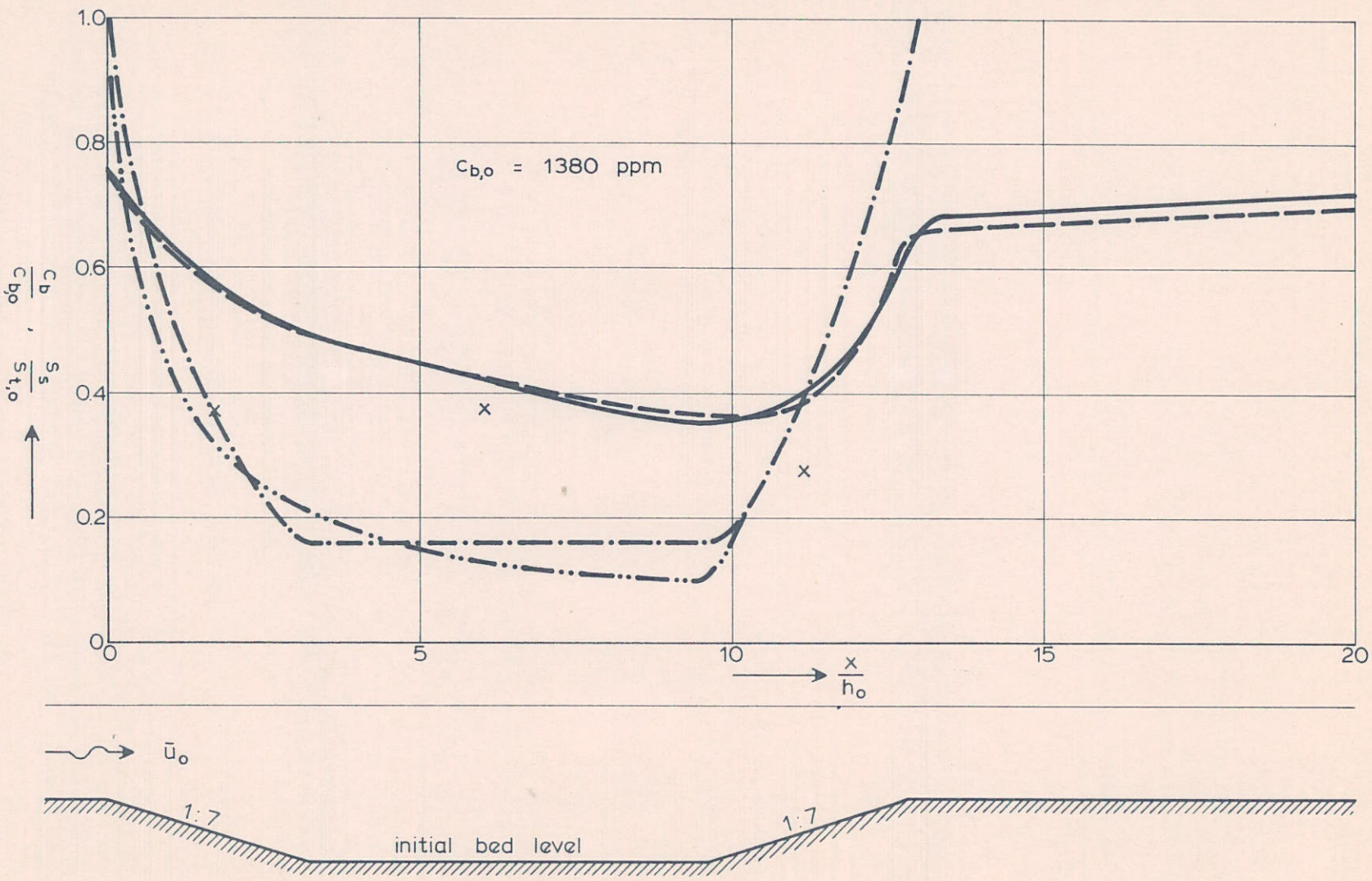

INFLUENCE OF BED BOUNDARY CONDITION ON BED CONCENTRATION AND SUSPENDED LOAD

DELFT HYDRAULICS LABORATORY

T 2

R1267-II/M1570

FIG. 25

DELFT HYDRAULICS LABORATORY

INFLUENCE OF FLOW VELOCITY FIELD ON LONGITUDINAL SUSPENDED LOAD

T 1

R1267-II/M1570

FIG. 26

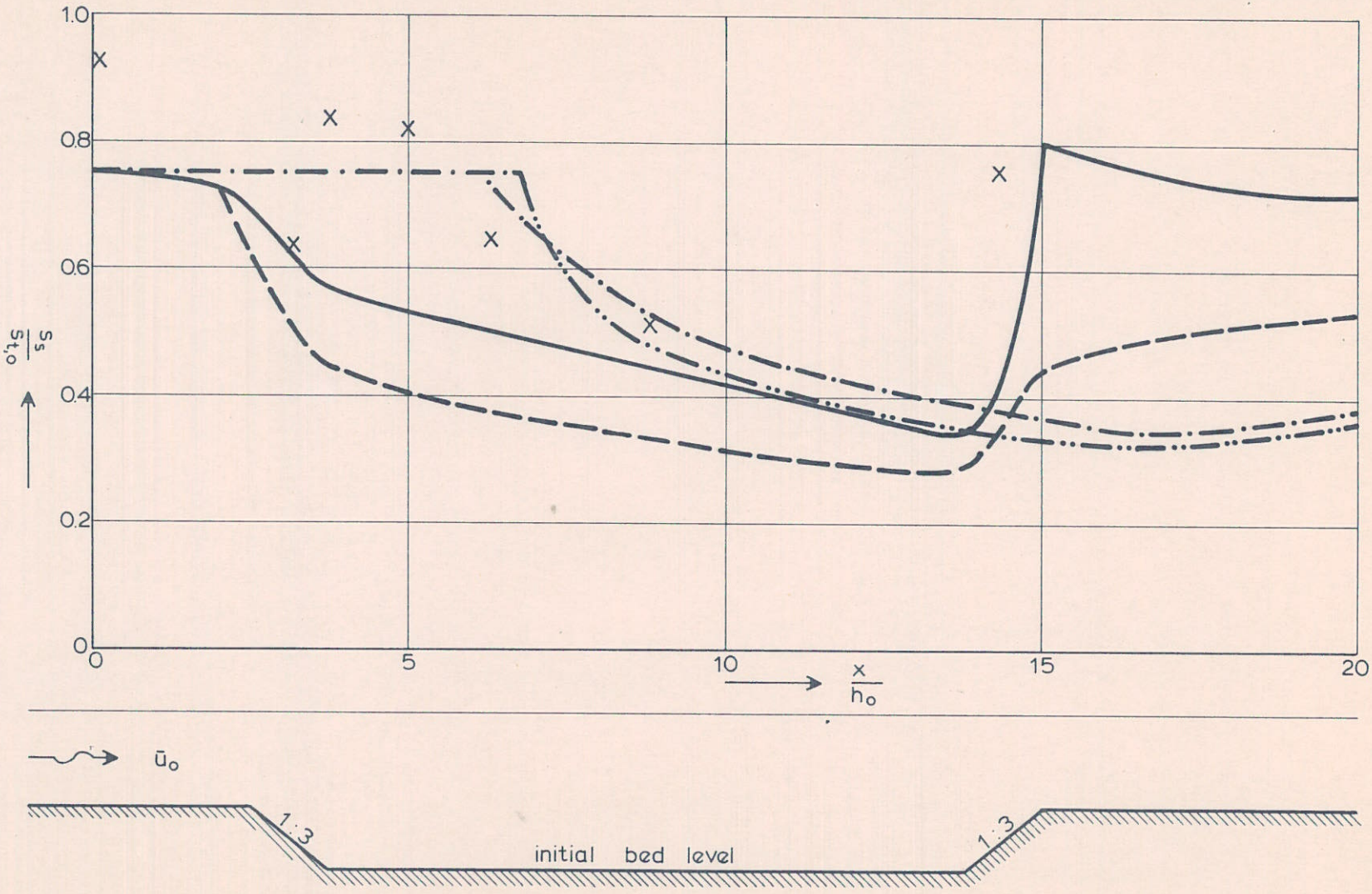

suspended load at t = 0 hours

——— computed for velocity profiles from semi-empiric model

– – – computed for logarithmic velocity profiles

x measured

suspended load at t = 7.5 hours

—·— computed for velocity profiles from semi-empiric model

—··— computed for logarithmic velocity profiles

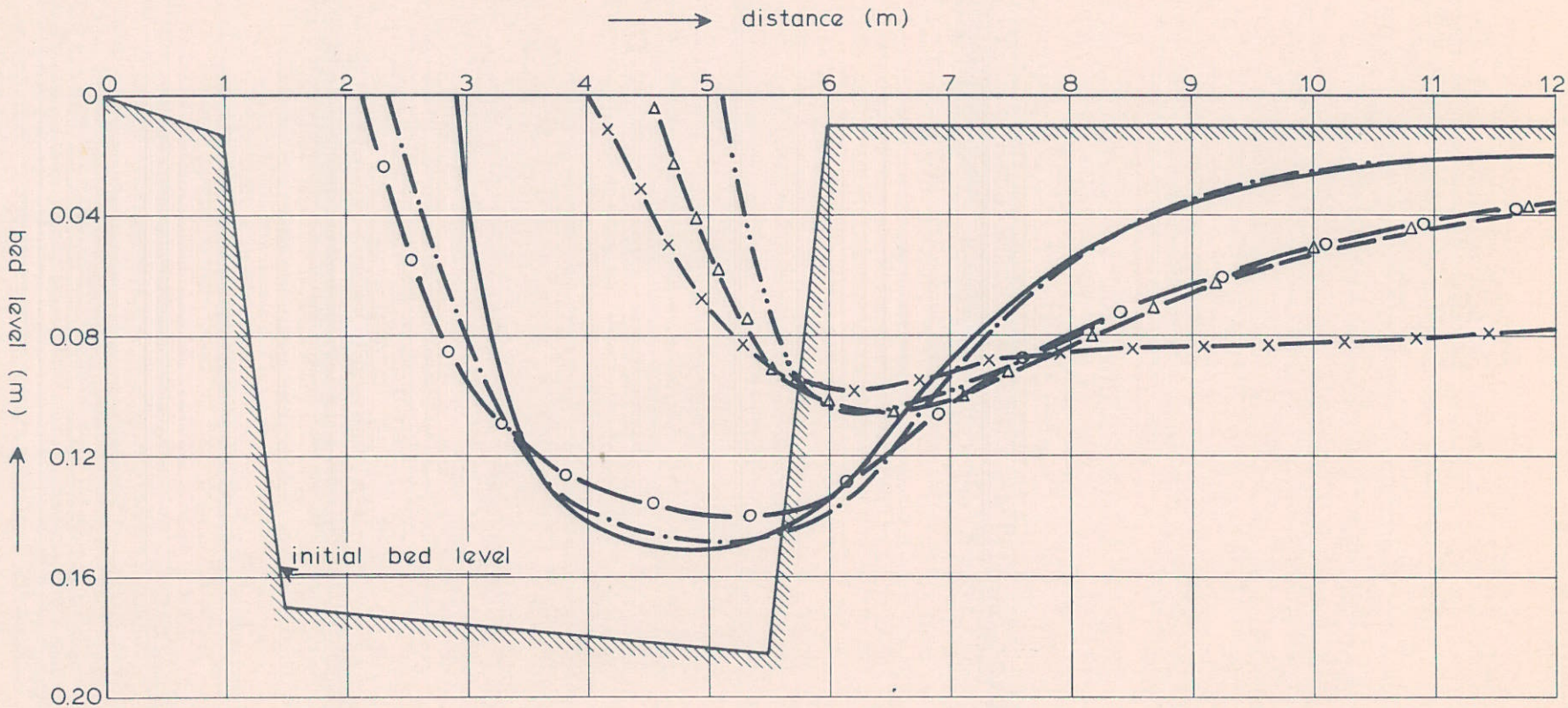

bed - level after t = 7.5 hours

- computed for logarithmic velocity profiles
- computed for velocity profiles from semi-empiric model
- o measured

bed - level after t = 15.0 hours

- computed for logarithmic velocity profiles
- Δ computed for velocity profiles from semi empiric model
- x measured

INFLUENCE OF FLOW VELOCITY FIELD ON BED LEVEL

T 1

DELFT HYDRAULICS LABORATORY

R1267-V/M1570 FIG. 27

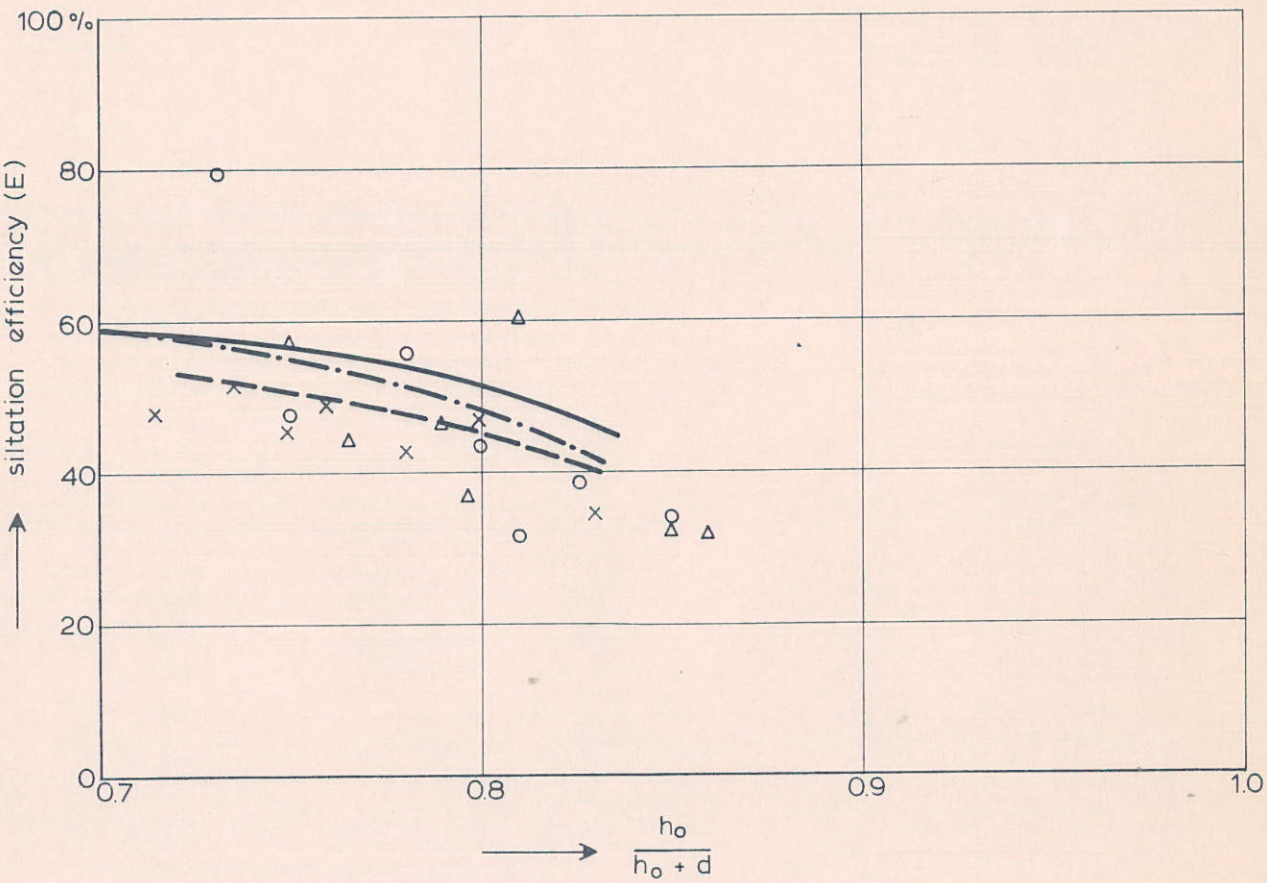

measured

× T1
o T2
Δ T3

computed

T1
T2
T3

SILTATION EFFICIENCY

DELFT HYDRAULICS LABORATORY | R1267-V/M1570 | FIG. 28

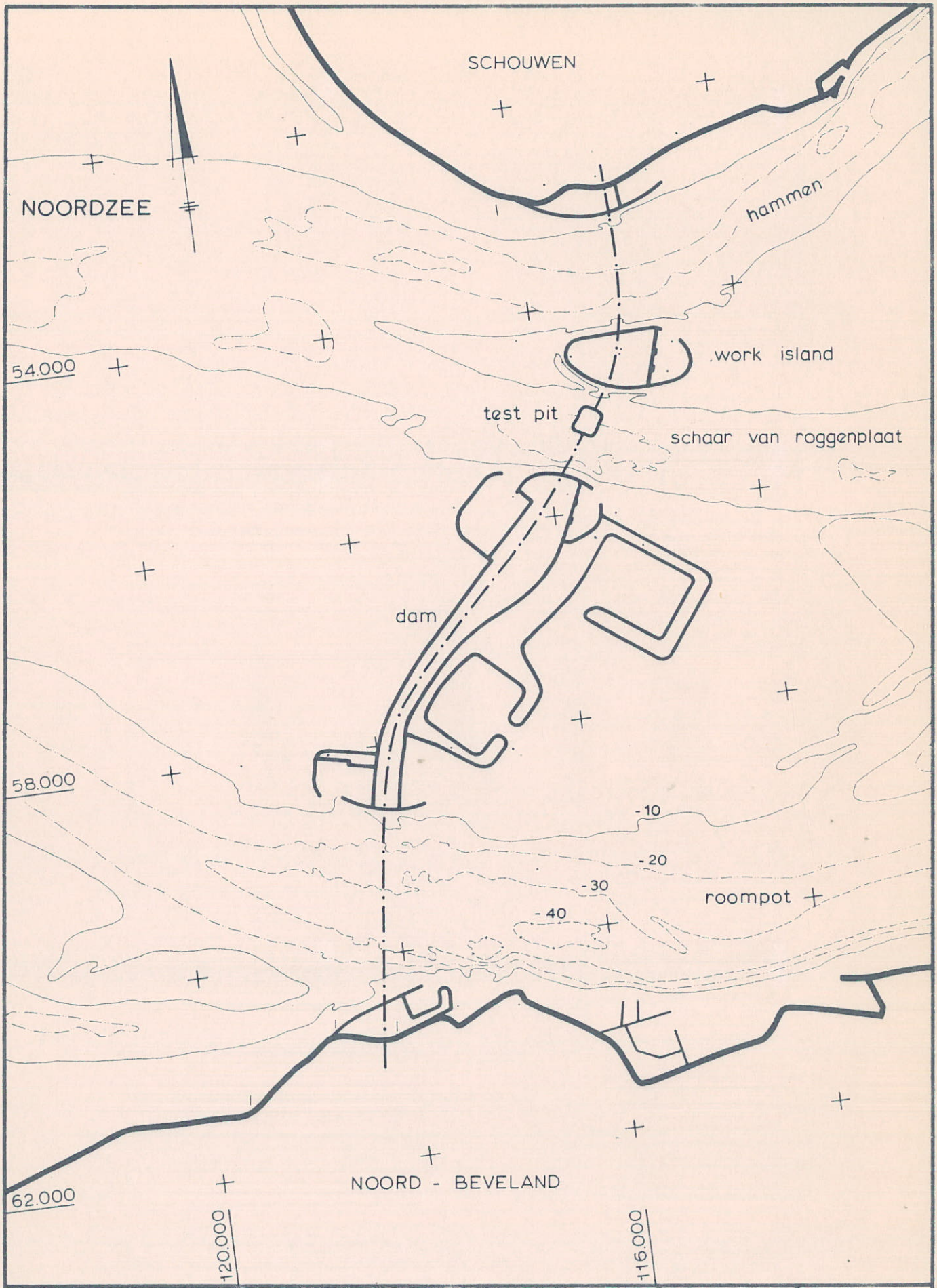

PLAN FORM OF OOSTERSCHELDE ENTRANCE

schaal 1 : 50.000

DELFT HYDRAULICS LABORATORY

R1267-V/M1570 FIG. 29

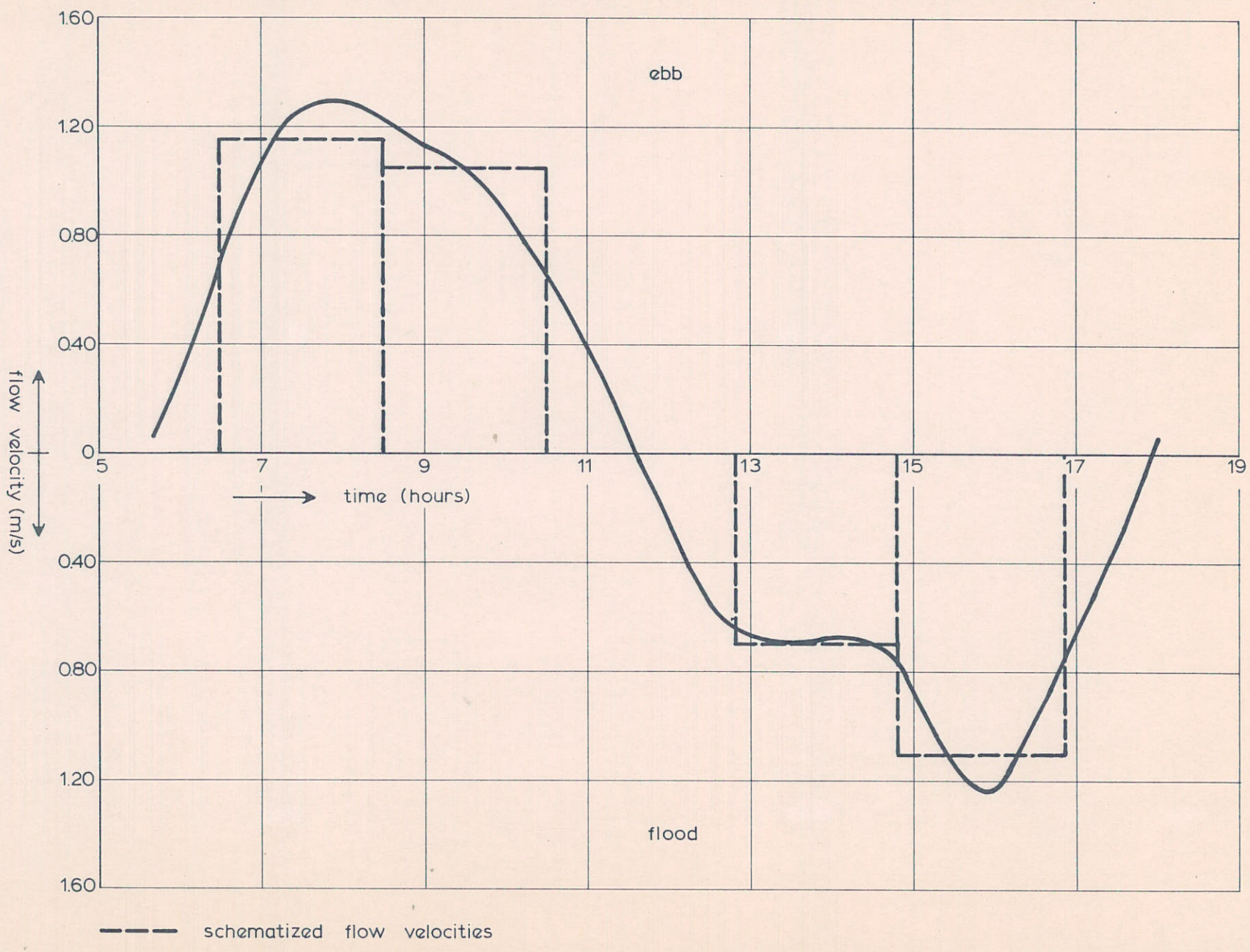

FLOW VELOCITIES FOR DESIGN TIDE

DELFT HYDRAULICS LABORATORY

R1267-IV/M1570

FIG. 30

DELFT HYDRAULICS LABORATORY

TIDAL RANGE FOR AVERAGE TIDE

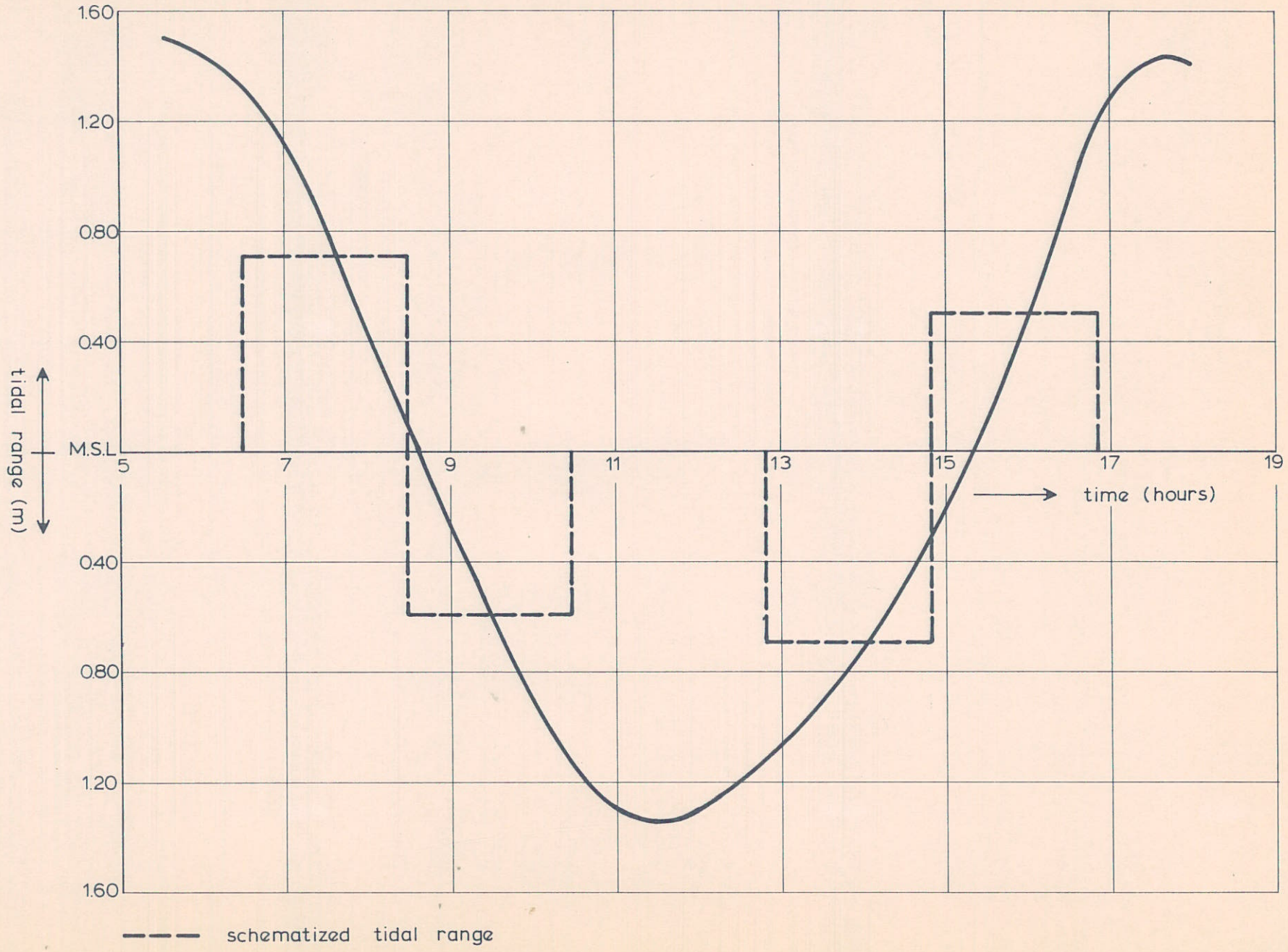

R1267-II/M1570

FIG. 31

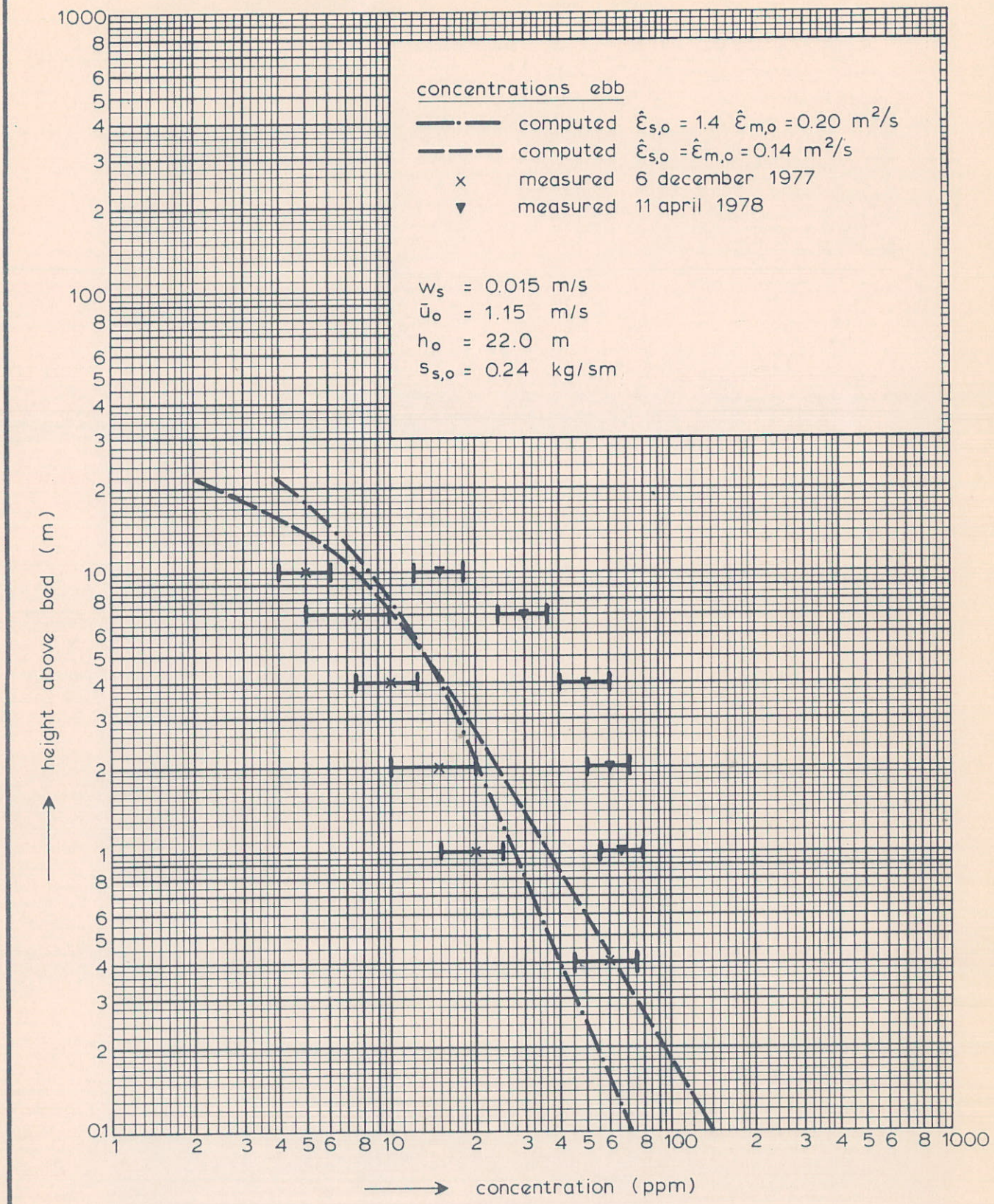

INFLUENCE OF DIFFUSION COEFFICIENT ON EQUILIBRIUM CONCENTRATION PROFILE (EBB)

DELFT HYDRAULICS LABORATORY | R1267-V/M1570 | FIG. 32

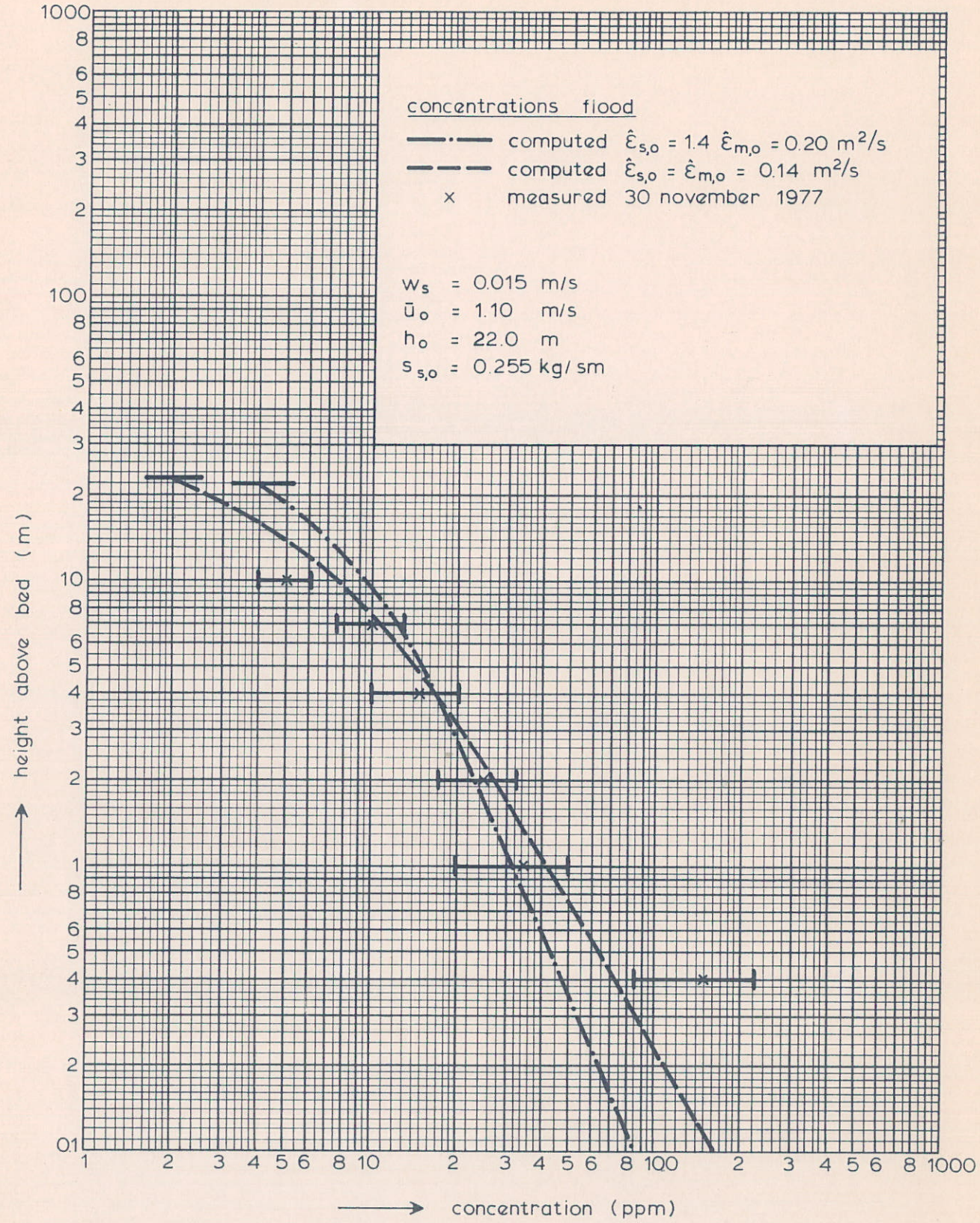

INFUENCE OF DIFFUSION COEFFICIENT ON EQUILIBRIUM CONCENTRATION PROFILE (FLOOD)

DELFT HYDRAULICS LABORATORY | R1267-V/M1570 | FIG. 33

FLOW VELOCITY AND SEDIMENT CONCENTRATION PROFILES (TEST PIT)

DELFT HYDRAULICS LABORATORY

R1267-II/M1570

FIG. 34

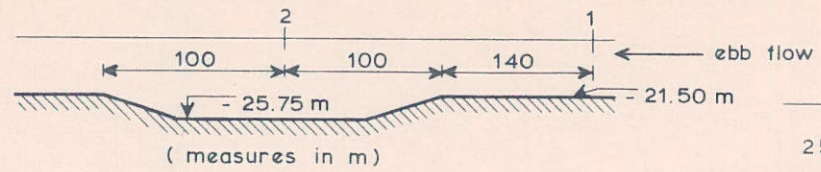

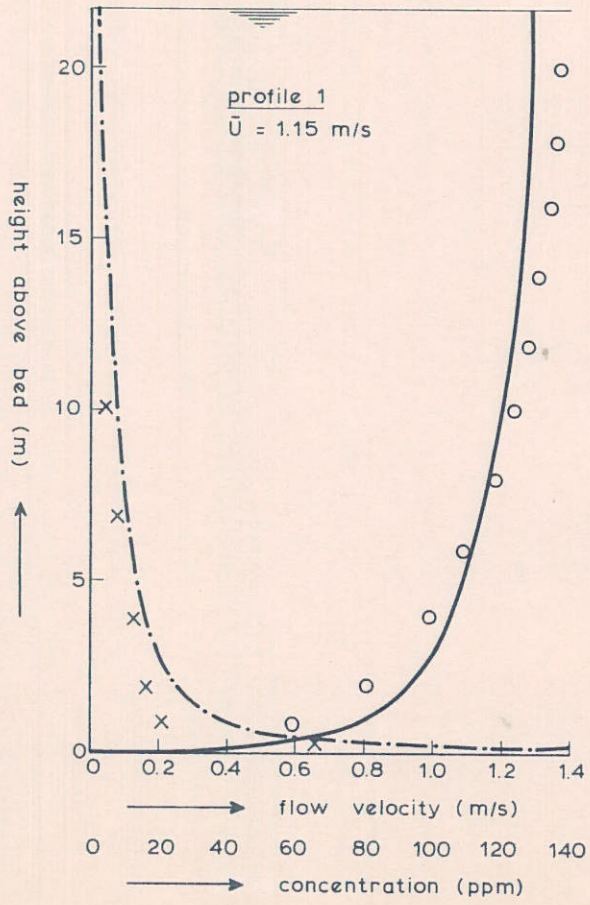

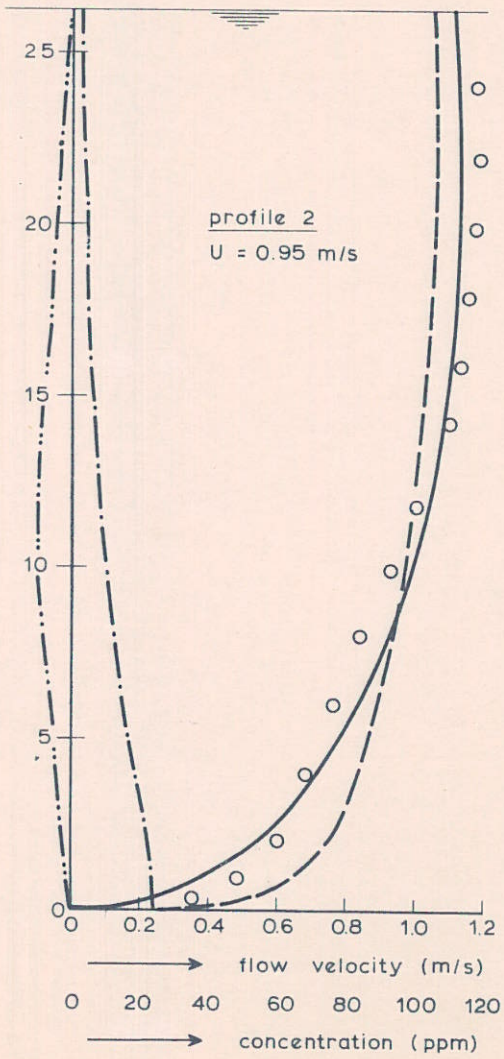

longitudinal flow velocity

——— computed (semi-empirical model)

– – – computed (logarithmic profile)

o measured 6 december 1977

vertical flow velocity

—··— computed

(scale is 10 times larger)

concentration

—·— computed

x measured 6 december 1977

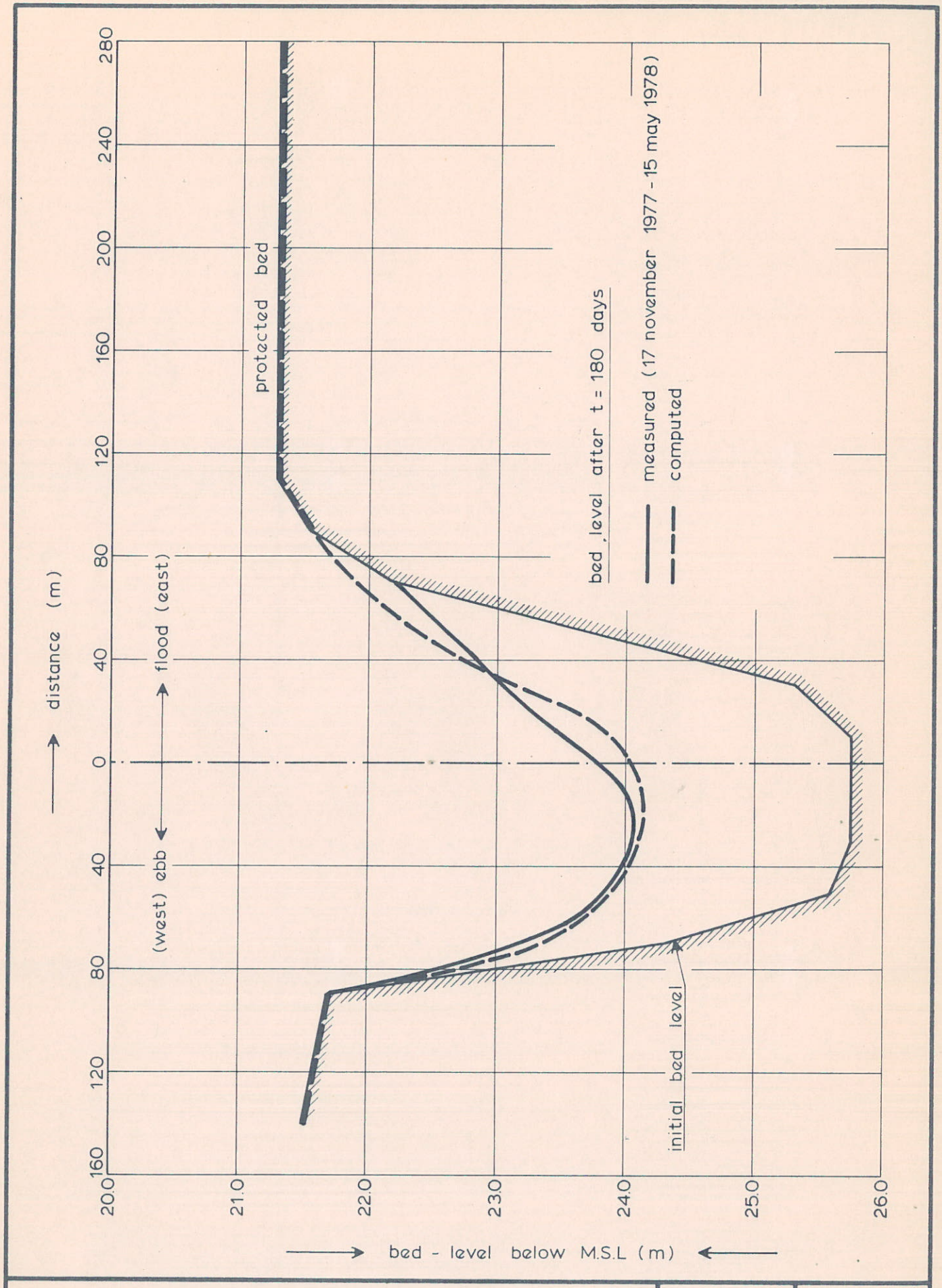

BED LEVELS (TESTPIT)

DELFT HYDRAULICS LABORATORY | R1267-V/M1570 | FIG. 35

computed maximum diffusion coefficient at t=0 hours

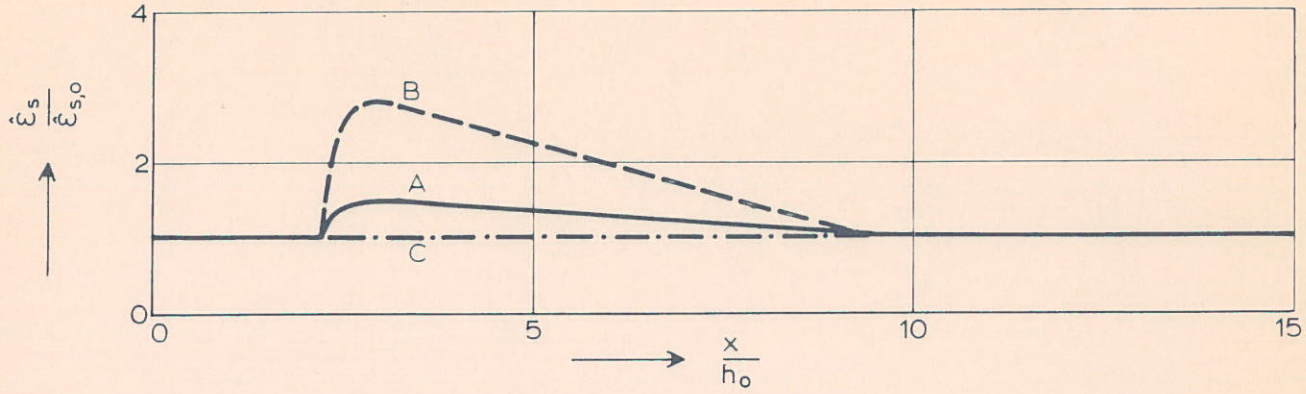

computed suspended load at t=0 hours

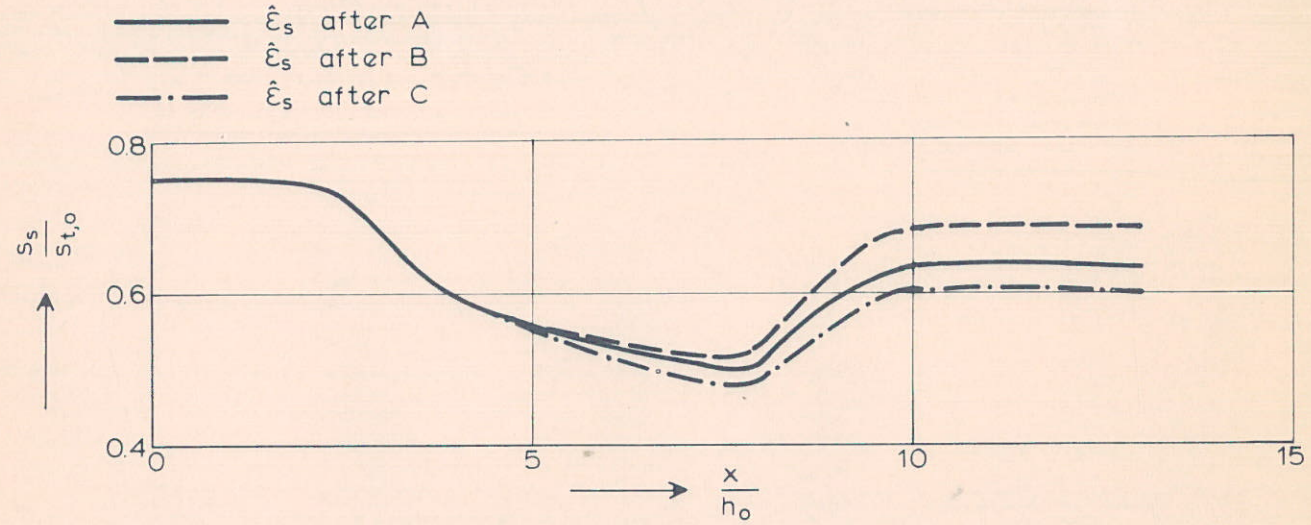

initial bed level of test pit

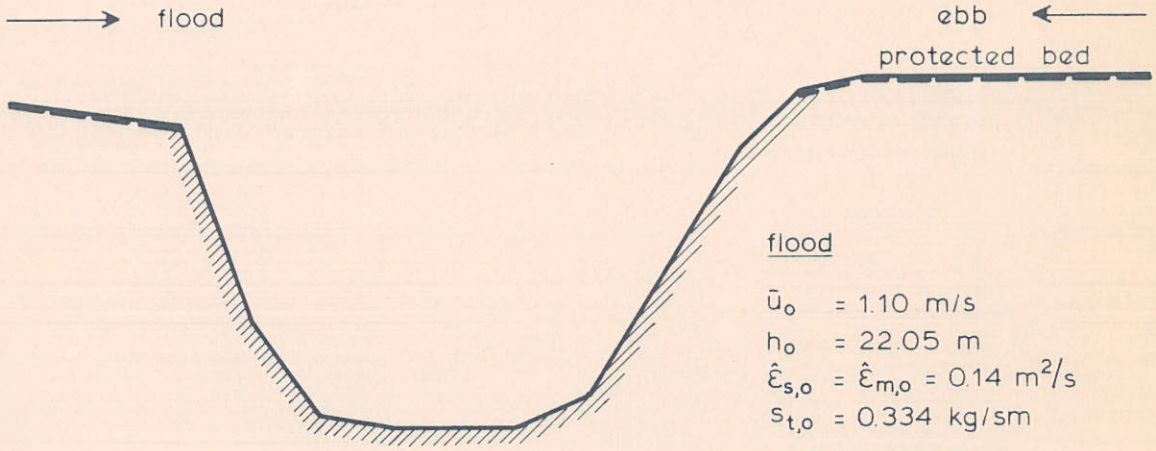

flood

$\bar{u}_o$ = 1.10 m/s
h_o = 22.05 m
$\hat{\varepsilon}_{s,o} = \hat{\varepsilon}_{m,o}$ = 0.14 m^2/s
$s_{t,o}$ = 0.334 kg/sm

INFLUENCE OF LONGITUDINAL DIFFUSION COEFFICIENT ON LONGITUDINAL SUSPENDED LOAD (TESTPIT)

DELFT HYDRAULICS LABORATORY | R1267-V/M1570 | FIG. 36

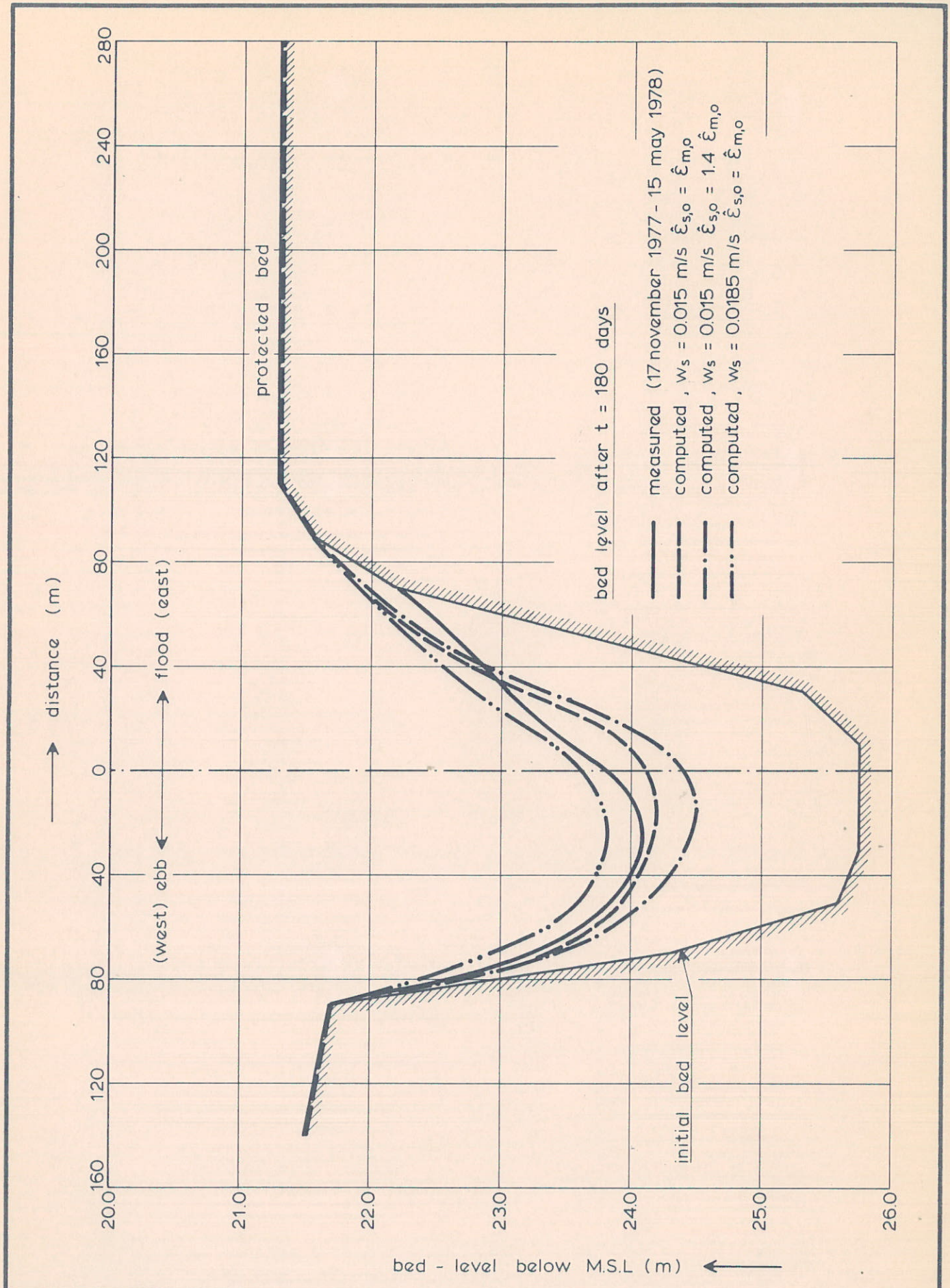

INFLUENCE OF PARTICLE FALL VELOCITY AND DIFFUSION COEFFICIENT ON BED LEVEL (TESTPIT)

DELFT HYDRAULICS LABORATORY | R1267-V/M1570 | FIG. 37

bed concentrations at t = 0 hours

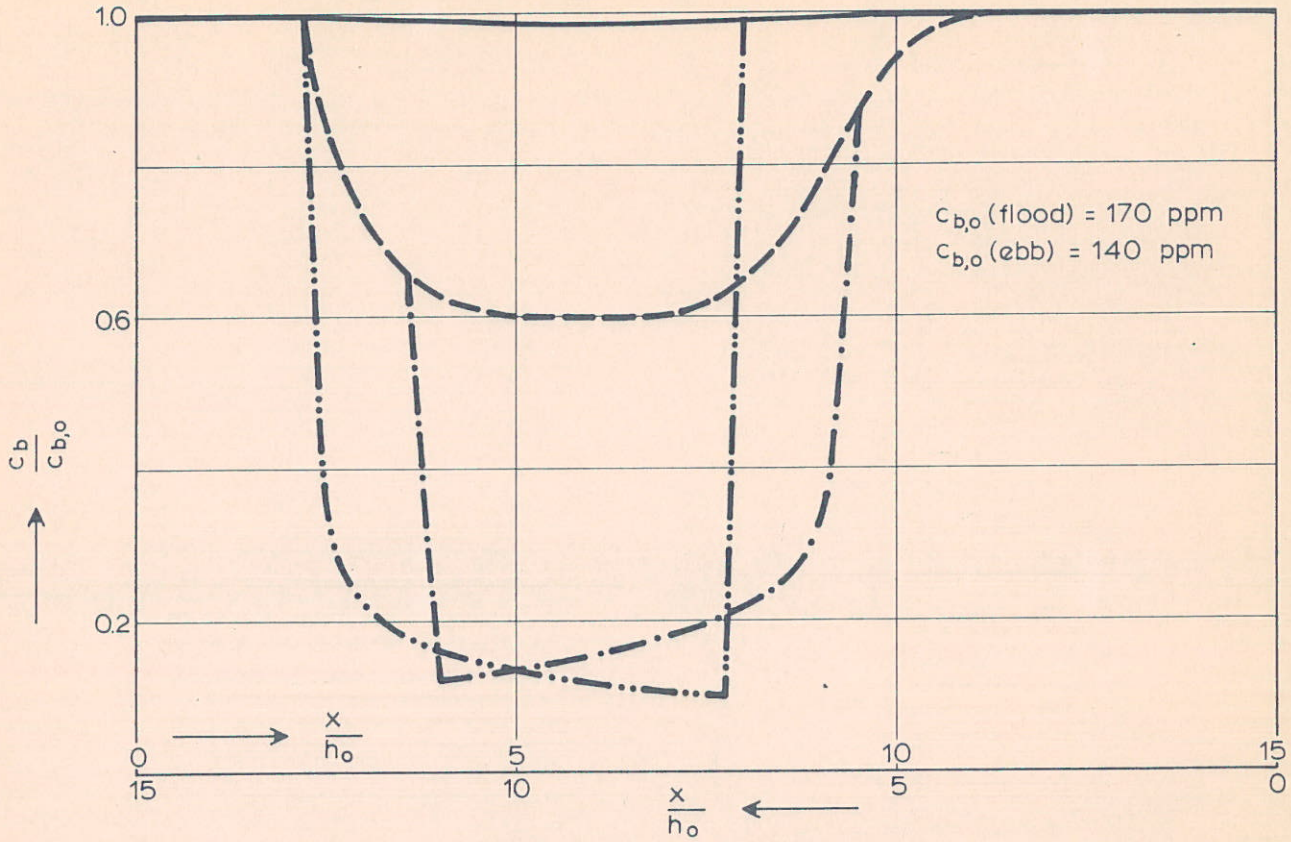

suspended load at t = 0 hours

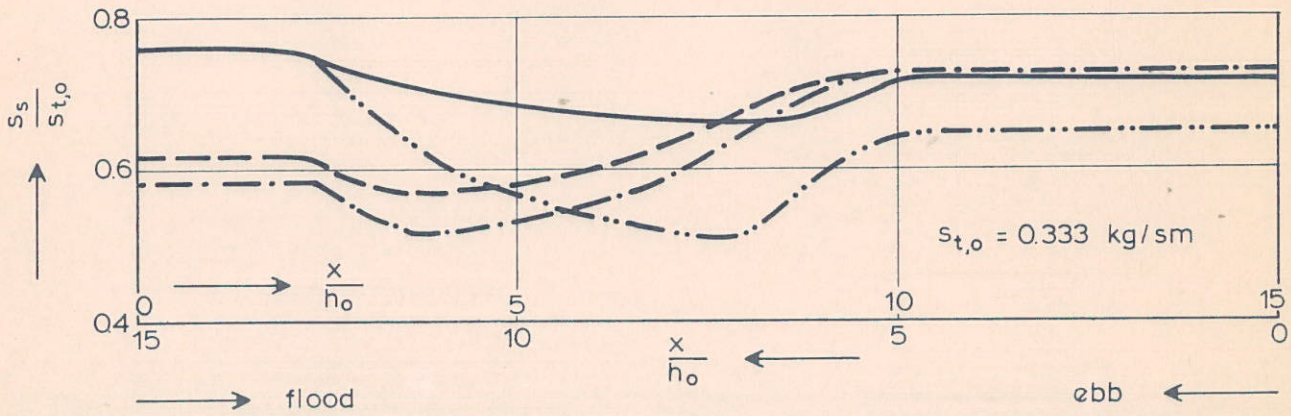

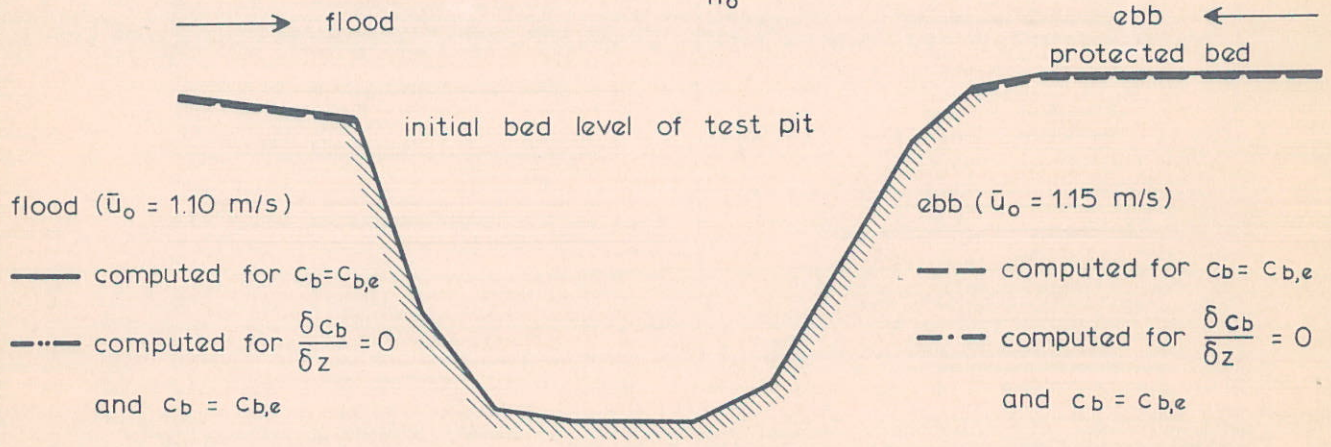

INFLUENCE OF BED BOUNDARY CONDITION ON LONGITUDINAL BED CONCENTRATION AND SUSPENDED LOAD (TESTPIT)

DELFT HYDRAULICS LABORATORY | R1267-V/M1570 | FIG. 38

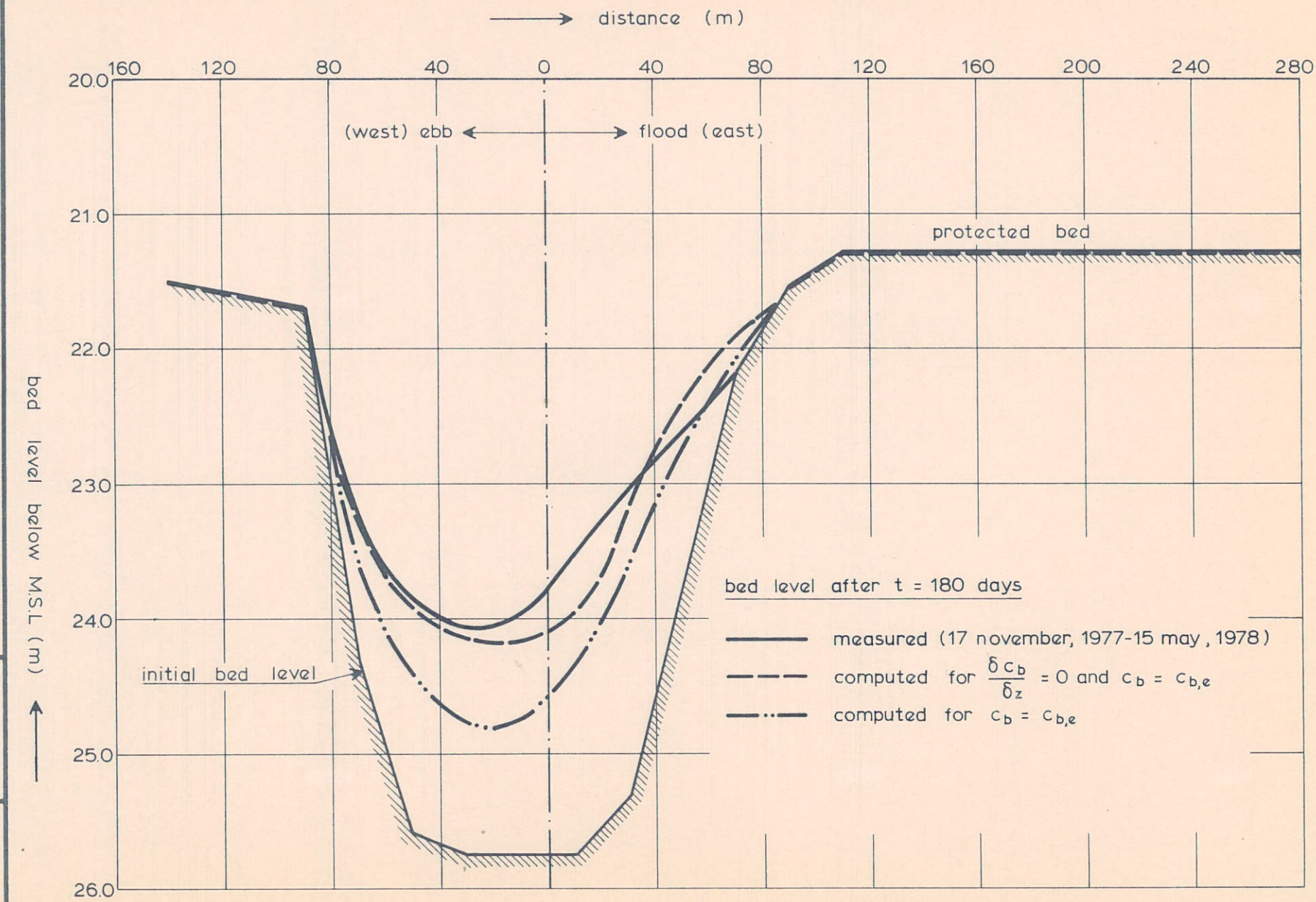

INFLUENCE OF BED BOUNDARY CONDITION ON BED LEVEL (TESTPIT)

DELFT HYDRAULICS LABORATORY

R1267-II/M1570 FIG. 39

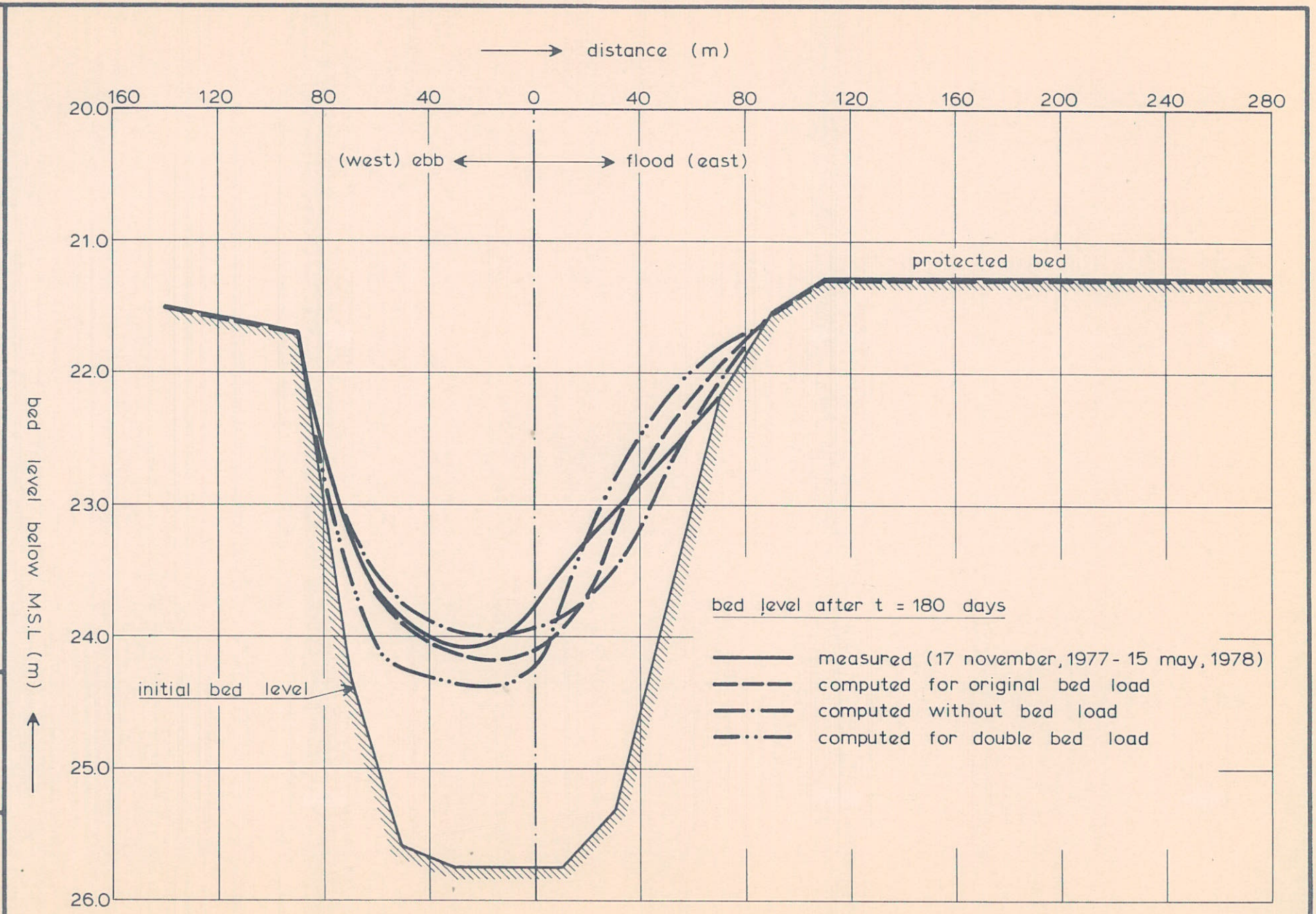

INFLUENCE OF UPSTREAM BED LOAD ON BED LEVEL (TEST PIT)

DELFT HYDRAULICS LABORATORY

R1267-II/M1570

FIG. 40

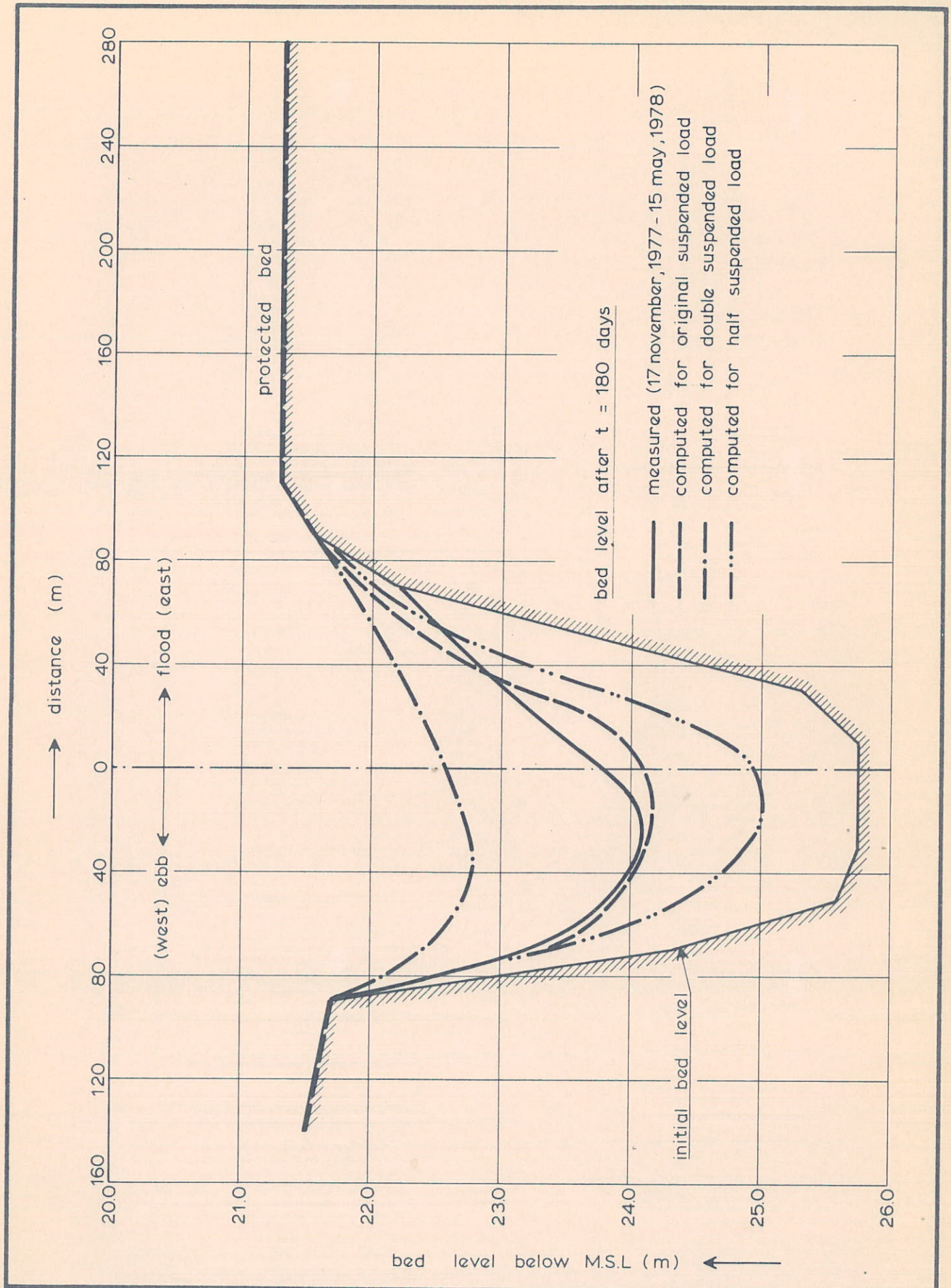

INFLUENCE OF UPSTREAM SUSPENDED LOAD ON BED LEVEL (TEST PIT)

DELFT HYDRAULICS LABORATORY | R1267-V/M1570 | FIG. 41

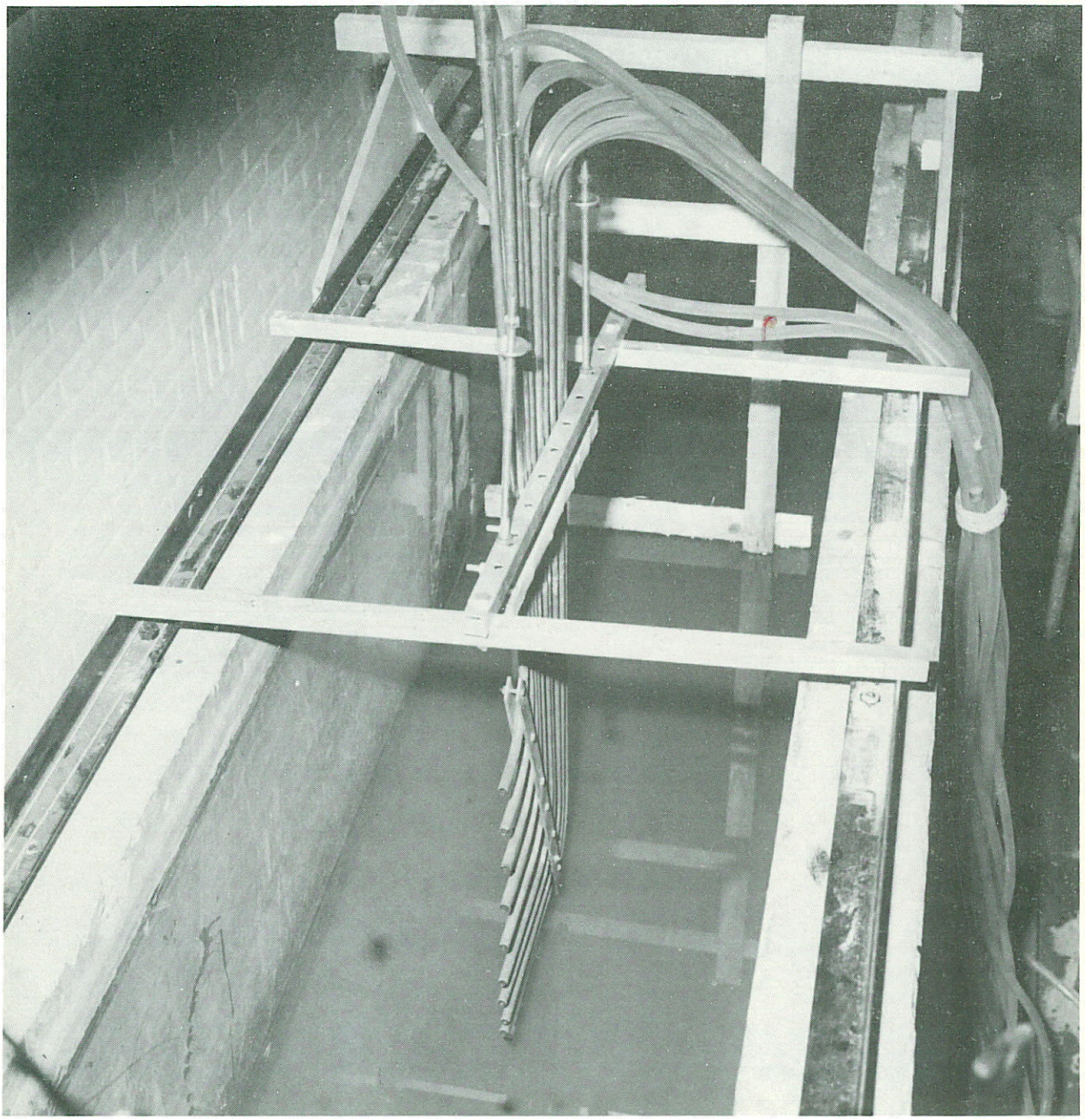

1. Instrument for measuring sediment concentration profiles

2. Separation of water and sediment by means of filter material (mesh size = 50 µm)

p.o. box 177 delft the netherlands